BIDGE Publications

Innovations in Nanomaterial Synthesis and Applications: from Heavy Metal Removal to Solid Oxide Fuel Cells and Beyond

Editor: Doç. Dr. Burak Tüzün

ISBN: 978-625-6707-53-5

Page Layout: Gözde YÜCEL

1st Edition:

Publication Date: 25.12.2023

BIDGE Publications,

Certificate No: 71374

www.bidgeyayinlari.com.tr - bidgeyayinlari@gmail.com

Krc Bilişim Ticaret ve Organizasyon Ltd. Şti.
Güzeltepe Mahallesi Abidin Daver Sokak Sefer Apartmanı No: 7/9 Çankaya / Ankara

PREFACE

All kinds of services for human health are one of the most basic and important priorities for societies. Scientific and technological advances make significant contributions to the field of health, engineering and basic sciences in our age. It is of great importance to follow these developments closely, to try to implement the developments and to pioneer innovations. As Bidge Publications, we are working towards becoming an important publishing house in the 100th anniversary of our republic.

This book titled "Innovations in Nanomaterial Synthesis and Applications: From Heavy Metal Removal to Solid Oxide Fuel Cells and Beyond", prepared on new scientific discoveries and innovations, examines in depth the complex world of advanced research and applications in various disciplines. From nanomaterials to catalysis, renewable energy to biotechnology, each chapter offers a unique perspective on the ever-evolving landscape of modern science. It takes you on a fascinating journey into the world of nanomaterials, investigating their synthesis and applications in combating the global problem of heavy metal pollution. In addition, the basic building blocks of solid oxide fuel cells are revealed and information can be obtained about the basic components that drive advances in sustainable energy technologies. In another, important insights into the field of computational chemistry are gained by exploring complex interactions between transition metals and aza-cryptans, providing valuable insights into molecular bonding. The next section describes the synthesis and characterization of a heterogeneous catalyst supported by mesoporous SBA-15 and sheds light on its catalytic ability in asymmetric transfer hydrogen reactions involving various aromatic ketones. in another, discover new materials designed for efficient adsorption, which play an important role in the pre-concentration and determination of heavy metal ions. In the next, delve into the fascinating world of

electrochemical biosensors, learning about their various types, their applications, and their capabilities in diagnostics and beyond. Next, important information is gained about sustainable energy with information on hydrogen production through solar water splitting using advanced photocatalytic and photoelectrochemical technologies. The next one provides important information about the environmentally friendly potential of polysaccharide gums by focusing on tragacanth-based hydrogels, which are effective tools for removing contaminants. The next one appears to explore the antibacterial properties of aromatic substances and their potential applications in the field of antibiotics.

This book aims to capture your curiosity and provide a comprehensive overview of groundbreaking discoveries and applications in various scientific fields. I hope this collection will inspire a new wave of curiosity and innovation, leading us towards a brighter and more sustainable future.

Editor
Associate Prof. Dr. Burak TÜZÜN

Contents

CHAPTER I

Synthesis Of Functionalized Iron Oxide Nanomaterials And Investigation Of Their Use In Heavy Metal Removal

Berrin TOPUZ

Introduction

Heavy metal ions have a strong affinity for protein, nucleic acids, and micro metabolites in living things. Due to the absence of crucial metals' homeostatic control, contaminated organic cells are altered or are unable to complete their biological tasks, which can have deadly health effects (Song & et al., 2011). Because of their toxic nature and tendency to bioaccumulate, heavy metal pollution has emerged into a significant environmental problem. Due to food chain transfers, heavy metal ions not only damage aquatic life, but they also have negative impacts on land animals, including people (Verma & Dwivedi, 2013). Thus, before releasing such dangerous heavy metal ions into the ecosystem, they must be removed from all

habitat. The need for new pollution standards to assess low levels of hazardous metal ions in the natural environment has led to the development of novel metal ion removal technologies (Carolin & et al., 2017).

Adsorption (Gao & et al., 2020), ion Exchange (Dąbrowski & et al., 2004), chemical precipitation (Chen & et al., 2018), electro-dialysis (Durairaj & et al., 2014), and membrane processes (Abdullah & et al., 2019) are a few of the techniques that have been used to remove toxic heavy metals from aqueous media. In terms of ease of design and implementation, the adsorption process using suitable and variable adsorbents is regarded as one of the most economical and efficient approaches among various separation processes. By using the adsorption of heavy metal ions with magnetic nanoparticulates, significant progress has recently been made in the production of environmentally benign solid material-based nanocomposites (Mehmood & et al.,2021).

Nanoparticles, particularly magnetic nanoparticles (MNPs), offer a wide range of uses due to their unique properties such as improved thermal and chemical endurance, high surface area and low toxicity (Binandeh, 2022). According to recent study, iron and iron oxide nanostructures are particularly effective materials for heavy metal removal via reduction/adsorption (Ali & et al., 2021).

Adsorption of the metal ion onto the modified or coated surface of nanopartices is the first stage in magnetic separation procedures. The metal ion was then preconcentrated, or removed from the solution, using an external magnetic field. Later, the same procedure can be carried out again using manufactured nanoparticles (Aguilar-Arteaga & et al., 2010,Gong & et al., 2007).

Iron oxide (II, III) (Fe_3O_4) is also known as magnetic iron oxide because it is a black crystal that is magnetized. The Schikorr reaction converts Fe(II) hydroxide ($Fe(OH)_2$) into Fe(II,III) oxide (Fe_3O_4). This transformation reaction follows. This transformation reaction follows:

$$Fe(OH)_2 \rightarrow Fe_3O_4 + H_2 + 2H_2O$$

Ferrous hydroxide Magnetite hydrogen water

Two separate mechanisms can be thought of as the Schikorr reaction: Fe(II) are anaerobically oxidized into Fe(III) by water protons. Two water protons are reduced, resulting in the creation of molecular hydrogen (H_2) and the dehydration of Fe(II) and Fe(III) hydroxides, which results in the synthesis of the thermodynamically more stable phase Fe (II,III) oxide (Ishikawa & et al., 1998). Due to the huge surface area/volume ratio, oxidation and aggregation are the most common issues in the synthesis of magnetic nanoparticles (Wu & et al., 2008). It is preferable to cover the surface with an appropriate and functional substance to prevent this. In addition to solving these issues, the coating procedure will increase the functionality of the composite construction.

Depending on the purpose, coating could be done with either organic or inorganic materials. As a result of coating, core/shell structures are formed. It matters for the formation of the shell in core/shell structures whether the environment is polar or nonpolar, and the shell structure forms successfully in polar environments. The new structures formed by different composite nanoparticle structures with each other are called multifunctional nanoparticles. Such structures are formed by additionally attaching different materials to the shell (Ahmed & et al., 2021; Zeng & Sun, 2008).

To protect the side effects of the released nanomaterials, scientific research is working to strengthen these nanoparticles into an easily detachable substrate. Magnetic nanoparticles can be integrated into the solid substrate using physical or chemical precipitation methods according to studies (Chen & et al., 2021a, Chen & et al., 2021b).

Comparing this process to other ones for chemical synthesis, it has some benefits. Chemical precipitation, for example, allows for quick synthesis without the need for high temperatures, and is simpler than other procedures because it uses water as a solvent. Controlling the modified magnetic nanoparticle is more challenging

than with other approaches due to its form. To obtain the appropriate sizes, the environmental conditions must be adjusted to the appropriate level. In numerous studies, various adsorbents such as activated carbon (Suhas & et al., 2016), chitosan (Begum & et al., 2021), functionalized polymer (Topuz & Macit, 2011) and silica (Wang & et al., 2009) have been investigated for the development of effective adsorption techniques.

Typically, polymers, noble metals, silica, active carbon, humic acid are utilized to create a shell structure that protects the magnetic nanoparticles from oxidation (Suo & et al., 2019, Donga & et al., 2021, Shan & et al., 2022).

Because of its strong affinity for magnetite nanoparticles, humic acid prevents particle agglomeration by sorption. Furthermore, the carboxylic and phenolic groups of humic acid have complicated interactions with heavy metals (Peña-Méndez & et al., 2005) .

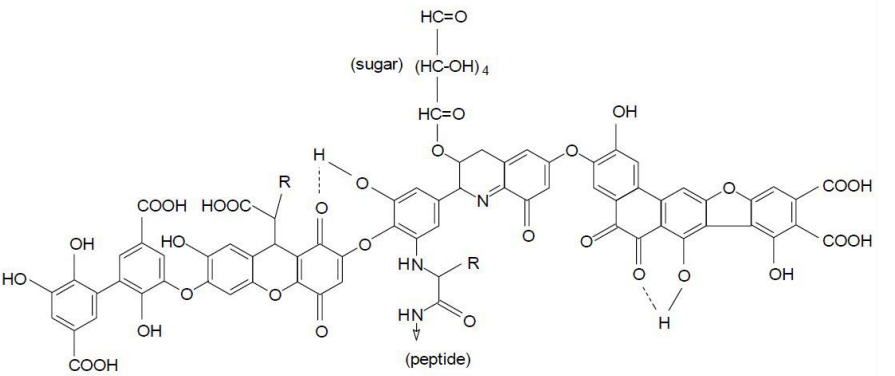

Fig. 1. *Chemical structure of Humic acid (HA)*

Some contaminants, particularly heavy metals in water, interact with Humic acid through hydrogen bonds, coordination bonds, hydrophobic bonds, and electrostatic bonds due to the presence of oxygen-containing functional groups, such as phenolic or carboxylic groups, in key binding sites (Andjelković & et al., 2006) . Technique for magnetic separation and concentration

typically involve removing metal ions from the environment after applying magnetic nanoparticles to an area with heavy metal pollution. This technique is quick, easy, and effective for analyzing heavy metals, which are hazardous and dangerous metals even at low concentrations.

Experimental Methods

Chemicals and Reagents

$FeCl_3.6H_2O$, $NH_4FeSO_4.6H_2O$, Humic Acid, NH_3, $AgNO_3$, NaOH, HCl, Sn (II) Chloride were purchased from the Sigma Aldrich. All of the chemicals were of analytical quality and were used without further purification.

Apparatus

UV-VIS Spectrophotometry (Spectroquant Pharo300, Merck, Darmstadt, Germany) (190-1100 nm) was used to measure cobalt and nickel in a 1-cm Quartz cuvette. The ISOLAB digital pH-meter was used to measure the pH. Weights were calculated using an analytical balance (Radwag, Poland) with a sensitivity of 0.00001. In the batch technique studies, the MEDISPEC roller mixer was used. ISOLAB magnetic stirrer was utilized to achieve homogenous heating during nanoparticle coprecipitation.

Synthesis of Silica-Functionalized Magnetite Nanoparticles

A chemical co-precipitation approach of ferric and ferrous ions in alkali solution was used to make silica-functionalized magnetite nanoparticles (Saberi & et al., 2020). The salts $FeCl_36H_2O$ (40 mmol) and $FeSO_47H_2O$ (20 mmol) were dissolved in 200 ml of deionized water while vigorously stirring (900 rpm). At room temperature, 1 $molL^{-1}$ of NaOH solution was then added to the mixture. To keep the reaction's pH between 11 and 12, where a black suspension was generated, NaOH solution was added next.

After 1 hour of steady stirring at room temperature, the resulting black dispersion was refluxed for another hour. Subsequently, silica (3.3 g) was added to the reaction vessel, the mixture was continuously stirred for 24 hr. The silica-coated nanoparticles (Fe_3O_4-SiO2) were collected using a magnet, followed by washing five times with EtOH solutions (50 % v/v, 40 mL) and drying at 80 °C in vacuum for 12 h.

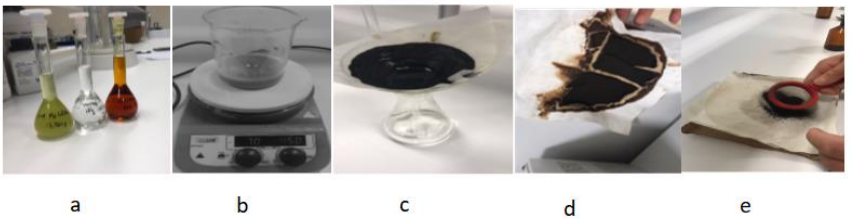

Fig. 2. *Preparation silica-functionalized magnetite nanoparticles. The solutions used (a), mixing with the silica of the solutions (b), filtration (c), drying (d), uniformity of nanoparticles by sieving (e).*

Synthesis of Fe_3O_4/HA/Ag Nanoparticles

By using a chemical co-precipitation approach with ferric and ferrous ions in an alkali solution and increasing heating and ultrasonication periods, HA/Ag-functionalized magnetite nanoparticles were created (Liu & et al., 2008). $FeCl_36H_2O$ (30 mmol) and $FeSO_47H_2O$ (20 mmol) salts were dissolved in 100 ml of deionized water with 900 rpm of vigorous stirring, and the mixture was then heated to 90^0C for 45 minutes.

Following the heating step, 10 mL of a 1000 mg/l sodium salt solution of humic acid was blended with solutions of ferrous and ferric chloride, and 10 mL of a 25% ammonia solution was added right away to precipitate humic acid-coated magnetite nanoparticles. Following reduction, an hour-long heating operation was conducted at 90^0C. The particles were sonicated for 30 minutes and being cleaned twice with milliQ pure water. Using a simple magnet for sonication, the supernatant was then gathered with a dropper. Very

small particles with very weak magnetic properties have been found in supernatant liquid. The liquid supernatant was discarded along with these particles. Existing particles were coated with silver using the redox reaction between tin and silver. Compared to silver, solid tin has a far higher tendency to generate its ions. Due to this, humic acid covered magnetite particles initially with tin particles before silver was substituted for tin during a redox reaction. Fe_3O_4/HA particles were combined with 0.063 M acidic Tin(II) chloride solution on the first step of the synthesis procedure, then sonicated for 30 minutes to form Fe_3O_4/HA/Sn particles that were then twice rinsed with milliQ water. The second stage involved mixing freshly prepared 0.13 M Tollen's reagent (ammonium silver nitrate) with Fe_3O_4/HA/Sn particles, sonicating the mixture for 30 minutes, and washing the mixture twice with milliQ water. Consequently, Fe_3O_4/HA/Ag magnet was used to extract the magnetic particles from the suspension, and they were then dried in the air at 60^0C.

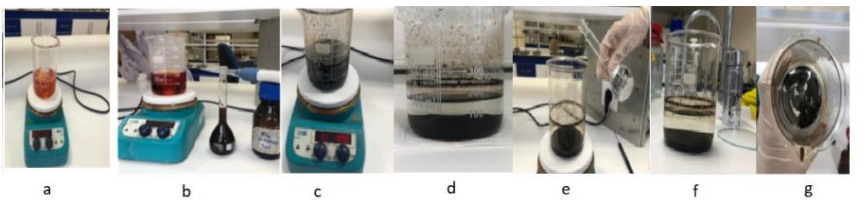

Fig. 3. *Preparation of Fe_3O_4/HA/Ag Nanoparticles. Creating of Fe_3O_4 with stoichiometric mixture of $FeCl_3.6H_2O$ and $NH_4FeSO_4.6H_2O$ (a), mixing with the Humic acid and ammonia of the Fe_3O_4 solutions (b), Mixing (c), precipitation of Fe_3O_4/HA (d), creating of Fe_3O_4/HA/Sn particles with Tollen's reagent (e) , precipitation of Fe_3O_4/HA/Ag nanoparticles (f), Drying of Fe_3O_4/HA/Ag nanoparticles.*

Procedure of Heavy Metal Adsorption

Adsorption process between Nickel and Cobalt metal ions and synthesized nanoparticles was investigated by using UV-VIS Spectrometer. 10 mgL of nickel and cobalt standard solutions were made by properly diluting stock solutions to concentrations of 1000

mg L^{-1}. (Merck, Darmstadt,Germany in 0.5 $molL^{-1}$ HNO3). Synthesized manyetic nanoparticles were mixed with standard solutions of 2 mL of 10 mgL^{-1} nickel and cobalt using the MEDISPEC roller mixer. After the adsorption particles were collected with a magnet. The adsorbed metal concentration values were calculated by subtracting the metal concentration values in each sample's filtrate from the initial concentration value with UV-VIS spectrometric method.

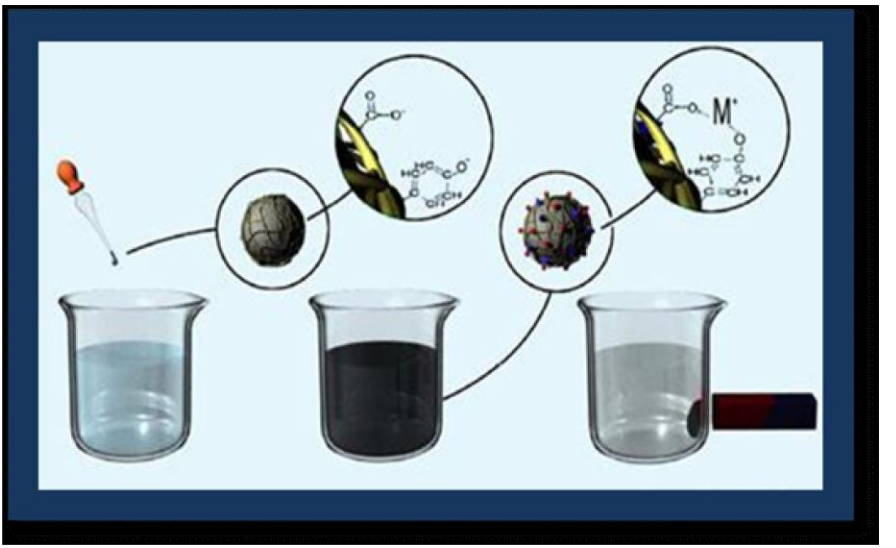

Fig. 4. *Removal of cobalt and nickel ions by using silica and Fe_3O_4/HA/Ag magnetic nanoparticules.*

Optimization

The effects of pH value, sorption period, and particle mass on heavy metal removal were explored for adsorption optimization. pH values were calculated using 0.01 M HCI and 0.01 M NaOH solutions, including standard metal solution and nanoparticule modifications.To acquire the best pH value, solutions were changed to a pH range of 5 to 13.17. With a contact time of 30 minutes, the particle mass was 150 mg. The best removal was obtained under these conditions with a pH of approximately 10.3.

Table 1. *pH effect on removal of cobalt ve nickel with magnetic nanoparticules*

Removal %					
Fe_3O_4/Si			**Fe_3O_4/HA/Ag**		
pH	Nickel	Cobalt	pH	Nickel	Cobalt
5.33	33	36	5,43	66	53
9.7	64	56	8,48	71	54
10.6	81	73	11,08	78	62
11.21	87	88	11,76	68	56
11,46	81,5	87	12,83	64	50
13.17	75	85	13,11	55	49

Effect of magneticnanoparticle mass on the removal of nickel and cobalt

The effect of magnetic nanoparticle mass on the removal of nickel and cobalt has been investigated using six different mass values: 0,05, 0,08, 0,1, 0,12, 0,15, 0,18, and 0.2. For each value solutions were adjusted to pH 11,21 and 10,36 for nickel and cobalt respectively. Sorption time was determined as 10 minutes. By using 0,05 and 0.08 g magnetic nonoparticle mass for the metal ions, the best removal percentages were obtained.

Table 2. Effect of magneticnanoparticle mass on the removal of nickel and cobalt

	Removal %	
	Fe_3O_4/Si	**Fe_3O_4/HA/Ag**

Amount of magnetic nanoparticul (g)	Nickel	Cobalt	Nickel	Cobalt
0,05	89,4	89,7	85	71
0,08	89,3	89,0	80	77
0,12	89,2	91,0	77	68
0,15	88,0	88,0	73	66
0,18	87,5	89,5	76	60
0,2	85,2	84,0	71	46

Effect of contact time on the removal of nickel and cobalt

The effect of contact time on the removal of nickel and cobalt has been investigated using eight different contact times: 1, 3, 5, 10, 20, 60, 80 and 100 minutes at pH 11 and with 100 mg of magnetic nanoparticulate.

Table 3. Effect of contact time on the removal of nickel and cobalt

Contact time (minute)	Fe_3O_4/Si		Fe_3O_4/HA/Ag	
	Removal %		Removal %	
	Nickel	Cobalt	Nickel	Cobalt
1	92	92,30	69	65
3	91,5	91,8	75	76,0
5	93,6	90,7	86	31,0
10	93,6	92,3	75	28,0
20	88,3	91,0	73	38,0
60	88,8	89,0	56	51,0
80	84,0	85,0	55	40,0
100	81,8	83,0	48	39,0

Conclusion

The purpose of this study was to investigate the efficiency of heavy metal removal from environmental samples using the synthesis of Fe3O4 magnetic nanoparticles modified with silica gel and humic acid. The co-precipitation method was used to develop nanoparticles. Synthesized Fe_3O_4/HA/Ag and Fe_3O_4/silica multifunctional nanoparticles were applied as effective adsorbent for

separation and preconcentration of trace nicel and cobalt. Heavy metals were separated using magnetic nanoparticles synthesized using the reduction/adsorption method. With this method, economical, environmentally friendly, and efficient work has been carried out. Dehydration of iron (II, III) hydroxides with the Schikorr reaction resulted in more stable iron (II, III) oxide (Fe_3O_4) synthesis. In order to examine the relationship between the amount of nickel and cobalt ions adsorbed by the synthesized nanoparticle and the sample pH, the nanoparticle amount and adsorption time were kept constant, and the adsorption efficiency of metal ions at variable pH values was investigated. Likewise, the effect of the nanoparticle amount and adsorption time on the adsorption of metal ions were investigated separately. In the adsorption of nickel metal with Fe_3O_4 modified with silica gel, 93.60% efficiency was reached with pH:11, 0.15g adsorbent amount and adsorption time of 5 min -10 min. In the adsorption of nickel metal with Fe_3O_4 modified with humic acid, 86.0% efficiency was reached with pH:11 and an adsorption time of 5 minutes with a 0.1 g adsorbent amount. The magnetic nanoparticle modified with humic acid and silica gel is environmentally friendly as it has no negative impact on the environment. The synthesis technique is simple and inexpensive.

Additionally, toxic metals could be easily recovered from water utilizing magnetic separations made with synthetic magnetic nanoparticles, potentially lowering water treatment costs.The magnetic nanoparticles that were created are expected to have a wide range of applications in the removal of heavy metals from various waters. The synthesis was produced by dehydrating iron(II) and iron(III) hydroxides with the Schikorr reaction under optimal conditions (pH:10.5, 50 mg particle, and 10 min contact time). The mean removal percentage of nickel and cobalt was determined to be 92.54% and 90%, respectively, with Fe_3O_4/silica. Using the optimal settings (pH:10.5, 50 mg particle, and 10 min contact time), the mean removal percentage of nickel and cobalt with Fe_3O_4/HA/Ag was determined to be 92.54% and 90%, respectively. Heavy metal

determination study was carried out with proposed UV-VIS spectrophotometric method.

The results demonstrate that in terms of magnetic nanoparticle mass and contact duration, Fe_3O_4/silica was more effective than Fe_3O_4/HA/Ag for the separation and preconcentration of trace heavy metals. Because very little contact time and a small amount of particles were employed to achieve the high removal percentages.

Acknowledgments We thank the Tubitak Scientific Research Projects of 2209-A University Students Research Projects Support for partial financial support. Graduate undergraduate students who supported this research we would like to express our gratitude to our students, Mervenur Başol and Beyza Aykurt.

References

Abdullah, N., Yusof, N., Lau, W. J., Jaafar, J., & Ismail, A. F. (2019). Recent trends of heavy metal removal from water/wastewater by membrane technologies. In *Journal of Industrial and Engineering Chemistry* (Vol. 76, pp. 17–38). Korean Society of Industrial Engineering Chemistry. https://doi.org/10.1016/j.jiec.2019.03.029

Aguilar-Arteaga, K., Rodriguez, J. A., & Barrado, E. (2010). Magnetic solids in analytical chemistry: A review. In *Analytica Chimica Acta* (Vol. 674, Issue 2, pp. 157–165). https://doi.org/10.1016/j.aca.2010.06.043

Ahmed, T., Noman, M., Manzoor, N., Shahid, M., Abdullah, M., Ali, L., Wang, G., Hashem, A., Al-Arjani, A. B. F., Alqarawi, A. A., Abd_Allah, E. F., & Li, B. (2021). Nanoparticle-based amelioration of drought stress and cadmium toxicity in rice via triggering the stress responsive genetic mechanisms and nutrient acquisition. *Ecotoxicology and Environmental Safety*, *209*. https://doi.org/10.1016/j.ecoenv.2020.111829

Ali, A., Shah, T., Ullah, R., Zhou, P., Guo, M., Ovais, M., Tan, Z., & Rui, Y. K. (2021). Review on Recent Progress in Magnetic Nanoparticles: Synthesis, Characterization, and Diverse Applications. In *Frontiers in Chemistry* (Vol. 9). Frontiers Media S.A. https://doi.org/10.3389/fchem.2021.629054

Andjelković, M., Van Camp, J., De Meulenaer, B., Depaemelaere, G., Socaciu, C., Verloo, M., & Verhe, R. (2006). Iron-chelation properties of phenolic acids bearing catechol and galloyl groups. *Food Chemistry*, *98*(1), 23–31. https://doi.org/10.1016/j.foodchem.2005.05.044

Begum, S., Yuhana, N. Y., Md Saleh, N., Kamarudin, N. H. N., & Sulong, A. B. (2021). Review of chitosan composite as a heavy metal adsorbent: Material preparation and properties. In

Carbohydrate Polymers (Vol. 259). Elsevier Ltd. https://doi.org/10.1016/j.carbpol.2021.117613

Binandeh, M. (2022). Performance of unique magnetic nanoparticles in biomedicine. In *European Journal of Medicinal Chemistry Reports* (Vol. 6). Elsevier Masson s.r.l. https://doi.org/10.1016/j.ejmcr.2022.100072

Carolin, C. F., Kumar, P. S., Saravanan, A., Joshiba, G. J., & Naushad, M. (2017). Efficient techniques for the removal of toxic heavy metals from aquatic environment: A review. In *Journal of Environmental Chemical Engineering* (Vol. 5, Issue 3, pp. 2782–2799). Elsevier Ltd. https://doi.org/10.1016/j.jece.2017.05.029

Chen, Q., Rong, S., Cen, Y., Xu, G., Xie, Z., Yang, J., Sun, Y., Hu, Q., & Wei, F. (2021a). A facile fluorescent sensor based on carbon dots and Fe3O4 nanoplates for the detection of hyaluronidase activity. *Sensors and Actuators, B: Chemical*, *346*. https://doi.org/10.1016/j.snb.2021.130434

Chen, Q., Rong, S., Cen, Y., Xu, G., Xie, Z., Yang, J., Sun, Y., Hu, Q., & Wei, F. (2021b). A facile fluorescent sensor based on carbon dots and Fe3O4 nanoplates for the detection of hyaluronidase activity. *Sensors and Actuators, B: Chemical*, *346*. https://doi.org/10.1016/j.snb.2021.130434

Chen, Q., Yao, Y., Li, X., Lu, J., Zhou, J., & Huang, Z. (2018). Comparison of heavy metal removals from aqueous solutions by chemical precipitation and characteristics of precipitates. *Journal of Water Process Engineering*, *26*, 289–300. https://doi.org/10.1016/j.jwpe.2018.11.003

Dąbrowski, A., Hubicki, Z., Podkościelny, P., & Robens, E. (2004). Selective removal of the heavy metal ions from waters and industrial wastewaters by ion-exchange method. In *Chemosphere* (Vol. 56, Issue 2, pp. 91–106). Elsevier Ltd. https://doi.org/10.1016/j.chemosphere.2004.03.006

Donga, C., Mishra, S. B., Abd-El-Aziz, A. S., & Mishra, A. K. (2021). Advances in Graphene-Based Magnetic and Graphene-Based/TiO2 Nanoparticles in the Removal of Heavy Metals and Organic Pollutants from Industrial Wastewater. *Journal of Inorganic and Organometallic Polymers and Materials*, *31*(2), 463–480. https://doi.org/10.1007/s10904-020-01679-3

Durairaj, S., Sivakumar, D., Shankar, D., Gomathi, V., & Nandakumaar, A. (2014). Application of electro-dialysis on removal of heavy metals. *Poll Res*, *33*(3), 627–631. https://www.researchgate.net/publication/287762453

Gao, X., Guo, C., Hao, J., Zhao, Z., Long, H., & Li, M. (2020). Adsorption of heavy metal ions by sodium alginate based adsorbent-a review and new perspectives. In *International Journal of Biological Macromolecules* (Vol. 164, pp. 4423–4434). Elsevier B.V. https://doi.org/10.1016/j.ijbiomac.2020.09.046

Gong, P., Li, H., He, X., Wang, K., Hu, J., Tan, W., Zhang, S., & Yang, X. (2007). Preparation and antibacterial activity of Fe3O4@Ag nanoparticles. *Nanotechnology*, *18*(28). https://doi.org/10.1088/0957-4484/18/28/285604

Ishikawa\, T., Kondo\, Y., Yasukawa, A., & Kandori, K. (1998). Formation of magnetite in the presence of ferric oxyhydroxides. In *Corrosion Science ,39(6), 1239-1251*).

Liu, J. F., Zhao, Z. S., & Jiang, G. Bin. (2008). Coating Fe3O4 magnetic nanoparticles with humic acid for high efficient removal of heavy metals in water. *Environmental Science and Technology*, *42*(18), 6949–6954. https://doi.org/10.1021/es800924c

Mehmood, A., Saleem Ahmed Khan, F., Mujawar Mubarak, N., Hua Tan, Y., Rao Karri, R., Khalid, M., Walvekar, R., Chan Abdullah, E., Nizamuddin, S., & Ali Mazari, S. (2021). *Magnetic nanocomposites for sustainable water purification-a comprehensive review*. https://doi.org/10.1007/s11356-021-12589-3/Published

Peña-Méndez, E. M., Havel, J., & Patočka, J. (2005). Humic substances-compounds of still unknown structure: applications in agriculture, industry, environment, and biomedicine. *J. Appl. Biomed*, *3*, 13–24.

Saberi, D., Hashemi, H., Ghanaatzadeh, N., Moghadam, M., & Niknam, K. (2020). Ruthenium/dendrimer complex immobilized on silica-functionalized magnetite nanoparticles catalyzed oxidation of stilbenes to benzil derivatives at room temperature. *Applied Organometallic Chemistry*, *34*(4). https://doi.org/10.1002/aoc.5563

Shan, X., Zhang, L., Ye, H., Shao, J., Shi, Y., Tan, S., Su, K., Zhang, L., & Cao, C. (2022). Magnetic solid phase extraction of lead ion from water samples with humic acid modified magnetic nanoparticles prior to its fame atomic absorption spectrometric detection. *Microchemical Journal*, *179*. https://doi.org/10.1016/j.microc.2022.107417

Song, J., Kong, H., & Jang, J. (2011). Adsorption of heavy metal ions from aqueous solution by polyrhodanine-encapsulated magnetic nanoparticles. *Journal of Colloid and Interface Science*, *359*(2), 505–511. https://doi.org/10.1016/j.jcis.2011.04.034

Suhas, Gupta, V. K., Carrott, P. J. M., Singh, R., Chaudhary, M., & Kushwaha, S. (2016). Cellulose: A review as natural, modified and activated carbon adsorbent. In *Bioresource Technology* (Vol. 216, pp. 1066–1076). Elsevier Ltd. https://doi.org/10.1016/j.biortech.2016.05.106

Suo, L., Dong, X., Gao, X., Xu, J., Huang, Z., Ye, J., Lu, X., & Zhao, L. (2019). Silica-coated magnetic graphene oxide nanocomposite based magnetic solid phase extraction of trace amounts of heavy metals in water samples prior to determination by inductively coupled plasma mass spectrometry. *Microchemical Journal*, *149*. https://doi.org/10.1016/j.microc.2019.104039

Topuz, B., & Macit, M. (2011). Solid phase extraction and preconcentration of Cu(II), Pb(II), and Ni(II) in environmental samples on chemically modified Amberlite XAD-4 with a proper

Schiff base. *Environmental Monitoring and Assessment*, *173*(1–4), 709–722. https://doi.org/10.1007/s10661-010-1417-4

Verma, R., & Dwivedi, P. (2013). Heavy metal water pollution-A case study. *Science and Technology*, *5*(5), 98–99. http://recent-science.com/

Wang, H., Kang, J., Liu, H., & Qu, J. (2009). Preparation of organically functionalized silica gel as adsorbent for copper ion adsorption. *Journal of Environmental Sciences*, *21*(11), 1473–1479. https://doi.org/10.1016/S1001-0742(08)62442-0

Wu, W., He, Q., & Jiang, C. (2008). Magnetic iron oxide nanoparticles: Synthesis and surface functionalization strategies. *Nanoscale Research Letters*, *3*(11), 397–415. https://doi.org/10.1007/s11671-008-9174-9

Zeng, H., & Sun, S. (2008). Syntheses, properties, and potential applications of multicomponent magnetic nanoparticles. In *Advanced Functional Materials* (Vol. 18, Issue 3, pp. 391–400). https://doi.org/10.1002/adfm.200701211

CHAPTER II

Fundamental Components of Solid Oxide Fuel Cells

Fatma AYDIN ÜNAL[1]

Introduction

The rapid increase in the world population and the parallel increase in energy demand have directed researchers to renewable energy sources (Van Ruijven, De Cian & Sue Wing, 2019; Sadigov, 2022). Of these energy sources, fuel cells are one of the most alluring energy conversion systems as they present high performance and low pollution (Unal & et al., 2015). Fuel cells draw attention with their advantages such as quiet operation, cleanness, efficiency, sustainability, and noiselessness. Another advantage of fuel cells is decentralized power generation and possible applications in mobile devices (Demir & Aydin, 2012). A fuel cell is an electrochemical

[1] Asst. Prof. Alanya Alaaddin Keykubat University, Faculty of Rafet Kayış Engineering, Department of Metallurgical and Materials Engineering, Antalya

appliance that can transform the chemical energy of a fuel and an oxidizer into heat and electrical energy (Scherer, 2012; Bakal & et al., 2014). In this respect, Solid oxide fuel cells(SOFCs) have been of primary importance among different types of fuel cells. SOFCs are technologies that are attracting more attention in the modern era due to optimum power generation with sufficient electrical efficiency for household appliances and automobiles. SOFCs are considered idealistic for future clean energy generation (Aydin, Demir & Mat, 2014). SOFC technology is not limited to conventional heat engines that accept leakage, lubrication, and heat loss issues (Hussain & Yangping, 2020). In this section, information about the structure, working principle, and components of the SOFC is given.

Structure and working principle of SOFC

A fuel cell typically consists of an anode, a cathode, and an electrolyte (Dwivedi, 2020). In SOFC, oxygen or air is sent to the flow channels on the cathode side and spreads to the flow channels where it becomes an O^{-2} ion. At the same time, hydrogen is sent to the flow channels on the anode side as fuel. The ceramic electrolyte only allows the oxygen ion to pass to the anode side. After the oxygen ion passes to the anode side, electrons are released as a result of the electrochemical reaction occurring in the cell. The exposed electrodes are collected with the help of current collectors and electrical energy is produced by the movement of electrons from the anode to the cathode (Figure 1). The electrons finally reach the cathode and continue the process (Kalra, Garg & Kumar, 2015; Golkhatmi, Asghar & Lund, 2022). The reactions occurring in the anode, cathode, and total cell in SOFC are as follows (Mudasir & et al., 2023; Yatoo & et al., 2023).

Cathode Reaction : $O_2(g) + 4e^- \rightarrow 2O^{2-}$

Anode Reaction: $2H_2(g) + 2O^{2-} \rightarrow 2H_2O(g) + 4e^-$

General Reaction: $2H_2(g) + O_2(g) \rightarrow 2H_2O(g)$

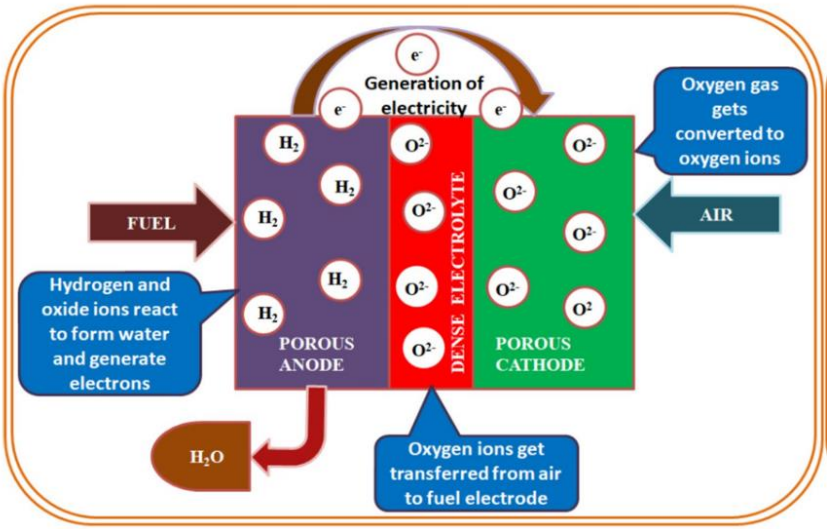

Figure 1. Schematic diagram of SOFC (Hussain & Yangping, 2020)

Components of SOFC

A typical SOFC cell; the Membrane electrode group (MEG) consists of a combination of anode, cathode, and electrolyte (Kee & et al., 2008; Dwivedi, 2020). The MEG is given visually in Figure 2.

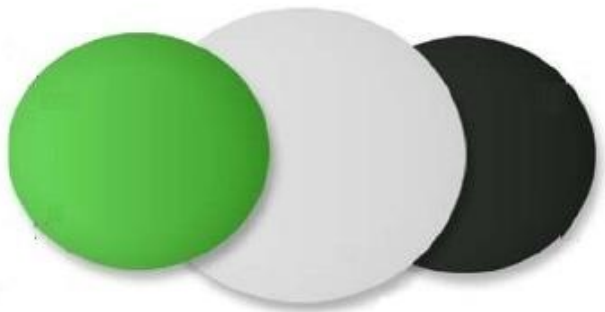

Figure 2. MEG groups (https://www.azom.com/equipment-details.aspx?EquipID=3946)

The basic components of SOFC are displayed in Figure 3.

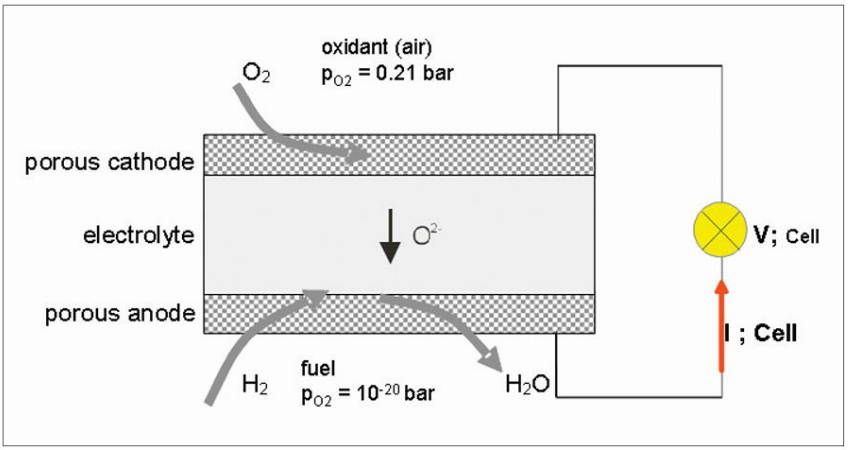

Figure 3. Schematic of a SOFC element with anode, cathode, and electrolyte (Gauckler & et al., 2004)

Membrane electrode groups can be combined to achieve higher power. The solid electrolyte is gas permeable and carries only oxygen ions between the cathode and the anode, filling the gap. While the oxidation of the fuel takes place at the anode, which is one of the two electrodes, the reduction of oxygen occurs at the cathode. These reactions occur at the interface of the electrolyte and the electrodes. A typical SOFC MEG; consists of a YSZ (yttria-stabilized zirconia) electrolyte, NiO-YSZ (nickel oxide- yttria-stabilized zirconia) anode, and LSM-YSZ (lanthanum strontium manganite-yttria-stabilized zirconia) cathode (Gauckler & et al., 2004; Hao & et al., 2017; Dwivedi, 2020; Shahsavari & et al., 2022; Mudasir & et al., 2023)

Electrolyte materials

Yttria (Y_2O_3) stabilized with YSZ or zirconia (ZrO_2) is generally used as the material for SOFC (Hussain & Yangping, 2020). Temperatures above 850°C are usually required for operation.

Due to the high temperature, temperature-resistant material is required.

Electrolyte materials should have the following properties (Hussain & Yangping 2020; Pigłowska & et al., 2021; Zaman & Hatzell, 2022):

1. The electrolyte should have high ion conductivity.

2. Solid electrolytes should have low electronic conductivity.

3. The solid and dense electrolyte between the two electrodes is essentially a ceramic material with ion permeability.

4. The mechanical strength of the electrolyte must be high enough.

5. The thermal stability of the electrolyte must be good so that it can distribute thermal stresses evenly.

6. Raw materials should not be costly and the processing method should be cost-effective.

Below is a graph of the ionic conductivity of the most commonly used electrolyte materials for SOFCs (Figure 4).

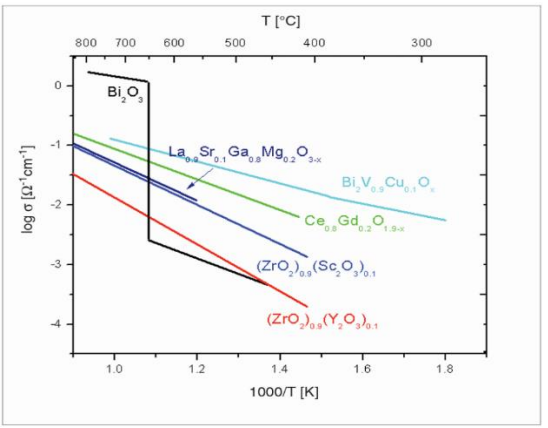

Figure 4. Ionic conductivities of different electrolyte materials (Gauckler & et al., 2004)

Anode materials

The anode is an important component in SOFC technology due to the microstructure that can give the best electrochemical performance. As it is known, the fuel oxidation reaction takes place at the anode. These reactions take place in regions called the anode triple-phase region where the fuel (pore), ion-conducting phase, and electronic-conducting phase coexist. Therefore, cell performance is directly dependent on the number and length of the triple-phase regions (Suzuki & et al., 2009; Dwivedi, 2020). In this context, both SOFC anode and SOFC cathode materials have a composite structure that includes an ion-conducting (usually electrolyte) phase as well as an electronically conductive catalyst material. In this way, electrochemical reactions occurring in the electrodes can take place in the entire electrode volume, and significant improvements in cell performance can be achieved due to increased electrochemical reaction zones. The anode material to be used should have a high degree of electronic conductivity, good chemical stability, and thermal compatibility with other system components. At the same time, the anode material must have sufficient porosity to conduct fuel effectively and high electrocatalytic efficiency for oxidation reactions. When all these factors are combined, it is seen that the oxidation reaction occurring at the anode will minimize the polarization losses and form high-performance SOFCs (Dwivedi, 2020; Develos-Bagarinao & et al., 2021).

Cathode materials

The cathode is an important component of the SOFC, which has the porosity that allows the passage of oxygen and converts the oxygen into ions by reducing it (Tahir & et al., 2022). Similar to the anode, this reduction reaction; develops in specific regions where oxygen ions, electrons, and oxygen molecules meet. These regions are called the cathode triple phase region, and similar to the anode, the number and length of these regions directly affect cell performance (Wang & et al., 2022). Table 1 gives the properties of some SOFC cathode materials.

Table I. Properties of some relevant SOFC cathode materials (Mudasir et al., 2023)

Material composition	Total conductivity (S/cm)	Ionic conductivity (S/cm)	TEC ($\times 10^{-6}$ °C^{-1})
$LaMnO_3$	71 (700°C)	–	9.5–10.75 (25–1000 °C)
$La_{0.8}Sr_{0.2}MnO_{3-\delta}$	150(500°C)	4.2×10^{-10} (750°C)	11.8 (30–1000 °C)
$La_{0.6}Sr_{0.4}MnO_{3-\delta}$	125 (700°C)	–	11.7–12.2 (25–1000 °C)
$La_{0.6}Sr_{0.4}CoO_{3-\delta}$	1084 (1000°C)	0.22 (800°C)	20.5 (30–1000°C)
$La_{0.8}Sr_{0.2}CoO_{3-\delta}$	1291 (1000°C)	4.9×10^{-4} (750°C)	19.7 (100–900°C)
$La_{0.6}Sr_{0.4}Co_{0.2}Fe_{0.8}O_{3-\delta}$	320 (700°C)	8×10^{-3} (800°C)	15.3 (100–600°C)
$La_2NiO_{4+\delta}$	85 (700°C)	4×10^{-2} (800°C)	13.8 (75–900°C)
$La_4NiO_{10\pm\delta}$	87 (800°C)	–	11.5 (250–800°C)
$Pr_4NiO_{10\pm\delta}$	90 (600°C)	–	12 (25–1000°C)

The properties that should be in a typical SOFC cathode material are listed below (Sun, Hui & Roller, 2010; Zhang & Hu, 2023):

1. It has both ionic and electronic conductivity.
2. Coefficient of thermal expansion to be compatible with other system components such as electrolyte, sealing element, and interconnector to avoid breakage and delamination during operation of SOFCs
3. Sufficient porosity to allow diffusion of oxygen to the cathode
4. High catalytic activity
5. It should not enter into a chemical reaction with other system components.

Conclusion

SOFCs are of great interest worldwide due to their fuel flexibility and real power generation devices with low environmental effects. However, there are some problems with the development of SOFCs. One of the basic difficulties of SOFCs is the high operating temperature, which leads to a rapid rate of degradation in cell performance. Due to the lower operating temperature of SOFCs and

the expensiveness of the materials used, the search for alternative materials for different components continues. In this chapter article, SOFC cell components and properties such as electrolyte, cathode, and anode are mentioned. Further development of SOFC technology is expected with the discovery of new materials and the development of already-known materials.

References

Aydin, F., Demir, I., & Mat, M. D. (2014). Effect of grinding time of synthesized gadolinium doped ceria (GDC_{10}) powders on the performance of solid oxide fuel cell. *Engineering Science and Technology, an International Journal,* 17 (1), 25-29. https://doi.org/10.1016/j.jestch.2014.02.003

Azo Materials (2023) Advanced-Electrolyte Planar Solid Oxide Fuel Cell (SOFC) – The NextCell (25/10/2023 tarihinde https://www.azom.com/equipment-details.aspx?EquipID=3946 adresinden ulaşılmıştır).

Bakal, A., Aydın, F., Mat, M. D., Ibrahimoğlu, B., & Pamuk, İ. (2014). A novel two-part interconnector for solid oxide fuel cells. International *Journal of Energy Research,* 38 (14), 1835-1842. https://doi.org/10.1002/er.3192

Demir, I., & Aydin, F. (2012). A novel method for GDC recovery during solid oxide fuel cell manufacturing. *Fuel Cells,* 12 (6), 1095-1098. https://doi.org/10.1002/fuce.201200029

Develos-Bagarinao, K., Ishiyama, T., Kishimoto, H., Shimada, H., & Yamaji, K. (2021). Nanoengineering of cathode layers for solid oxide fuel cells to achieve superior power densities. *Nature Communications*, 12 (1), 3979. https://doi.org/10.1038/s41467-021-24255-w

Dwivedi, S. (2020). Solid oxide fuel cell: Materials for anode, cathode and electrolyte. *International Journal of Hydrogen Energy,* 45 (44), 23988-24013. https://doi.org/10.1016/j.ijhydene.2019.11.234

Gauckler, L. J., Beckel, D., Buergler, B. E., Jud, E., Muecke, U. P., Prestat, M., ... & Richter, J. (2004). Solid oxide fuel cells: systems and materials. *Chimia,* 58 (12), 837-837. https://doi.org/10.2533/000942904777677047

Golkhatmi, S. Z., Asghar, M. I., & Lund, P. D. (2022). A review on solid oxide fuel cell durability: Latest progress,

mechanisms, and study tools. *Renewable and Sustainable Energy Reviews,* 161, 112339. https://doi.org/10.1016/j.rser.2022.112339

Hao, S. J., Wang, C., Liu, T. L., Mao, Z. M., Mao, Z. Q., & Wang, J. L. (2017). Fabrication of nanoscale yttria stabilized zirconia for solid oxide fuel cell. *International Journal of Hydrogen Energy,* 42 (50), 29949-29959. https://doi.org/10.1016/j.ijhydene.2017.08.143

Hussain, S., & Yangping, L. (2020). Review of solid oxide fuel cell materials: Cathode, anode, and electrolyte. *Energy Transitions,* 4:113–126. https://doi.org/10.1007/s41825-020-00029-8

Kalra, P., Garg, R., & Kumar, A. (2015). Modelling of a High temperature Solid oxide Fuel cell. *J. Energy Technol. Policy,* 5, 76-84. https://api.core.ac.uk/oai/oai:ojs.localhost:article/20159

Kee, R. J., Zhu, H., Sukeshini, A. M., & Jackson, G. S. (2008). Solid oxide fuel cells: operating principles, current challenges, and the role of syngas. *Combustion Science and Technology*, 180 (6), 1207-1244. https://doi.org/10.1080/00102200801963458

Mudasir A. Yatoo, Faiza Habib, Akhtar Hussain Malik, Mohsin Jahan Qazi, Sharique Ahmad, Mohd Azhardin Ganayee, Zubair Ahmad. (2023). Solid-oxide fuel cells: A critical review of materials for cell components, *MRS Communications,*13:378–384. https://doi.org/10.26434/chemrxiv-2023-txrf8

Pigłowska, M., Kurc, B., Galiński, M., Fuć, P., Kamińska, M., Szymlet, N., & Daszkiewicz, P. (2021). Challenges for Safe Electrolytes Applied in Lithium-Ion Cells—A Review. *Materials*, 14 (22), 6783. https://doi.org/10.3390/ma14226783

Sadigov, R. (2022). Rapid growth of the world population and its socioeconomic results. *The Scientific World Journal, 8110229, 1-8.* https://doi.org/10.1155/2022/8110229

Scherer, G.G. (2012). Fuel cell types and their electrochemistry . In: Meyers, R.A. (eds) Encyclopedia of Sustainability Science and Technology. *Springer, New York, NY*, pp. 97-119.

https://doi.org/10.1007/978-1-4419-0851-3_132

Shahsavari, E., Jafari, M., Yadollahi Farsani, F., Ekraminezhad, N., Ranjbar, M., & Salamati, H. (2022). Fabrication of YSZ electrolyte layers using thermally assisted slurry spin coating method for IT-SOFC application. *Monatshefte für Chemie-Chemical Monthly*, 153 (2), 183-192. https://doi.org/10.1007/s00706-021-02884-7

Sun, C., Hui, R., & Roller, J. (2010). Cathode materials for solid oxide fuel cells: a review. *Journal of Solid State Electrochemistry*, 14, 1125-1144. https://doi.org/10.1007/s10008-009-0932-0

Suzuki, T., Hasan, Z., Funahashi, Y., Yamaguchi, T., Fujishiro, Y., & Awano, M. (2009). Impact of anode microstructure on solid oxide fuel cells. *Science*, 325 (5942), 852-855. https://www.science.org/doi/10.1126/science.1176404

Tahir, N. N. M., Baharuddin, N. A., Samat, A. A., Osman, N., & Somalu, M. R. (2022). A review on cathode materials for conventional and proton-conducting solid oxide fuel cells. *Journal of Alloys and Compounds*, 894, 162458. https://doi.org/10.1016/j.jallcom.2021.162458

Unal, F. A., Mat, M. D., Demir, I., Kaplan, Y., & Veziroglu, N. (2015). Application of a coating mixture for solid oxide fuel cell interconnects. *International Journal of Hydrogen Energy*, 40 (24), 7689-7693. https://doi.org/10.1016/j.ijhydene.2015.03.031

Van Ruijven, B. J., De Cian, E., & Sue Wing, I. (2019). Amplification of future energy demand growth due to climate change. *Nature Communications*, 10 (1), 2762. https://doi.org/10.1038/s41467-019-10399-3

Wang, M., Su, C., Zhu, Z., Wang, H., & Ge, L. (2022). Composite cathodes for protonic ceramic fuel cells: Rationales and materials. *Composites Part B: Engineering*, 238, 109881. https://doi.org/10.1016/j.compositesb.2022.109881

Yatoo, M. A., Habib, F., Malik, A. H., Qazi, M. J., Ahmad, S., Ganayee, M. A., & Ahmad, Z. (2023). A Critical Review on Materials for Solid Oxide Fuel Cell Components. *Materials Chemistry*. https://doi.org/10.26434/chemrxiv-2023-txrf8

Zaman, W., & Hatzell, K. B. (2022). Processing and manufacturing of next generation lithium-based all solid-state batteries. *Current Opinion in Solid State and Materials Science*, 26 (4), 101003. https://doi.org/10.1016/j.cossms.2022.101003

Zhang, W., & Hu, Y. H. (2023). Recent progress in design and fabrication of SOFC cathodes for efficient catalytic oxygen reduction. *Catalysis Today*, 409, 71-86. https://doi.org/10.1016/j.cattod.2022.05.008

CHAPTER III

Computational Investigation for Lone-Pair Interactions with Transition Metals: The Complexes Formed by Cr^+, Mn^+, Fe^+, Co^+, Ni^+, Cu^+, and Zn^+ Binding with Aza-Cryptands

Abdurrahman ATALAY[1]
Emel EKİNCİ[2]
Harun ÇİFTÇİ[3]

Introduction

Noncovalent interactions (NCIs) are often the dominant kind of intermolecular interactions in processes including drug binding, protein folding, and nanomaterial self-assembly (Mahadevi &

[1] Asst. Prof., Avrasya University, Department Of Nutrition And Dietetics, Orcıd: 0000-0002-9018-7264
[2] Lecturer, Çankırı Karatekin University, Department of Chemistry, Orcıd: 0000-0003-2323-2747
[3] Prof. Dr., Kırşehir Ahi Evran University, Department of Medical Biochemistry, Orcıd: 0000-0002-3210-5566 - Prof. Dr., Çankırı Karatekin University, Institute of Science, Department of Chemistry, Orcıd: 0000-0002-3210

Sastry, 2013, 2016; Müller-Dethlefs & Hobza, 2000; Saha & Sastry, 2015; Schug & Lindner, 2005; Wheeler & Bloom, 2014). They cover a broad spectrum of weak interactions, such as hydrogen bonding, cation–π, and π–π interactions, anion–π, halogen bond, and metal ion–lone pair (Kumar vd., 2021; Mahadevi & Sastry, 2013, 2016; Müller-Dethlefs & Hobza, 2000; Saha & Sastry, 2015; Schug & Lindner, 2005; Sharma vd., 2015, 2016; Wheeler & Bloom, 2014). Because of their unique properties, NCIs also have a lot of potential applications in supramolecular chemistry, biochemistry, pharmaceutics, and materials science research (Ayinla vd., 2023; Jena vd., 2022; Ravva vd., 2017; Schug & Lindner, 2005). This makes it easier to create functional materials and develop new technologies. Because experimental measurements of NCIs are very difficult, particularly for big molecules that include a significant number of NCIs, efficient tools—highly precise first-principles approaches, in particular—are frequently used (Mahadevi & Sastry, 2013, 2016; Müller-Dethlefs & Hobza, 2000; Saha & Sastry, 2015; Schug & Lindner, 2005; Wheeler & Bloom, 2014).

Cryptands are large, bicyclic or polycyclic structures that have the ability to encapsulate ions like a cage and form complexes with them (Alibrandi vd., 2015; Bharadwaj, 2017; Dietrich, 1996; Gupta vd., 2019; Montà-González vd., 2022; Sarkar vd., 2003; Taschner vd., 2020; Zhang vd., 2014). An essential family of chemical compounds is macrocyclic cryptands containing amine groups, namely aza-cryptands (Bharadwaj, 2017; Gupta vd., 2019; Sarkar vd., 2003; Taschner vd., 2020). These compounds can combine with various transition and main group metal ions to produce inclusion complexes. By taking advantage of the tendency of the cryptand to form metal complexes, the structure and energetics of the complexes formed by the 3^6adamanzane (3^6adz) aza-cryptand (**Figure 1**) with transition metal (M) cations (Cr^+, Mn^+, Fe^+, Co^+, Ni^+, Cu^+, and Zn^+) were computationally investigated.

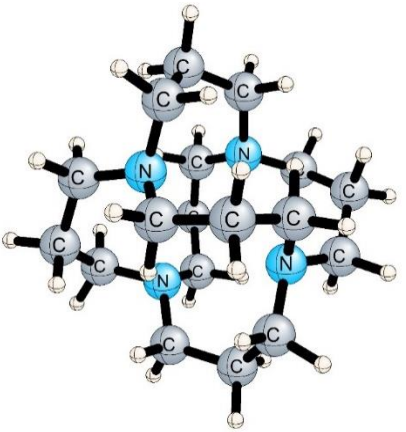

Figure 1. Optimized Structure of 36adz Aza-Cryptand at the ωB97XD/6-31+G(d,p) level.

Computational Details

Geometry optimization and harmonic vibrational frequency computations were performed by employing the density functional theory (DFT) and the ωB97XD functional (Chai & Head-Gordon, 2008) for the complexes formed by 3^6adz with M cations such as Cr^+, Mn^+, Fe^+, Co^+, Ni^+, Cu^+, and Zn^+. In this regard, the 6-31+G(d,p) basis set (Ditchfield vd., 2003; Hehre vd., 2003) was utilized for all complexes. To determine the structures with the lowest energy for 3^6adz−M^+ complexes, doublet, quartet, and sextet spin states of 3^6adz−Cr^+, 3^6adz−Fe^+, 3^6adz−Ni^+, 3^6adz−Zn^+ complexes, and singlet, triplet, quintet, and septet spin states of 3^6adz−Co^+ and 3^6adz−Cu^+, and 3^6adz−Mn^+ complexes were optimized at the ωB97XD/6-31+G(d,p) level. All interaction energies for all complexes studied were computed with the counterpoise procedure (Boys & Bernardi, 1970) at the ωB97XD/6-311++G(d,p) level. In addition, the Douglas-Kroll-Hess (DKH) approximation was used to account for scalar relativistic effects on the complexes considered.

Results and Discussion

The optimized geometries of all complexes studied at the ωB97XD/6-31+G(d,p) level is illustrated in **Figure 2**. The structures with the lowest energy are sextet for 3^6adz−Cr^+ and 3^6adz−Fe^+, septet for 3^6adz−Mn^+, triplet for 3^6adz−Co^+, doublet state for 3^6adz−Ni^+ and 3^6adz−Cu^+, and 3^6adz−Zn^+ complexes at the ωB97XD/6-31+G(d,p) level. The 3^6adz is recognized as an S_4-symmetric structure containing the four lone pairs of the N atom oriented toward the center of the cage. The M^+−N1 and M^+−N2 distances are 2.104−2.104 Å, 2.078−2.046 Å, 2.021−2.021 Å, 2.038−2.020 Å, 2.015−2.015 Å, 2.020−2.020 Å, and 2.004−1.986 Å for the 3^6adz−M^+ (M: Cr^+, Mn^+, Fe^+, Co^+, Ni^+, Cu^+, and Zn^+) complexes at their optimized geometries, respectively. This clearly shows that in the 3^6adz−Cr^+, Fe^+, Ni^+, and Cu^+ complexes studied the metal cations were symmetrically placed to the center of the 3^6adz to which they are attached, while in the 3^6adz−Mn^+, Co^+, and Zn^+ complexes metal cations were not symmetrically placed to it. The critical structural parameters for all 3^6adz−M^+ complexes are shown in **Table 1**. As seen in **Figure 2**, the 3^6adz−Cr^+, Fe^+, Ni^+, and Cu^+ complexes maintain the S_4 symmetry of 3^6adz, whereas the 3^6adz−Mn^+, Co^+, and Zn^+ complexes is lowered to C_1.

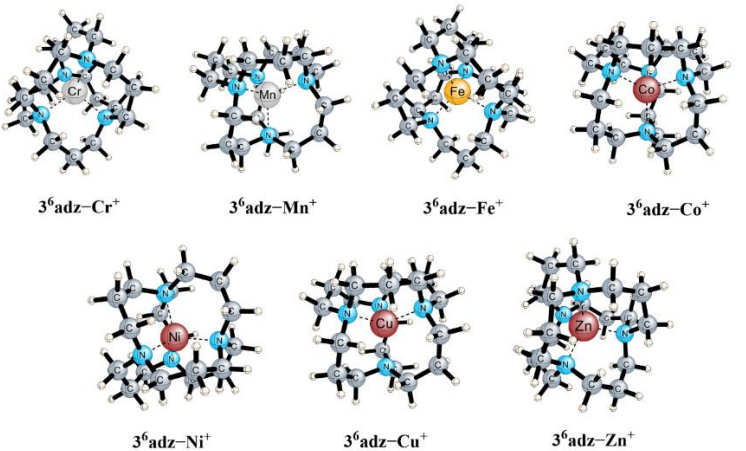

Figure 2. *The optimized geometries of the $3^6adz{-}M^+$ (M: Cr, Mn, Fe, Co, Ni, Cu and Zn) complexes at the ωB97XD/6-31+G(d,p) level.*

Table 1. *$M^+\cdots N1/N2$ Distances (in Å) at the ωB97XD/6-31+G(d,p) Level, Nonrelativistic Interaction Energies and Interaction Energies Including Relativistic Corrections (in kcal mol^{-1}) at the ωB97XD/6-311++G(d,p) Level for the $3^6adz{-}M^+$ (M: Cr, Mn, Fe, Co, Ni, Cu and Zn) Complexes Considered.*

	M···N1 Distance (Å)	M···N2 Distance (Å)	Non-relativistic IEs (kcal/mol)	IEs Including Relativistic Corrections (kcal/mol)
$3^6adz{-}Cr^+$	2.104	2.104	−108.5	−112.6
$3^6adz{-}Mn^+$	2.078	2.046	−73.3	−73.5
$3^6adz{-}Fe^+$	2.021	2.021	−92.4	−92.7
$3^6adz{-}Co^+$	2.038	2.020	−146.7	−152.4
$3^6adz{-}Ni^+$	2.015	2.015	−155.6	−162.0
$3^6adz{-}Cu^+$	2.020	2.020	−151.6	−158.4
$3^6adz{-}Zn^+$	2.004	1.986	−87.8	−89.0

Table 1 shows the computed nonrelativistic interaction energies (IE) for the 3^6adz−M^+ complexes considered at the ωB97XD/6-311++G(d,p) level. The computed nonrelativistic IE values for the 3^6adz−M^+ complexes are −108.5 kcal mol^{-1} for 3^6adz−Cr^+, −73.3 kcal mol^{-1} for 3^6adz−Mn^+, −92.4 kcal mol^{-1} for 3^6adz−Fe^+, −146.7 kcal mol^{-1} for 3^6adz−Co^+, −155.6 kcal mol^{-1} for 3^6adz−Ni^+, −151.6 kcal mol^{-1} for 3^6adz−Cu^+ and −87.8 kcal mol^{-1} for 3^6adz−Zn^+at the ωB97XD/6-311++G(d,p) level.

The computed IE values with relativistic corrections for the 3^6adz−M^+ complexes at the ωB97XD/6-311++G(d,p) level are reported in **Table 1**. The computed relativistic energy correction for interaction energy is −4.1 kcal mol^{-1} for 3^6adz−Cr^+, −0.2 kcal mol^{-1} for 3^6adz−Mn^+, −0.3 kcal mol^{-1} for 3^6adz−Fe^+, −5.7 kcal mol^{-1} for 3^6adz−Co^+, −6.4 kcal mol^{-1} for 3^6adz−Ni^+, −6.8 kcal mol^{-1} for 3^6adz−Cu^+ and −1.2 kcal mol^{-1} for 3^6adz−Zn^+ complex at the ωB97XD/6-311++G(d,p) level, indicating that these energy correction values are not negligible except for 3^6adz−Mn^+ and 3^6adz−Fe^+ complexes, and therefore they should take into account for an accurate description of the corresponding 3^6adz−M^+ complexes.

The computed IE values including relativistic energy correction for the 3^6adz−M^+ complexes are −112.6 kcal mol^{-1} for 3^6adz−Cr^+, −73.5 kcal mol^{-1} for 3^6adz−Mn^+, −92.7 kcal mol^{-1} for 3^6adz−Fe^+, −152.4 kcal mol^{-1} for 3^6adz−Co^+, −162.0 kcal mol^{-1} for 3^6adz−Ni^+, −158.4 kcal mol^{-1} for 3^6adz−Cu^+ and −89.0 kcal mol^{-1} for 3^6adz−Zn^+at the ωB97XD/6-311++G(d,p) level. The bigger negative value for the 3^6adz−Ni^+ complex indicates that it is more stable than the other complexes because it fits into the cage cavity more easily. Overall, the negative values demonstrate the stability of the all complexes considered.

Conclusion

In this study, we undertake an extensive study to elucidate the structures and interaction energies of the complexes formed by

transition metals, such as Cr^+, Mn^+, Fe^+, Co^+, Ni^+, Cu^+ and Zn^+, with 3^6adamanzane aza-cryptand employing DFT method and ωB97XD functional. At their optimized geometries of complexes studied, the 3^6adz−Cr^+, Fe^+, Ni^+, and Cu^+ complexes maintain the S_4 symmetry of 3^6adz, whereas the 3^6adz−Mn^+, Co^+, and Zn^+ complexes is lowered to C_1. The computed relativistic energy correction for interaction energy is −4.1, −0.2, −0.3, −5.7, −6.4, −6.8 and −1.2 kcal mol^{-1} for 3^6adz−Cr^+, Mn^+, Fe^+, Co^+, Ni^+, Cu^+ and Zn^+ complexes, respectively, at the ωB97XD/6-311++G(d,p) level, indicating that these energy correction values are not negligible except for 3^6adz−Mn^+ and 3^6adz−Fe^+ complexes. The computed IE values including relativistic energy correction for the 3^6adz−M^+ complexes are −112.6 kcal mol^{-1} for 3^6adz−Cr^+, −73.5 kcal mol^{-1} for 3^6adz−Mn^+, −92.7 kcal mol^{-1} for 3^6adz−Fe^+, −152.4 kcal mol^{-1} for 3^6adz−Co^+, −162.0 kcal mol^{-1} for 3^6adz−Ni^+, −158.4 kcal mol^{-1} for 3^6adz−Cu^+ and −89.0 kcal mol^{-1} for 3^6adz−Zn^+ at the ωB97XD/6-311++G(d,p) level.

References

Alibrandi, G., Amendola, V., Bergamaschi, G., Fabbrizzi, L., & Licchelli, M. (2015). Bistren cryptands and cryptates: Versatile receptors for anion inclusion and recognition in water. *Organic & Biomolecular Chemistry*, *13*(12), 3510-3524. https://doi.org/10.1039/C4OB02618G

Ayinla, R. T., Shiri, M., Song, B., Gangishetty, M., & Wang, K. (2023). The pivotal role of non-covalent interactions in single-molecule charge transport. *Materials Chemistry Frontiers*, *7*(17), 3524-3542. https://doi.org/10.1039/D3QM00210A

Bharadwaj, P. K. (2017). Metal ion binding by laterally non-symmetric macrobicyclic oxa–aza cryptands. *Dalton Transactions*, *46*(18), 5742-5775. https://doi.org/10.1039/C7DT00722A

Boys, S. F., & Bernardi, F. (1970). The calculation of small molecular interactions by the differences of separate total energies. Some procedures with reduced errors. *Molecular Physics*, *19*(4), 553-566. https://doi.org/10.1080/00268977000101561

Chai, J.-D., & Head-Gordon, M. (2008). Long-range corrected hybrid density functionals with damped atom–atom dispersion corrections. *Physical Chemistry Chemical Physics*, *10*(44), 6615-6620. https://doi.org/10.1039/B810189B

Dietrich, B. (1996). Cryptands. İçinde D. Parker (Ed.), *Macrocycle Synthesis: A Practical Approach* (s. 0). Oxford University Press. https://doi.org/10.1093/oso/9780198558415.003.0005

Ditchfield, R., Hehre, W. J., & Pople, J. A. (2003). Self-Consistent Molecular-Orbital Methods. IX. An Extended Gaussian-Type Basis for Molecular-Orbital Studies of Organic Molecules. *The Journal of Chemical Physics*, *54*(2), 724-728. https://doi.org/10.1063/1.1674902

Douglas, M., & Kroll, N. M. (1974). Quantum electrodynamical corrections to the fine structure of helium. *Annals of Physics*, *82*(1), 89-155. https://doi.org/10.1016/0003-4916(74)90333-9

Gupta, M., Tomar, K., Pandey, S. K., & Bharadwaj, P. K. (2019). Weak and Reversible Binding of Alkali Metal Ions (Na+/K+) by an Aza-Oxa Cryptand. *ChemistrySelect*, *4*(5), 1785-1788. https://doi.org/10.1002/slct.201803353

Hehre, W. J., Ditchfield, R., & Pople, J. A. (2003). Self—Consistent Molecular Orbital Methods. XII. Further Extensions of Gaussian—Type Basis Sets for Use in Molecular Orbital Studies of Organic Molecules. *The Journal of Chemical Physics*, *56*(5), 2257-2261. https://doi.org/10.1063/1.1677527

Hess, B. A. (1985). Applicability of the no-pair equation with free-particle projection operators to atomic and molecular structure calculations. *Physical Review A*, *32*(2), 756-763. https://doi.org/10.1103/PhysRevA.32.756

Hess, B. A. (1986). Relativistic electronic-structure calculations employing a two-component no-pair formalism with external-field projection operators. *Physical Review A*, *33*(6), 3742-3748. https://doi.org/10.1103/PhysRevA.33.3742

Jansen, G., & Hess, B. A. (1989). Revision of the Douglas-Kroll transformation. *Physical Review A*, *39*(11), 6016-6017. https://doi.org/10.1103/PhysRevA.39.6016

Jena, S., Dutta, J., Tulsiyan, K. D., Sahu, A. K., Choudhury, S. S., & Biswal, H. S. (2022). Noncovalent interactions in proteins and nucleic acids: Beyond hydrogen bonding and π-stacking. *Chemical Society Reviews*, *51*(11), 4261-4286. https://doi.org/10.1039/D2CS00133K

Kumar, N., Gaur, A. S., & Sastry, G. N. (2021). A perspective on the nature of cation-π interactions. *Journal of*

Chemical Sciences, *133*(4), 97. https://doi.org/10.1007/s12039-021-01959-6

Mahadevi, A. S., & Sastry, G. N. (2013). Cation−π Interaction: Its Role and Relevance in Chemistry, Biology, and Material Science. *Chemical Reviews*, *113*(3), 2100-2138. https://doi.org/10.1021/cr300222d

Mahadevi, A. S., & Sastry, G. N. (2016). Cooperativity in Noncovalent Interactions. *Chemical Reviews*, *116*(5), 2775-2825. https://doi.org/10.1021/cr500344e

Montà-González, G., Sancenón, F., Martínez-Máñez, R., & Martí-Centelles, V. (2022). Purely Covalent Molecular Cages and Containers for Guest Encapsulation. *Chemical Reviews*, *122*(16), 13636-13708. https://doi.org/10.1021/acs.chemrev.2c00198

Müller-Dethlefs, K., & Hobza, P. (2000). Noncovalent Interactions: A Challenge for Experiment and Theory. *Chemical Reviews*, *100*(1), 143-168. https://doi.org/10.1021/cr9900331

Ravva, M. K., Risko, C., & Brédas, J.-L. (2017). Chapter 9—Noncovalent Interactions in Organic Electronic Materials. İçinde A. Otero de la Roza & G. A. DiLabio (Ed.), *Non-Covalent Interactions in Quantum Chemistry and Physics* (ss. 277-302). Elsevier. https://doi.org/10.1016/B978-0-12-809835-6.00011-6

Saha, S., & Sastry, G. N. (2015). Cooperative or Anticooperative: How Noncovalent Interactions Influence Each Other. *The Journal of Physical Chemistry B*, *119*(34), 11121-11135. https://doi.org/10.1021/acs.jpcb.5b03005

Sarkar, B., Mukhopadhyay, P., & Bharadwaj, P. K. (2003). Laterally non-symmetric aza-cryptands: Synthesis, catalysis and derivatization to new receptors. *Coordination Chemistry Reviews*, *236*(1), 1-13. https://doi.org/10.1016/S0010-8545(02)00058-9

Schug, K. A., & Lindner, W. (2005). Noncovalent Binding between Guanidinium and Anionic Groups: Focus on Biological- and Synthetic-Based Arginine/Guanidinium Interactions with

Phosph[on]ate and Sulf[on]ate Residues. *Chemical Reviews*, *105*(1), 67-114. https://doi.org/10.1021/cr040603j

Sharma, B., Neela, Y. I., & Narahari Sastry, G. (2016). Structures and energetics of complexation of metal ions with ammonia, water, and benzene: A computational study. *Journal of Computational Chemistry*, *37*(11), 992-1004. https://doi.org/10.1002/jcc.24288

Sharma, B., Srivastava, H. K., Gayatri, G., & Sastry, G. N. (2015). Energy decomposition analysis of cation–π, metal ion–lone pair, hydrogen bonded, charge-assisted hydrogen bonded, and π–π interactions. *Journal of Computational Chemistry*, *36*(8), 529-538. https://doi.org/10.1002/jcc.23827

Taschner, I. S., Walker, T. L., M, S. C., Schrage, B. R., Ziegler, C. J., Gao, X., & Wheeler, S. E. (2020). Topomeric aza/thia cryptands: Synthesis and theoretical aspects of in/out isomerism using n-alkyl bridging. *Organic Chemistry Frontiers*, *7*(9), 1164-1176. https://doi.org/10.1039/D0QO00123F

Wheeler, S. E., & Bloom, J. W. G. (2014). Toward a More Complete Understanding of Noncovalent Interactions Involving Aromatic Rings. *The Journal of Physical Chemistry A*, *118*(32), 6133-6147. https://doi.org/10.1021/jp504415p

Zhang, M., Yan, X., Huang, F., Niu, Z., & Gibson, H. W. (2014). Stimuli-Responsive Host–Guest Systems Based on the Recognition of Cryptands by Organic Guests. *Accounts of Chemical Research*, *47*(7), 1995-2005. https://doi.org/10.1021/ar500046r

CHAPTER IV

Synthesis and characterization of a heterogeneous catalyst supported with mesoporous SBA-15 and investigation of its catalytic activity in asymmetric transfer hydrogen reactions in various aromatic ketones

Osman Tayyar ARLI[1]
Yaşar GÖK [2]
Halil Zeki GÖK [3]

Introductıon

Since the importance of stereoisomerism in various fields, especially in the pharmaceutical industry, has been understood, studies on the synthesis of enantiomerically pure chemicals have come to the fore. One of the important methods in the synthesis of

[1] Doctorand, Burdur Mehmet Akif Ersoy University, Department of Chemistry, Orcid: orcid.org/0000-0001-7619-2668
[2] Prof.Dr., Burdur Mehmet Akif Ersoy University, Department of Chemistry, Orcid: orcid.org/0000-0003-3134-7560
[3] Prof.Dr., Burdur Mehmet Akif Ersoy University, Department of Chemistry, Orcid: orcid.org/0000-0001-7641-2683

enantiomerically pure compounds is enantioselective catalysts. (Gök, Aykut, & Gök, 2020) For example, enantioselective catalysts used in asymmetric hydrogen transfer reactions involving the transformation of carbonyl compounds into alcohols, which have an important place in organic chemistry, generally catalyze the reactions by forming a complex with a chiral ligand carrying asymmetric information and transition metals such as iron, cobalt and ruthenium (Foubelo, Nájera, & Yus, 2015). Although these catalysts stand out with their advantages such as easy processability and usability in low quantities, they also have some disadvantages in terms of environmental damage, recyclability and reusability in industrial processes. In order to cope these disadvantages, studies on the immobilization of various catalysts on solid support materials are being carried out intensively (Ghorbani-Choghamarani, Tahmasbi, Hudson, & Heidari, 2019). Various solid support materials in nanoparticle structure play an important role in increasing catalytic efficiency, reusability and enantioselectivity. Among the solid support materials, **SBA-15** and **MCM-41** regularly porous structures are very interesting with their features such as high surface areas and controllable pore structures (Xu, Bing, Jia, Bai, & Sun, 2022). Studies on the development of heterogeneous catalysts that provide more efficient catalytic activity, functionalized with various modifications of these support materials in the silica structure, such as **SBA-15**, continue in a wide range of reactions. In addition, regular mesoporous structures such as **SBA-15** can generally be synthesized by the sol-gel method in an aqueous environment under mild conditions, starting from a silane compound such as tetraethyl orthosilicate (Croissant, Fatieiev, Almalik, & Khashab, 2018).

Based on the aforementioned information, the scope of this study was to synthesize an organic ligand and graft it onto mesoporous **SBA-15**. It was also aimed to examine the characterization of the obtained heterogeneous catalyst and its catalytic activity in asymmetric transfer hydrogen reactions of various aromatic ketones.

Materıals And Methods

Mesoporous SBA-15 and triethoxy(3-isothiocyanatopropyl)silane **(1)** used in the study were synthesized by our group in previously published studies (Gök & Gök, 2020). (1*R*, 2*R*)-1,2-diphenylethane-1,2-diamine, p-toluenesulfonyl chloride and the other reagents were purchased from commercial suppliers (Sigma-Aldrich or Merck). Purification and drying of all solvents used in the experiments carried out within the scope of the study were carried out using the procedures in Perrin and Armarego. Nuclear magnetic resonance measurements **(NMR)** for ^{1}H and ^{13}C were performed in $CDCl_3$ with a Bruker AVANCE III 400 MHz Nanobay instrument. Mass spectrometry **(MS)** and matrix assisted laser desorption ionization-time of flight measurements **(MALDI-TOF)** were performed with an Agilent LC-MS/MS 6460 Triple QUAD and a Bruker Daltonics spectrometer instrument. Fourier transform infrared spectroscopy measurements **(FT-IR)** were performed with a Perkin Elmer Spectrum 65 instrument using the KBr pellet technique. X-ray diffraction measurements **(XRD)** were performed using Cu-K_α radiation (λ= 0.154056 nm) with a PANalytical Empyrean X-ray diffractometer device in the range of 1-10° and 10-80° 2θ scattering angles. A Jeol SEM-7100-EDX device was used to record field emission scanning electron microscope images **(FESEM)**. Thermogravimetric analysis measurements **(TGA)** were carried out with a Seiko SII TG/DTA 7200 instrument with a flow rate of 2 ml min^{-1} N_2 and a heat rate of 10 C° min^{-1}. N_2 adsorption - desorption isotherms were measured using a Micrometrics Surface Area and Porosity Tristar II analyzer. The Brunauer-Emmett-Teller **(BET)** method was utilized to calculate the surface area and the Barrett, Joyner and Gelenda **(BJH)** method was utilized to calculate the pore diameter distribution. Optical activity measurements were performed using a Rudolph Autopol I polarimeter. Enantiomeric excesses were measured with a Shimadzu GC-2010 Plus instrument equipped with a chiral column (HP-Chiral-20B).

Synthesis of triethoxy(3-isothiocyanatopropyl)silane (1)

Triethoxy(3-isothiocyanatopropyl)silane was previously synthesized in a published study by our group (Gök & Gök, 2020). Briefly, freshly distilled dry THF (14.5 mL) and dry NEt_3 (1.5 mL) at 0 °C were added to commercially available 3-aminopropyl)triethoxysilane (APTES) (0.864 mL) under N_2. 488 µL thiophosgene was added dropwise to the reaction medium and the color change was observed. At the finish of the reaction monitoring by TLC, the reaction was terminated after 3 hours and 15 minutes. It was extracted with DCM, dried with Na_2SO_4, and purified by flash chromatography in the hexane/EtOAc (5/95) system. Yield: 0.54 g (57%). FT-IR (disk) ν = 2974, 2927, 2886, 2178, 2097, 1679, 1443, 1390, 1345, 1192, 1165, 1099, 1071, 954, 873, 779 cm^{-1}. ^{1}H-NMR (400 MHz, $CDCl_3$, ppm) δ: 1.83 (s, 2H, NH_2), 2.35 (s, 3H), 4.17 (d, *J* = 5.4 Hz, 1H), 4.42 (d, *J* = 5.4 Hz, 1H), 7.00 (m, 2H), 7.13–7.20 (m, 11H), 7.34–7.36 (m, 2H). ^{13}C-NMR (100 MHz, $CDCl_3$, ppm) δ: 7.7 (CH_2), 18.3 (CH_3), 24.1 (CH_2), 47.3 (CH_2), 58.5 (CH_2), 171.0 (C).

Synthesis of N-((1*R*,2*R*)-2-amino-1,2-diphenylethyl)-4-methylbenzenesulfonamide (2)

N-((1*R*,2*R*)-2-amino-1,2-diphenylethyl)-4-methylbenzenesulfonamide **(2)** was synthesized using a previously published method (Giuffredi, Purser, Sawicki, Thompson, & Gouverneur, 2009). (1*R*, 2*R*)-1,2-diphenylethane-1,2-diamine (1 g, 4.71 mmol) was putted to the flask containing newly distilled dry THF (35 mL) and dry NEt_3 (0.364 g, 3.6 mmol) as the base under argon atmosphere at 0 °C. The reaction medium was stirred for 1 h at these conditions. Then a solution of p-toluenesulfonyl chloride (0.982 g, 5.15 mmol) in dry THF (15 mL) was added dropwise with the help of a dropping funnel to the reaction medium at 0 °C, under argon atmosphere. The reaction medium was stirred for further 21 h. Formation of products and depletion of reactants were tracked by TLC. At the end of the reaction period, the resulting reaction mixture

evaporated under reduced pressure. Then a saturated sodium bicarbonate solution was added to the remaining product and extracted with saturated sodium chloride solution and dichloromethane solvent system. The organic layer of the mixture was dried with anhydrous sodium sulfate, and then the solvent of the mixture was evaporated under vacuum to give a crude product. The remaining crude product was subjected to the flash chromatography. The solvent system was hexane/ethyl acetate (10/90), affording pure product as a white powder. Yield: 0.41 g (%79). $[\alpha]_D^{20}$= -15 (c, 1.0, $CHCl_3$). FT-IR (disk) ν = 3344, 3286, 3084, 3065, 3028, 2924, 2863, 1944, 1880, 1808, 1737, 1597, 1492, 1454, 1329, 1155, 1086, 1055, 1017, 983, 912, 812, 767, 697 cm^{-1}. ^{1}H-NMR (400 MHz, $CDCl_3$, ppm) δ: 1.83 (s, 2H, NH_2), 2.35 (s, 3H), 4.17 (d, *J* = 5.4 Hz, 1H), 4.42 (d, *J* = 5.4 Hz, 1H), 7.00 (m, 2H), 7.13–7.20 (m, 11H), 7.34–7.36 (m, 2H). ^{13}C-NMR (100 MHz, $CDCl_3$, ppm) δ: 21.4 (CH_3), 60.5 ($CHNH_2$), 63.2 (CHNHTs), 126.5 (CH), 126.8 (CH), 127.0 (CH), 127.3 (CH), 127.4 (CH), 128.2 (CH), 128.4 (CH), 129.1 (CH), 137.3 (C), 139.2 (C), 141.4 (C), 142.4 (C). MS (ESI^+) MS calculated $[M+H]^+$ for $C_{21}H_{22}N_2O_2S$: 366.48 found: 367.8 $[M+H]^+$, 389.8 $[M+Na]^+$, 405.7 $[M+K]^+$.

Synthesis of N-((11*R*,12*R*)-4,4-diethoxy-11,12-diphenyl-9-thioxo-3-oxa-8,10-diaza-4-siladodecan-12-yl)-4-methylbenzenesulfonamide (3)

Compound (2) (0.271 g, 0.74 mmol) was dissolved in dry DCM (12.5 mL) in an inert atmosphere and at room temperature, and stirring was started. Then, **compound (1)** (0.178 g, 0.68 mmol) was dissolved in dry DCM (10 mL) and transferred to a dropping funnel using a cannula. It was slowly dropped into the reaction medium, which was mixed under an inert atmosphere. Product formation and depletion of reactants were monitored using TLC. After 24 hours, the temperature of the reaction medium was increased to 30 °C and a reflux was added. The reaction was terminated at 48 hours. The reaction medium was transferred to an evaporation flask and the solvents were evaporated under vacuum. The obtained crude product

was subjected to flash chromatography. DCM:MeOH (98/2) was used as the solvent system and pure **compound (3)** was obtained as a yellowish oil. Yield: 0.45 g (%97). $[\alpha]_D^{20}$= 6.7 (c, 1.0, $CHCl_3$). FT-IR (disk) ν = 3346, 3277, 3062, 3032, 2968, 2924, 2872, 1598, 1544, 1494, 1454, 1415, 1384, 1303, 1290, 1153, 1066, 935, 812, 796, 758, 696, 663 cm^{-1}. ^{1}H-NMR (400 MHz, $CDCl_3$, ppm) δ: 0.63 (t, 2H, CH_2), 0,88 (t, 2H, CH_2), 1.2-1.3 (m, 9H), 2.31 (s, 3H, CH_3), 3.4 (m, 2H, CH_2), 3.8 (m, 6H, CH_2), 4.14 (d, 1H), 4.39 (d, 1H), 7.5-7.0 (m, 16H), 9.3 (m, 2H, NH). ^{13}C-NMR (100 MHz, $CDCl_3$, ppm) δ: 7.7, 18.3, 21.3, 22.2, 22.7, 29.4, 29.7, 30.2, 31.2, 58.5, 60.5, 63.2, 63.8, 126.9, 127.6, 127.7, 128.0, 128.2, 128.4, 128.6, 129.1, 129.2, 137.8, 137.9, 138.0, 142.9, 156.0. MS (ESI^+) MS calculated $[M+H]^+$ for $C_{31}H_{43}N_3O_5S_2Si$: 629.91 found: 629.04 $[M+H]^+$.

Synthesis of mesoporous SBA-15 supported heterogenous catalyst (4)

First, mesoporous SBA-15 was kept under vacuum at 120 °C for 2 hours to activate it. Then, **compound (3)** (0.163 g) was dissolved in dry toluene (40 mL) under an inert atmosphere and transferred to a dropping funnel using a cannula. Activated SBA-15 (1 g) was dissolved in dry toluene (10 mL) and mixed at room temperature. **Compound (3)** began to be added dropwise to the reaction medium. After the dripping was completed, the temperature was increased to 110 °C and the reaction medium was stirred for 24 hours. At the end of this period, the reaction medium was filtered under vacuum and washed with toluene, ethanol and methanol respectively. Heterogeneous catalyst **(4)** was acquired as white powder (1.10 g).

Monitoring the catalytic activity of mesoporous SBA-15 supported heterogenous catalyst (4) in asymmetric transfer hydrogen reactions in various aromatic ketones

As a general procedure, in each test reaction to determine the catalytic activity of catalyst **(4)**, **heterogeneous catalyst (4)** and

[Ru(p-cymene)Cl_2]$_2$ were added to 7 mL of isopropyl alcohol under an inert atmosphere and at room temperature, then the temperature was increased to 82 °C and mixed for 2 hours. At the end of the second hour, aromatic ketone was added to the reaction medium at room temperature and then the temperature was increased to 82 °C again. Finally, the reactions were initiated by adding base at this temperature. In order to monitor the conversion rates and enantiomeric excesses of aromatic ketones into their corresponding alcohols, a few drops were taken from the reaction medium at certain intervals, diluted with isopropyl alcohol and filtered with the help of a microfilter. The filtrates were loaded into the GC equipped with a chiral column and the results of the conversions and enantiomeric excesses were obtained. The results were calculated based on the areas under the peaks of ketones and their corresponding alcohols.

Results And Dıscussıons

Characterization studies of compound 3 and mesoporous SBA-15 supported heterogeneous catalyst (4)

The synthesis route of the heterogeneous catalyst **(4)** starting from (1*R*, 2*R*)-1,2-diphenylethane-1,2-diamine is given in **Scheme 1**.

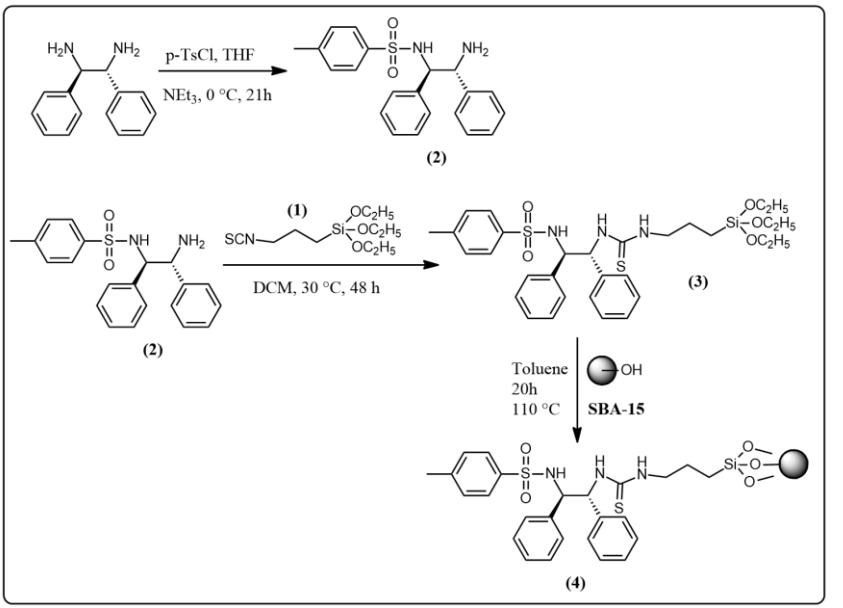

Scheme 1 *- Synthesis of* ***heterogeneous catalyst (4)*** *grafting with mesoporous* ***SBA-15***

FT-IR spectroscopy was first used for the characterization of the synthesized **compound (3)** and **heterogeneous catalyst (4)**. FT-IR spectra of **compound (3)** and **heterogeneous catalyst (4)** are shown in **Figure 1** along with the spectrum of **SBA-15**. When the spectrum of **compound (3)** is examined, the stretching vibration band of the **C=S** bond is seen around 1065 cm^{-1}. In addition, stretching vibrations of the **S=O** bond are also seen in the 1415 cm^{-1} region. In the 3300 cm^{-1} regions, stretching of the **N-H** bonds are observed. These results indicate that **compound (3)** was successfully synthesized. In the spectrum of **heterogeneous catalyst (4)**, characteristic out of plane, bending and stretching vibrations of **Si-O** bonds are seen in the regions of 460, 805 1085 cm^{-1}, similar to **SBA-15**. Finally, in the 3420 cm^{-1} regions, the stretching vibration of the **N-H** bond is seen superposed with the **O-H** stretching vibration in the silanol groups. These spectral data demonstrate successful grafting of **compound (3)** onto mesoporous SBA-15.

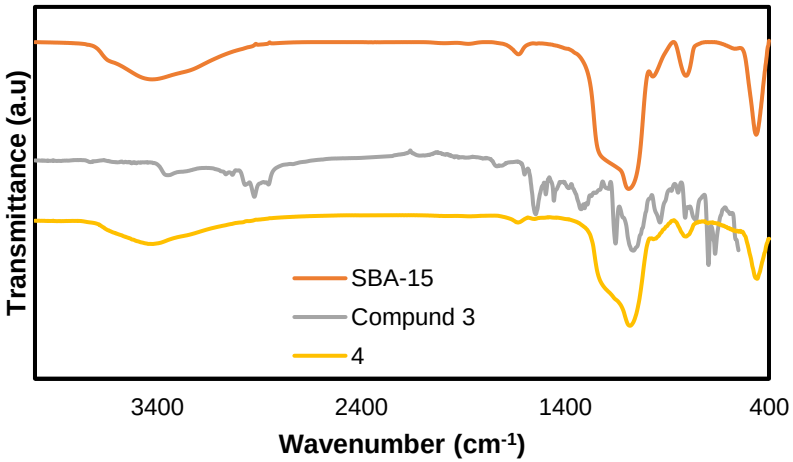

Figure 1 - FT-IR spectra of SBA-15, compound 3 and heterogeneous catalyst (4)

FESEM analysis was performed to determine the morphological structure of **heterogeneous catalyst (4)** and to compare the similarity of the synthesized catalyst to **SBA-15**, it was also examined by SEM analysis. According to the obtained FESEM micrographs, it was observed that **heterogeneous catalyst (4)** had a worm-like morphology similar to **SBA-15**. The resulting micrographs are shown in **Figure 2**.

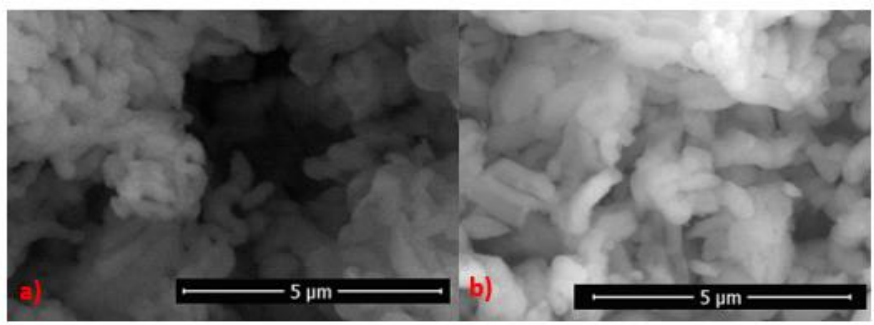

Figure 2 - FESEM micrographs of a) SBA-15 and b) heterogeneous catalyst (4)

The crystallinity of the **heterogeneous catalyst (4)** and **SBA-15** was examined by low angle XRD. In the obtained XRD diffraction patterns, **SBA-15** indicate robust diffraction reflection at (100) **2θ=0.90**. This result demonstrates the regular hexagonal symmetry of mesoporous **SBA-15**. The XRD pattern of the **heterogeneous catalyst (4)** shows the characteristic peaks of **SBA-15.** This result shows that **compound (3)** was successfully grafted into the mesoporous ordered structure of **SBA-15** without any structural distortion. Low angle XRD patterns are shown in **Figure 3**.

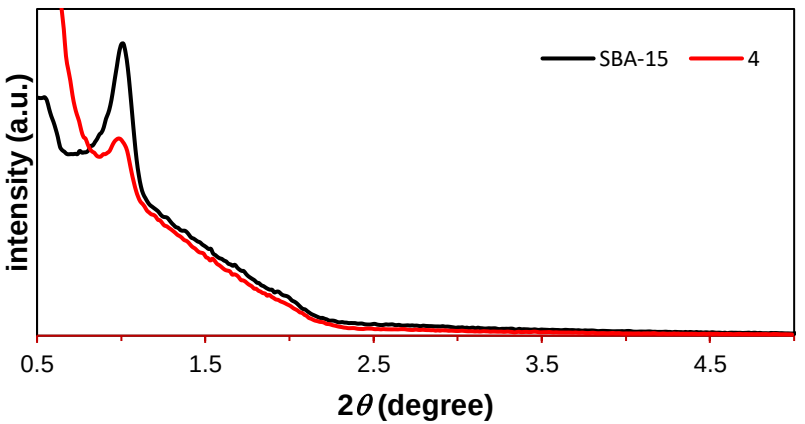

Figure 3 - Low angle XRD patterns of SBA-15 and heterogeneous catalyst (4)

Structural parameters of **SBA-15** and **heterogeneous catalyst (4)** were calculated based on N_2 adsorption-desorption measurements. According to the IUPAC adsorption isotherm classification, N_2 sorption isotherms of **SBA-15** and **heterogeneous catalyst (4)** are compatible with H1 hysteresis and Type 4 adsorption isotherm. Sorption isotherms and pore diameter distribution curves of **SBA-15** and the **heterogeneous catalyst (4)** are shown in **Figure 4.**

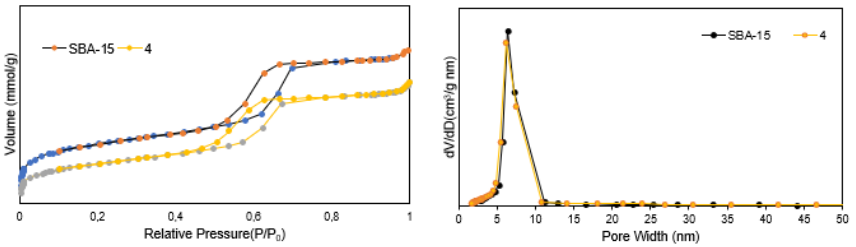

Figure 4 *- N_2 sorption isotherms and pore size distributions of* ***SBA-15*** *and* ***heterogeneous catalyst 4***

According to the N_2 adsorption-desorption results obtained, the amount of N_2 increased in the range of $0.5 < P/P_0 < 0.7$. Surface areas (S_{BET}), pore volumes (V_P) and pore diameters (D_P) calculated according to the results obtained from the measurements are given in **Table 1**. According to the obtained results shown in **Table 1**, **heterogeneous catalyst (4)** has lower pore volume, average pore diameter and surface area compared to **SBA-15**, these results indicate the successful grafting of **compound (3)** onto **SBA-15**.

Table 1 - Structural parameters of SBA-15 and heterogeneous catalyst (4)

Specimens	**Surface Area (m^2g^{-1})**	**Pore Diameter (nm)**	**Pore Volume (cm^3g^{-1})**
SBA-15[i]	459[d]	5.68[d]	0.51[d]
4	393	5.39	0.47

[i]results from previously published study of our group (Gök & Gök, 2020)

Thermogravimetric analysis of **heterogeneous catalyst (4)** and **SBA-15** was performed to calculate the amount of **compound (3)** grafted onto **SBA-15**. The resulting TGA curves are shown in **Figure 5**.

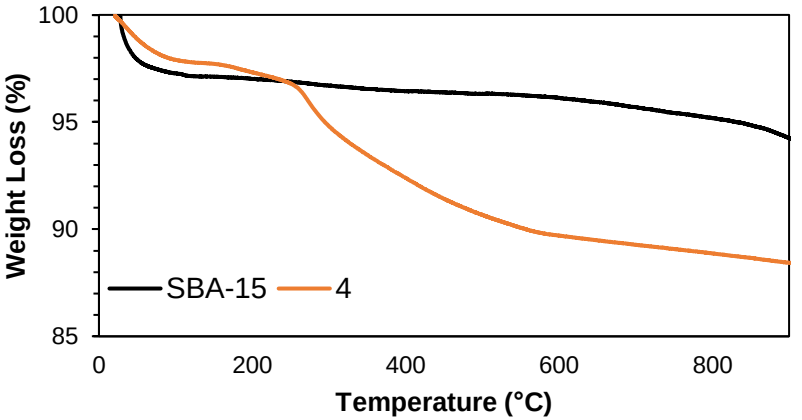

Figure 5 - TGA curves of SBA-15 and heterogeneous catalyst (4)

When looking at the curve of **SBA-15**, **approximately 3%** mass loss is seen in the first region between 20 - 115 °C. The mass loss in this region is due to the loss of water and/or organic solvents over the surface and pores of mesoporous **SBA-15**. In the curve of **SBA-15**, the second mass loss appears between 125 and 650 °C. The mass loss in this range **(about 2%)**, where the curve almost flattens, can be attributed to silanol condensation in the mesoporous structure. When looking at the curve of **heterogeneous catalyst (4)**, it is observed that the initial mass loss is between 20 - 115 °C, similar to **SBA-15**. Similarly, this loss **(about 3%)** is due to the removal of water and/or solvents within the mesoporous structure. On the other hand, it is seen that **heterogeneous catalyst (4)** loses mass before **SBA-15** in this region. This result can be attributed to its hydrophobic character. Finally, when looking at the second mass loss region of **heterogeneous catalyst (4)**, it is seen that this loss is **approximately 7%** between 250 - 675 °C. This loss can be referred to the cast out of covalently bonded organic groups from the mesoporous structure.

Catalytic activity of mesoporous SBA-15 supported heterogeneous catalyst (4) in ATH reactions of various aromatic ketones

In determining the catalytic activity of the heterogeneous catalyst **(4)**, the optimum reaction conditions were first investigated with various test reactions, choosing the asymmetric transfer hydrogenation reaction of acetophenone as a model reaction. These test reactions primarily involved the formation of a complex between the catalyst and $[Ru(p\text{-cymene})Cl_2]_2$, isopropyl alcohol serving as a hydrogen donor, and the relevant base catalyzing the reaction. While the effects of base type, base amount and substrate/catalyst ratio were examined in determining the best catalytic activity, the catalytic activities **without catalyst, $[Ru(p\text{-cymene})Cl_2]_2$ and base** were also examined. The results obtained are shown in **Table 2**.

Table 2 *- Reaction optimization for heterogeneous catalyst (4) at asymmetric transfer hydrogenation of acetophenone*[a]

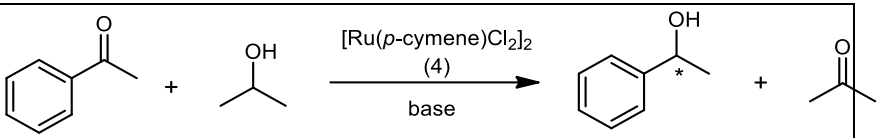

Entry	Time (h)	Base	mmol	Conversion (%)[b]	%ee[c]	S/C
1	24	NaOH	1	93	*ras.*	250/1
2	24	KOH	1	53	*ras.*	250/1
3	24	NEt_3	1	58	*ras.*	250/1
4	24	t-BuOK	1	69	*ras.*	250/1
5[d]	24	NaOH	1	79	*ras.*	250/1
6[e]	24	NaOH	1	97	*ras.*	250/1
7[d, e]	24	NEt_3	1	0	-	250/1
8[e]	24	NEt_3	1	44	*ras.*	250/1
9[f]	24	-	-	0	-	250/1
10	24	NEt_3	1	92	*ras.*	100/1
11	24	NEt_3	1	54	*ras.*	500/1

12	24	NEt_3	1	27	*ras.*	1000/1
13	24	NEt_3	0,8	90	*ras.*	100/1
14[h]	24	-	-	8	*ras.*	100/1

[a] Reactions were performed in 7 mL of isopropanol with Ru:ligand = 1:2. Substrate/catalyst ratio was 250/1 for the entries 1-9. [b] Determined by GC (HP-Chiral-20B). [c] The absolute configuration was confirmed by comparing the retention times of the enantiomers on the GC traces with those reported in the literature. [d] Without of $[Ru(p\text{-cymene})Cl_2]_2$ [e] Without of catalyst. [f] Without of $[Ru(p\text{-cymene})Cl_2]_2$ and base. [h] Without of base.

As the beginning of the test reactions, reactions containing various bases (NaOH, KOH, NEt_3 and *t*-BuOK) were carried out in the **base type**, 250/1 substrate/catalyst ratio and **1 mmol base amount.** As a result of these test reactions, the highest conversion rate was obtained in the reaction **(93%)** (Table 2, entry 1) in which **NaOH** was used as a base, but since bases containing alkali metals already gave high conversion in this reaction type even without catalyst and $[Ru(p\text{-cymene})Cl_2]_2$, the organic base **$NEt_3$** with a relatively higher conversion rate **(58%)** (Table 2, entry 3) was chosen as the optimum base. To verify the influence of the **base type on the catalytic effect**, a Ru(II)-free test reaction and an additional catalyst-free test reaction were also carried out. The first test reaction was again carried out with a 250/1 substrate/catalyst ratio and 1 mmol base amount, with NaOH, **without $[Ru(p\text{-cymene})Cl_2]_2$**. In the other reaction, this time it was carried out **without a catalyst instead of $[Ru(p\text{-cymene})Cl_2]_2$**. As a result of these reactions, the reaction **without $[Ru(p\text{-cymene})Cl_2]_2$** had a conversion rate of **(79%)** (Table 2, entry 5), while the reaction **without a catalyst** had a conversion rate of **(97%)** (Table 2, entry 6). No enantiomeric excess was observed in either of these test reactions.

In the continuation of these test reactions, reactions in which **NEt_3** was used as the base, the **substrate/catalyst ratio was 250/1** and the **base amount was 1 mmol**. They were carried out separately **without ruthenium and catalyst**. As a result of these test reactions, while no conversion (Table 2, entry 7) occurred in the reaction **without $[Ru(p\text{-cymene})Cl_2]_2$**, a conversion rate of **(44%)** (Table 2, entry 8) was observed in the reaction **without a catalyst.** This

conversion rate obtained was less than the conversion rate that occurred in the presence of the catalyst. In addition to these test reactions, no conversion (Table 2, entry 9) was observed in the reaction without **both [Ru(p-cymene)Cl_2]$_2$ and base** under the same conditions. Besides these results, no enantiomeric excess was observed in any of these reactions.

Test reactions were carried out with various **substrate/catalyst ratios (100/1, 500/1 and 1000/1)** to determine the optimum substrate/catalyst ratio at which the best catalytic activity occurs. The reaction conditions were **NEt_3 as base and 1 mmol as base amount**, based on the results obtained from previous test reactions. As a result of these test reactions, the highest conversion rate **(92%)** (Table 2, entry 10) occurred at a substrate/catalyst ratio of **100/1.** Following these test reactions, a reaction was carried out with **0.8 mmol NEt_3** containing less base amount, taking into account the substrate/catalyst ratio where the best catalytic activity was exhibited. In addition, a test reaction was also carried out under the same conditions but **without base**. As a result, a lower conversion **(90%)** (Table 2, entry 13) occurred in the test reaction containing less base compared to the test reaction containing 1 mmol NEt_3 **(92%)** (Table 2, entry 10). On the other hand, a very low conversion rate **(8%)** (Table 2, entry 14) was observed in the reaction that **did not contain any base.** Considering the overall results, no enantiomeric excess was observed in these test reactions as in the previous reactions, and the optimum reaction conditions where the **heterogeneous catalyst (4)** showed the best catalytic activity occurred at a ratio of **100/1 substrate/catalyst** with **1 mmol NEt_3 base.**

After determining the optimum reaction conditions, the catalytic activity of the **heterogeneous catalyst (4)** was examined in the asymmetric transfer hydrogenation reactions of various aromatic ketones **(4'-methoxyacetophenone, 4'-methylacetophenone, 4'-chloroacetophenone and 4'-bromoacetophenone)** using the same general reaction procedures. The results obtained are shown in **Table 3**. As a result of the test reactions carried out with various ketones,

the **heterogeneous catalyst (4)** showed the best catalytic activity with a conversion rate of **(97%)** (Table 3, entry 5) in the reaction of **4'-bromoacetophenone** under optimum reaction conditions (1 mmol NEt_3 and 100/1 substrate/catalyst ratio).

Table 3 - *ATH reactions of various aromatic ketones with heterogenous catalyst (4)*[a]

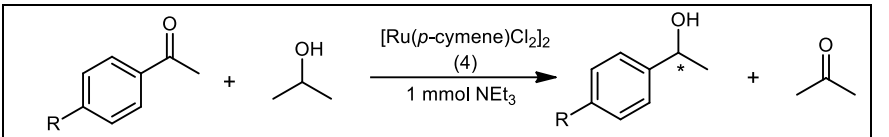

Entry	Time (h)	R	Base	mmol	Conversion (%)[b]	%ee[c]	S/C
1	24	H	NEt_3	1	92	*ras.*	100/1
2	24	OCH_3	NEt_3	1	81	*ras.*	100/1
3	24	CH_3	NEt_3	1	95	*ras.*	100/1
4	24	Cl	NEt_3	1	94	*ras.*	100/1
5	24	Br	NEt_3	1	97	*ras.*	100/1

[a] Reactions were performed in 7 mL of isopropanol with Ru:ligand = 1:2. Substrate/catalyst ratio was 100/1 for all entries. [b] Determined by GC (HP-Chiral-20B). [c] The absolute configuration was confirmed by comparing the retention times of the enantiomers on the GC traces with those reported in the literature.

CONCLUSIONS

Within the scope of this study, tosylated **compound (2)** was synthesized by first reacting commercial substance (1*R*, 2*R*)-1,2-diphenylethane-1,2-diamine with p-TsCl. Based on this substance **compound (1)**, which was previously synthesized by our group, was reacted it and **compound (3)**, which contains a silyl group ready for

heterogenization was obtained. **Heterogeneous catalyst (4)** was synthesized by grafting **compound (3)** onto mesoporous **SBA-15.** The structures of **compound (3)** and **heterogeneous catalyst (4**) were successfully characterized and their structures were confirmed. The catalytic activity of the **heterogeneous catalyst (4)**, which was successfully grafted with mesoporous **SBA-15**, in asymmetric transfer hydrogen reactions of various aromatic ketones was examined. According to the results obtained from catalytic studies, it was observed **that heterogeneous catalyst (4)** catalyzed the conversion of acetophenone to 4-phenylethanol with a **92%** conversion rate at a 100/1 substrate/catalyst ratio with 1 mmol NEt_3, which is the optimum conditions in the asymmetric transfer hydrogenation reaction of acetophenone. With the results obtained here, it was observed that **heterogeneous catalyst (4)** catalyzed the asymmetric transfer hydrogenation reaction of 4-bromoacetophenone under similar conditions with a conversion rate of **97%**. Although the tosylation reaction of **compound (3)**, which is in the structure of **heterogeneous catalyst (4)**, from **compound (2)** was carried out in order to increase the enantioselectivity, no enantiomeric excess was observed in the above-mentioned reactions. This result can also be thought to be due to the steric hindrances applied by the pores in the mesoporous structure to the organic ligand. Considering the advantages of heterogeneous catalysts, our group continues to work on the development of new heterogeneous catalysts without loss of chirality.

REFERENCES

Croissant, J. G., Fatieiev, Y., Almalik, A., & Khashab, N. M. (2018). Mesoporous Silica and Organosilica Nanoparticles: Physical Chemistry, Biosafety, Delivery Strategies, and Biomedical Applications. *Adv. Healthcare Mater*, 7:e1700831.

Foubelo, F., Nájera, C., & Yus, M. (2015). Catalytic asymmetric transfer hydrogenation of ketones: recent advances. *Tetrahedron: Asymmetry*, 769-790.

Ghorbani-Choghamarani, A., Tahmasbi, B., Hudson, R. H., & Heidari, A. (2019). Supported organometallic palladium catalyst into mesoporous channels of magnetic MCM-41 nanoparticles for phosphine-free Csingle bondC coupling reactions. *Microporous and Mesoporous Materials*, 366-377.

Giuffredi, G., Purser, S., Sawicki, M., Thompson, A., & Gouverneur, V. (2009). Asymmetric de novo synthesis of fluorinated D-glucitol and D-mannitol analogues. *Tetrahedron: Asymmetry*, 910-920.

Gök, Y., & Gök, H. Z. (2020). Synthesis, characterization and catalytic performance in enantioselective reactions by mesoporous silica materials functionalized with chiral thiourea-amine ligand. *Research on Chemical Intermediates*, 853-874.

Gök, Y., Aykut, İ. T., & Gök, H. Z. (2020). Readily accessible mesoporous silica nanoparticles supported chiral urea-amine bifunctional catalysts for enantioselective reactions. *Applied Organometallic Chemistry*, 34:e6015.

Perrin, D., & Armarego, W. (1989). *Purification of Laboratory Chemicals.* UK: Permagon Press.

Xu, G., Bing, L., Jia, B., Bai, S., & Sun, J. (2022). Comparison of mesoporous fractal characteristics of silica-supported organocatalysts derived from bipyridine-proline and

resultant effects on the catalytic asymmetric aldol performances. *RSC Adv.*, 10800–10814.

CHAPTER V

Some Novel Materials Used as a Sorbent for Preconcentration and Determination of Heavy Metal Ions

Rukiye SAYGILI CANLIDİNÇ[1]

Introduction

Heavy metal pollution, especially in terms of food and the environment, has been among the issues that have attracted increasing attention for years (Yavuz & et. al., 2016, Tüzen, Elik & Altunay 2021, Ali & et. al., 2023). Because there are a wide variety of pollutant sources in the spread of heavy metals to the environment, air, water and soil all over the world. Mining-metallurgy activities, agricultural activities, dye industry, fuel consumption, pesticides, etc. are examples of these resources (Gümüş & Soylak, 2021). Metals such as lead, copper, cadmium,

[1] Assoc. Prof., Kütahya Dumlupınar University

iron, chromium, cobalt, mercury and nickel can be given as examples of metals released from these sources (Elsayed, Alatawi & Monier 2020, Özdemir & et. al., 2021). Heavy metal pollution is extremely important as these metals reach the food chain from these sources and thus to human health. These metals, which are exposed directly or indirectly through food, air, water and soil, tend to accumulate in the body over time and have toxic effects (Domingo & et. al., 2020, Yılmaz & et. al., 2023, Ullah & Tüzen, 2022).

So, determination of these metals from different matrices are very important but difficult because of their low concentrations (Mendil & et. al., 2019). Several techniques such as, flame atomic absorption spectrometry (FAAS) (Kazantzi & et. al., 2019, Soylak & et. al., 2024), graphite furnace atomic absorption spectrometry (GFAAS), inductively coupled plasma optical emission spectrometry (ICP-OES) (Yamini & Safari, 2018) and inductive coupled plasma mass spectrometry (ICP-MS) (Aydın & et. al., 2020) are used to determine these metal ions. Because sample media are complex matrices, a sample separation step is needed beforehand. Therefore, a sample pretreatment step is crucial in the analytical process (Faraji, Yamini, & Gholami, 2019). For this purpose, different separation techniques are used. The most common methods for preconcentration are such as solid phase extraction (SPE) (Özdemir, Yalçın & Kılınç, 2021), solid phase micro-extraction (SPME) (Mei & et. al., 2019, Khan Arain & Soylak, 2020), liquid-liquid extraction (LLE) (Mahandra, Singh & Gupta, 2017, Lukomska & et. al., 2020), dispersive liquid-liquid micro-extraction (DLLE) (Sorouraddin, Farajzadeh & Dastoori, 2020, Hong & et. al., 2022) because of easy, fast, economical and eco-friendly. SPE is one of the most used separation technique for decades, because it has a simple preparation technique and some important advantages such as reusability, automation, low organic solvent consumption and high extraction capacity. But for the extraction procedure, the most important step is the selection of the sorbent. For this purpose, several materials, are considered as sorbents (Azzouz & et. al., 2018), but the majority of such materials are limited by low

efficiency and low reusability. Thus, seeking more economic and efficient sorbents to eliminate heavy metals. New sorbent materials have been prepared to increase the performance of solid-phase sorption-based extraction techniques and satisfy the requirements of highly sensitive and highly selective green analytical chemistry (Su & et. al., 2016).

In recent years, some reported sorbents are graphene oxide (Soylak & et. al., 2017) imprinted polymers, (Wan & et. al. 2021, Saygılı Canlıdinç, Turan & Kalfa, 2022) activated carbon (Turan, Saygılı Canlıdinç & Kalfa, 2022), carbon nanotube (Turan, Saygılı Canlıdinç & Kalfa, 2018, Duman, Erbas & Soylak, 2020), biosorbents (Saygili Canlıdinç, 2022), zeolite (Yazani & et. al., 2019), resins (Iwase & et. al., 2023), DESs-based sorbent material (Jagirani & Soylak, 2022), magnetic sorbents (Montoro-Leal & et. al., 2020, Sajid, Nazal & Ihsanullah, 2021) and metal organic frameworks (MOFs) (Li & et. al., 2020).

Graphene Oxide

Graphene oxide is the oxidized form of graphene that is easily made using Hummer's method from natural graphite powder after reacting with an anhydrous mixture of potassium permanganate, sodium nitrate, and sulfuric acid. Graphene (G) and graphene oxide (GO) have garnered significant attention in recent times as sorbent materials for solid phase extraction. due to their distinctive mechanical and thermal characteristics, which include their large surface area, chemical stability, and high adsorption capacity. Two-dimensional, one-atom-thick layers of sp^2 connected carbon make up graphene oxide. Rich functional groups found in GO, such as hydroxyl, carboxyl and epoxy groups, facilitate strong π-π stacking, hydrophobic contact, and hydrogen bonding between the sorbent and metal ions. Thus, GO has been successfully used in analytical chemistry to prepare a wide range of samples, including biological, food and environmental matrices (Saygili Canlıdinç & et. al., 2017; Manousi & et. al., 2020).

Biosorbents

In solid phase extraction method, different sorbent materials have already been evaluated for the preconcentration of heavy metal ions. New reports focus on agricultural waste materials because they have been recognized as low-cost, renewable, biodegradable and eco-friendly biosorbents with significant adsorption capacity for heavy metal ions. Therefore, they are potential low-cost sorbents such as clay, natural zeolites, chitosan, walnut shell, rice husk, leaves, peels of fruits and vegetables, seeds and so on. They rich source of lignocellulosic material, lignin, cellulose, hemicellulose, pectin, proteins, flavonoids, terpenoids and other secondary metabolites having polyhydroxyl, carboxyl, amine, and aldehydes, functionalities with high affinity for metal ions (Özkalkan & Saygili Canlidinç, 2021; Saygili Canlidinç, 2022).

The compact lattice structure of cellulose and hemicelluloses in lignocellulosic materials restricts the amount of free hydroxyl groups that can bind with heavy metal ions. They have a very low adsorption capacity as a result. As a result, their ability to adsorb heavy metal ions has been demonstrated to be low. It is common practice to employ a number of modification treatments to address these drawbacks. These agricultural waste products have an easy functionalization process, which makes them a good choice for heavy metal adsorption. Evaluation of these sorbents made from agricultural waste is also crucial. Because using agricultural waste as a biosorbent offers a sustainable way to manage and make use of the ever-increasing amount of waste produced by home cooking, industrial food processing, and agricultural operations (Garg & et. al., 2023).

Metal Organic Frameworks

Novel functional materials known as metal organic frameworks (MOFs) are made up of different transition metal ions that bind to a wide range of organic ligands (Ma & et. al., 2018). MOFs possess many of the superior qualities of both organic

complexes and inorganic porous materials, including a large specific surface area, extremely high porosity, adjustable polarity, adjustable pore size, and simple functionalization. The use of MOFs in solid phase extraction makes sense in light of these benefits (Ma & et. al., 2016). Thus, these nanoparticles are employed in various samples as sorbents for the preconcentration of analytes. Nevertheless, MOFs are limited to use with water and some other liquid samples because many of their nanomaterials are not stable in liquid environments. In an effort to get around this, a large body of research on magnetic MOFs for use as sorbents in SPE has quickly spread (Gümüş & Soylak, 2021).

Conclusion

Determination of trace heavy metal concentrations in environmental and biological samples is becoming increasingly important in pollution monitoring studies. Despite the increased sensitivity and selectivity of modern instrumental analyzes such as FAAS, ICP-MS, ICP-OES and GFAAS, there are many difficulties in the analysis of trace heavy metals due to both their low levels in samples and the very complexity of sample matrices. Therefore, a preconcentration/separation step is usually required. Preconcentration is needed at trace levels in analytical procedures, mainly when the complex environmental sample analysis. The most important goal of the sample preparation step is to separate and concentrate the analyte of interest and convert the analyte into an instrument-friendly environment for final analytical measurement. Here one of the most important step is selection of the sorbent material. The sorbent to be selected is expected to have some features such as being economical, reusable and high adsorption capacity. Several sorbent materials are used for this purpose. Recently some materials are considered as most used sorbents, because of some of are economical, reusability and large adsorption capacity. Especially, several biosorbents, nanomaterials such as GO, magnetic materials and MOFs have attracted increasing attention as new sorbents in analytical chemistry in recent years.

REFERENCES

Yavuz, E., Tokalıoğlu, Ş., Şahan, H. & Patat, Ş. (2016) Nanosized spongelike Mn3O4 as an adsorbent for preconcentration by vortex assisted solid phase extraction of copper and lead in various food and herb samples. *Food Chemistry, 194*, 463-469. Doi: 10.1016/j.foodchem.2015.08.035

Tuzen, M., Elik, A. & Altunay, N. (2021) Ultrasound-assisted supramolecular solvent dispersive liquid-liquid microextraction for preconcentration and determination of Cr(VI) in waters and total chromium in beverages and vegetables. *Journal of Molecular Liquids, 329*, 115556. Doi: 10.1016/j.molliq.2021.115556

Ali, Z., Ullah, R., Tuzen, M., Ullah, S., Rahim, A. & Saleh, T.A. (2023) Colorimetric sensing of heavy metals on metal doped metal oxide nanocomposites: A review. *Trends in Environmental Analytical Chemistry, 37,* e00187. Doi: 10.1016/j.teac.2022.e00187

Gümüş, Z.P. & Soylak, M. (2021) Metal organic frameworks as nanomaterials for analysis of toxic metals in food and environmental applications. *TrAC Trends in Analytical Chemistry, 143*, 116417. Doi: 10.1016/j.trac.2021.116417

Elsayed, N.H., Alatawi, A. & Monier, M. (2020) Diacetylmonoxine modified chitosan derived ion-imprinted polymer for selective solid-phase extraction of nickel (II) ions. *Reactive and Functional Polymers, 151*, 104570. Doi: 10.1016/j.reactfunctpolym.2020.104570

Özdemir, S., Kılınç, E., Acer, Ö. & Soylak, M. (2021) Simultaneous preconcentrations of Cu(II), Ni(II), and Pb(II) by SPE using E. profundum loaded onto Amberlite XAD-4. *Microchemical Journal, 171,* 106758. Doi: 10.1016/j.microc.2021.106758

Domingo, J.L., Marquès, M., Mari, M. & Schuhmacher, M (2020) Adverse health effects for populations living near waste incinerators with special attention to hazardous waste incinerators.

A review of the scientific literature. *Environmental Research, 187*, 109631. Doi: 10.1016/j.envres.2020.109631

Yılmaz, S., Ullah, N., Citak, D., Hazer, B. & Tuzen, M. (2023) Vortex-assisted dispersive solid-phase microextraction of cadmium and copper on magnetic polystyrene-b- poly dimethyl siloxane hydrophobic block copolymer for their atomic absorption spectrometric determination in water, soft drink and food samples. *Journal of Food Composition and Analysis, 123,* 105487. Doi: 10.1016/j.jfca.2023.105487

Ullah, N. & Tuzen, M. (2022) A New Trend and Future Perspectives of the Miniaturization of Conventional Extraction Methods for Elemental Analysis in Different Real Samples: A Review. *Critical Reviews in Analytical Chemistry*. DOI: 10.1080/10408347.2022.2128635

Mendil, D., Uluozlu, O.D., Tuzen, M. & Soylak, M. (2019) Multi-element determination in some foods and beverages using silica gel modified with 1-phenylthiosemicarbazide. *Food Additives & Contaminants: Part A, 36:11*, 1667-1676. Doi: 10.1080/19440049.2019.1662954

Kazantzi, V., Drosaki, E., Skok, A., Vishnikin, A.B. & Anthemidis, A. (2019) Evaluation of polypropylene and polyethylene as sorbent packing materials in on-line preconcentration columns for trace Pb(II) and Cd(II) determination by FAAS. *Microchemical Journal, 148,* 514-520. Doi: 10.1016/j.microc.2019.05.033

Soylak, M., Hassan Ahmed, H.E. & Coban, A.N. (2024) Micro-solid phase extraction of cobalt at trace levels as 1-nitroso-2-naphthol chelates on magnetic date palm fiber-WSe2 (mDPF@WSe2) nanocomposite from food, tobacco, and water samples. *Journal of Food Composition and Analysis, 125,* 105716. Doi: 10.1016/j.jfca.2023.105716

Yamini, Y. & Safari, M. (2018) Modified magnetic nanoparticles with catechol as a selective sorbent for magnetic solid

phase extraction of ultra-trace amounts of heavy metals in water and fruit samples followed by flow injection ICP-OES. *Microchemical Journal, 143,* 503-511. Doi: 10.1016/j.microc.2018.08.018

Aydin, F., Yilmaz, E., Ölmez, E. & Soylak, M. (2019) Cu2O-CuO ball like/multiwalled carbon nanotube hybrid for fast and effective ultrasound-assisted solid phase extraction of uranium at ultra-trace level prior to ICP-MS detection. *Talanta, 207,* 120295. Doi: 10.1016/j.talanta.2019.120295

Faraji, M., Yamini, Y. & Gholami, M. (2019) Recent Advances and Trends in Applications of Solid-Phase Extraction Techniques in Food and Environmental Analysis. *Chromatographia 82,* 1207–1249. Doi: 10.1007/s10337-019-03726-9

Özdemir, S., Yalçın, M.S. & Kılınç, E. (2021) Preconcentrations of Ni(II) and Pb(II) from water and food samples by solid-phase extraction using Pleurotus ostreatus immobilized iron oxide nanoparticles. *Food Chemistry, 336,* 127675. Doi: 10.1016/j.foodchem.2020.127675

Mei, M., Pang, J., Huang, X. & Luo, Q. (2019) Magnetism-reinforced in-tube solid phase microextraction for the online determination of trace heavy metal ions in complex samples. *Analytica Chimica Acta, 1090,* 82-90. Doi: 10.1016/j.aca.2019.09.028

Khan, W.A., Arain, M.B. & Soylak, M. (2020) Nanomaterials-based solid phase extraction and solid phase microextraction for heavy metals food toxicity. *Food and Chemical Toxicology, 145,* 111704. Doi: 10.1016/j.fct.2020.111704

Mahandra, H., Singh, R. & Gupta, B. (2017) Liquid-liquid extraction studies on Zn(II) and Cd(II) using phosphonium ionic liquid (Cyphos IL 104) and recovery of zinc from zinc plating mud. *Separation and Purification Technology, 177,* 281-292. Doi: 10.1016/j.seppur.2016.12.035

Łukomska, A., Wiśniewska, A., Dąbrowski, Z. & Domańska, U. (2020) Liquid-liquid extraction of cobalt(II) and zinc(II) from aqueous solutions using novel ionic liquids as an extractants. *Journal of Molecular Liquids, 307,* 112955. Doi: 10.1016/j.molliq.2020.112955

Sorouraddin, S.M., Farajzadeh, M.A. & Dastoori, H. (2020) Development of a dispersive liquid-liquid microextraction method based on a ternary deep eutectic solvent as chelating agent and extraction solvent for preconcentration of heavy metals from milk samples. *Talanta, 208,* 120485. Doi: 10.1016/j.talanta.2019.120485

Hong, J., Liu, X., Yang, X., Wang, Y. & Zhao, L. (2022) Ionic liquid-based dispersive liquid–liquid microextraction followed by magnetic solid-phase extraction for determination of quinolones. *Microchimica Acta 189:8.* Doi: 10.1007/s00604-021-05077-5

Azzouz, A., Kailasa, S.K., Lee, S.S., Rascón, A.J., Ballesteros, E., Zhang, M. & Ki-Hyun, K. (2018) Review of nanomaterials as sorbents in solid-phase extraction for environmental samples. *TrAC Trends in Analytical Chemistry, 108,* 347-369. Doi: 10.1016/j.trac.2018.08.009

Su, H., Lin, Y., Wang, Z., Wong, Y.L.E., Chen, X. & Dominic Chan, T.W. (2016) Magnetic metal–organic framework–titanium dioxide nanocomposite as adsorbent in the magnetic solid-phase extraction of fungicides from environmental water samples. *Journal of Chromatography A, 1466,* 21-28. Doi: 10.1016/j.chroma.2016.08.066

Soylak, M., Acar, D., Yilmaz, E., El-Khodary, S.A., Morsy, M. & Ibrahim, M. (2017) Magnetic Graphene Oxide as an Efficient Adsorbent for the Separation and Preconcentration of Cu(II), Pb(II), and Cd(II) from Environmental Samples. *Journal of AOAC INTERNATIONAL, 100,* Pages 1544–1550. Doi: 10.5740/jaoacint.16-0230

Wan, Q., Liu, H., Deng, Z., Bu, J., Li, T., Yang, Y. & Zhong, S. (2021) A critical review of molecularly imprinted solid phase

extraction technology. *Journal of Polymer Research, 28,* 401. Doi: 10.1007/s10965-021-02744-2

Saygili Canlidinç, R., Turan, K. & Kalfa, O.M. (2022) Investigation of chromium preconcentration conditions by solid phase extraction method using activated carbon based ion-imprinted sorbent. *International Journal of Environmental Analytical Chemistry*. Doi: 10.1080/03067319.2022.2119141

Turan, K., Saygili Canlidinç, R. & Kalfa, O.M. (2022) Preconcentration of trace amount Cu(II) by solid-phase extraction method usingactivated carbon-based ion-imprinted sorbent. *Turkish Journal of Chemistry, 46:*2. Doi: 10.55730/1300-0527.3328

Turan, K., Saygılı Canlıdinç R. & Kalfa, O.M. (2018) Selective Preconcentration of Trace Amounts of Cu(II)With Surface-Imprinted Multiwalled Carbon Nanotubes. *Clean–Soil, Air, Water, 46,* 1700580. Doi: 10.1002/clen.201700580

Duman, S., Erbas, Z. & Soylak, M. (2020) Ultrasound-assisted magnetic solid phase microextraction of patent blue V on magnetic multiwalled carbon nanotubes prior to its spectrophotometric determination. *Microchemical Journal, 159,* 105468. Doi: 10.1016/j.microc.2020.105468

Saygili Canlidinç, R. (2022) Determination of the Cadmium Ions from Aqueous Solution Using EDTA Functionalized Prunus Dulcis L. Peels by Solid-Phase Extraction Method. *Bulletin Environmental Contamination Toxicology, 108,* 976–984. Doi: 10.1007/s00128-021-03450-x

Amiri-Yazani, T., Zare-Dorabei, R., Rabbani, M. & Mollahosseini, A. (2019) Highly efficient ultrasonic-assisted pre-concentration and simultaneous determination of trace amounts of Pb (II) and Cd (II) ions using modified magnetic natural clinoptilolite zeolite: Response surface methodology. *Microchemical Journal, 146,* 498-508. Doi: 10.1016/j.microc.2019.01.050

Iwase, M., Isobe, K., Zheng, L., Takano, S. & Sohrin, Y. (2023) Solid-phase extraction of palladium, platinum, and gold from water samples: comparison between a chelating resin and a chelating fiber with ethylenediamine groups. *Analytical Sciences, 39,* 695–704. Doi: 10.1007/s44211-023-00270-3

Jagirani, M.S. & Soylak, M. (2022) Deep eutectic solvents-based adsorbents in environmental analysis. *TrAC Trends in Analytical Chemistry, 157,* 116762. Doi: 10.1016/j.trac.2022.116762

Montoro-Leal, P., García-Mesa, J.C., Siles Cordero, M.T., López Guerrero, M.M. & Vereda Alonso, E. (2020) Magnetic dispersive solid phase extraction for simultaneous enrichment of cadmium and lead in environmental water samples. *Microchemical Journal, 155,* 104796. Doi: 10.1016/j.microc.2020.104796

Sajid, M., Nazal, M.K. & Ihsanullah, I. (2021) Novel materials for dispersive (micro) solid-phase extraction of polycyclic aromatic hydrocarbons in environmental water samples: A review. *Analytica Chimica Acta, 1141,* 246-262. Doi: 10.1016/j.aca.2020.07.064

Li, B., Zheng, J.Q. Guo, J.Z. & Dai, C.Q. (2020) A novel route to synthesize MOFs-derived mesoporous dawsonite and application in elimination of Cu(II) from wastewater. *Chemical Engineering Journal, 383,* 123174. Doi: 10.1016/j.cej.2019.123174

Saygili Canlidinç, R., Kalfa, O.M., Üstündağ, Z. & Erdoğan Y. (2017) Graphene oxide modified expanded perlite as a new sorbent for Cu(II) and Pb(II) prior to determination by high-resolution continuum source flame atomic absorption spectrometry. *Separation Science and Technology, 52:13,* 2069-2078. Doi: 10.1080/01496395.2017.1328443

Manousi, N., Rosenberg, E., Deliyanni, E., Zachariadis G.A. & Samanidou, V. (2020) Magnetic Solid-Phase Extraction of Organic Compounds Based on Graphene Oxide Nanocomposites. *Molecules, 25,* 1148. Doi: 10.3390/molecules25051148

Özkalkan, H. & Saygili Canlidinç, R. (2021) Investigation of the Conditions for Preconcentration of Cadmium Ions by Solid Phase Extraction Method Using Modified Juglans regia L. Shells. *Journal of AOAC INTERNATIONAL, 104*, 1246–1254. Doi: 10.1093/jaoacint/qsab042

Garg, R., Garg, R., Sillanpää, M., A., Khan, M.A., Mubarak N.M. & Tan, Y.H. (2023) Rapid adsorptive removal of chromium from wastewater using walnut derived biosorbents. *Scientifc Reports 13*, 6859. Doi: 10.1038/s41598-023-33843-3

Ma, J., Wu, G., Li, S., Tan, W., Wang, X., Li, J. & Chen, L. (2018) Magnetic solid-phase extraction of heterocyclic pesticides in environmental water samples using metal-organic frameworks coupled to high performance liquid chromatography determination. *Journal of Chromatography A, 1553,* 57-66. Doi: 10.1016/j.chroma.2018.04.034

Ma, J., Yao, Z., Hou, L., Lu, W., Yang, Q., Li, J. & Chen, L. (2016) Metal organic frameworks (MOFs) for magnetic solid-phase extraction of pyrazole/pyrrole pesticides in environmental water samples followed by HPLC-DAD determination. *Talanta, 161*, 686-692. Doi: 10.1016/j.talanta.2016.09.035

CHAPTER VI

Electrochemical biosensors, types, applications and future aspects

Elif Esra ALTUNER[1]
Fatih ŞEN[2]

Introduction

All living things have to adapt to nature and the living conditions it brings to continue their lives. Otherwise, living things cannot continue and lose their vitality as a result of natural selection. The adaptation of living things to the differences and conditions brought by nature creates the so-called in vitro state of sensors [1]. This means that living things increase their sensitivity by developing

[1] Assist.Prof.Dr., Program of Medical Laboratuary and Techniques, Department of Medical Services and Techniques, Avrupa Vocational School, University of Kocaeli Health and Technology, 41090, Kocaeli, Turkey
[2] Prof. Dr., Sen Research Group, Department of Biochemistry, University of Dumlupinar, 43000 Kutahya, Turkey

sensitivity to the conditions of nature. For example; Butterflies' discovery of pheromones secreted by their partners, eels' perception of foreign substances in the form of droplets in water with a weight of hundreds of thousands, dogs' sense of smell are one hundred thousand times ahead of humans [1], [2]. The sensitivity development of living things explains the basic functioning of sensors.

Sensors are systematically classified as active sensors and passive sensors [3]–[5]. Active sensors are natural sensors that produce their own energy. Active sensors include millimeter wave radar, synthetic array radar (SAR and inverse SAR), and imaging radars such as microwave radars. Passive sensor systems rely on natural or man-made radiation from the target for detection. The passive sensor encompasses the acoustic sensor, the thermal sensor (electro-optical system such as infrared search and monitoring or forward-looking infrared sensor) and electronic support measure (ESM). Passive sensors are; It is a man-made sensor system that cannot produce its own energy. For example, electronic and electrochemical sensors, thermal sensors, optical sensors, etc. are in this group [5]. It is an important factor to get a continuous result in sensors [6]. One of the important advantages of the sensors is that the tip of the sensors is simple, practical, economical and fast [5], [6], [7]. There are various types of sensors in terms of structure. These species are; biosensors , chemical sensors [8], colorimetric sensors [8], [9], fluorimetric [10] and optical sensors [11], aptasensors [6], [12], [13], microbial sensors [14], [15] and electronic and electrochemical sensors [6], [16]. Electrochemical sensors are faster sample-response time, more intense sensitivity and more practical than normal sensors [17] [18]. For this reason, researchers tend to focus more on electrochemical sensors in sensor studies [6], [18].

Electrochemical sensors are sensors that work with electrical energy and receive a permanent signal result through electricity. It is intended for the diagnosis of various chemical analytes with electrical energy [18]. Electrochemical sensors are an important

method of choice for environmental monitoring, traffic and medical monitoring, and control in metabolic research [19]. According to the data in the literature, this type of sensor works in different temperature matrices (usually from -30 to 1600 ^{o}C) according to the structure and type of electrolytes used [20]–[22]. If there is an aqueous solution in electrochemical sensors, this temperature can go up to 140 ^{o}C [23], [24]. Electrochemical sensors are divided into types within themselves as amperometric, potentiometric or impedimetric [25]. It is important to pay attention to temperature, pressure, chemical environment and external factors, as all sensors are generally affected by measurement conditions. Electrochemical sensors generally operate at low temperatures [26], [27].

In this review, the structure of electrochemical sensors and their working systems are explained in detail with reference to the relevant places. At the same time, the future place of electrochemical sensors, the perspective from the past to the present, what kind of future studies will be supported and the application areas of electrochemical sensors are explained.

1.Electrochemical sensors and types

Electrochemical sensors are miniaturized devices that selectively and reversibly respond to chemical compounds or ions and generate concentration-dependent electrical signals. It contains the largest group of chemical sensors in terms of diversity [28], [29]. The electrochemical sensor converts the data received with electrical energy into digital data with a transducer tool. These data are then permanently converted into signals and recorded in the detector [29]. Figure 1 shows the working mechanism of an electrochemical sensor.

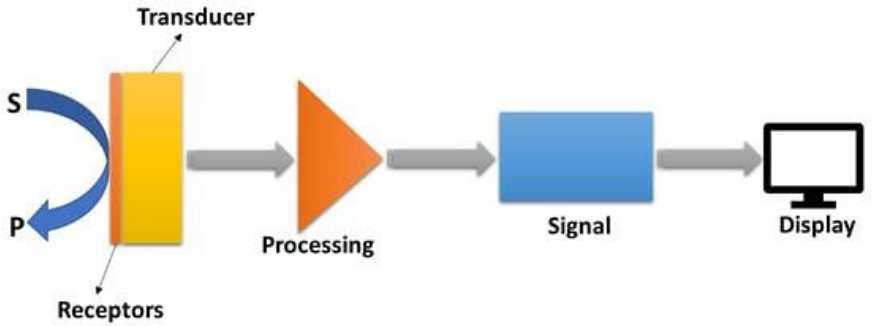

Figure 1. *The illustration structure of one electrochemical sensor [29].*

"Reprinted (adapted) with permission from [29] Copyright (2023) MDPI–Chemosensors"

If a receptor (eg DNA, antibodies and enzymes) is of biological origin, this device is called a biosensor. The analyte binds to the receptor to convert the recognition [30], [31]. Maintaining a high level of specificity for the target analyte in the presence of chemical species that might interfere is the major need for sensors. This is essential to prevent undesirable positive outcomes. Another crucial component of the sensors is the transducer, which transforms the signal produced by the interaction of the receptor and the analyte into a value that can be read [32]. As a result, catalytic or affinity-based sensors can be used as both chemical and biological sensors. In the case of enzymatic, DNAzyme, or functionalized surfaces that may execute redox reactions under specific circumstances, catalytic sensors employ catalytic activity to create signals [33], [34]. Analyte-receptor interactions that are extremely specific, such as those involving nucleic acids (such as ssDNA and aptamers), antibodies and antigens, or host-guest interactions, are the foundation of affinity-based devices. Optical, gravimetric, or electrochemical techniques can be employed to monitor identification event, depending on the type of transducer utilized [35], [36].

2.Types of electrochemical sensors

Sensors of electrochemical applications can be divided into many derivatives such as potentiometric, impedimetric, amperometric, photoelectrochemical, and chemiluminescence, etc. according to their application areas. In the operation mechanism of potentiometric sensors, if there is no current at the interface in the interaction of the sensor and analyte, a Nernstian equilibrium occurs. In amperometric sensors, the voltage between the electrodes is provided to initiate electrochemical reduction or oxidation according to the analyte concentration accordin to cottrell equilibrium (Eq.1) [29].

$$i = nFAc_j\sqrt{D_j / \prod t} \quad \text{(Eq.1) [29]}$$

where:

i = Current (ampere unit);
n = Electrons' number;
F = Faraday constant (96,485 C/mol);
A = Area of the (planar) electrode in cm^2;
c^0_j = Initial concentration of the reducible analyte {\displaystyle j}in mol/cm^3;
D_j = Diffusion coefficient for species {\displaystyle j}in cm^2/s;
t = Seconds.

2.1.Potentiometric sensors

Potentiometric sensors are an electrochemical analytical technique based on ion-selective electrodes. It is found in almost every laboratory because it is practical, inexpensive and simple [37], [38]. Analyzing the ion content in real (and synthetic) samples can easily interpret electromotive force (EMF) signals versus time under near-zero current conditions [39]. The conversion of an ion exchange event into a voltage signal provides in-depth information on ISE [40]. The electrode is designed to detect any perturbation occurring in the local equilibrium created at the interface between the ion selective membrane (ISM) and the sample solution [41]. This allows

for a sufficiently large perturbation. Consequently, the membrane potential is affected by a change in the activity of the primary ion in the bulk sample solution [41]–[44]. As shown in Figure 2a, the electromagnetic current (EMF) of the electrochemical cell is due to the difference between this potential and that provided by the reference electrode. However, the concentration dependence of the potentiometric signal on the activity of the primary ion is defined using the Nernst equation. Also, a logarithmic activity plot of ISE (aqueous) versus EMF used to determine unknown ion concentrations in (aqueous) samples is self-contained (Fig. 2b) [44].

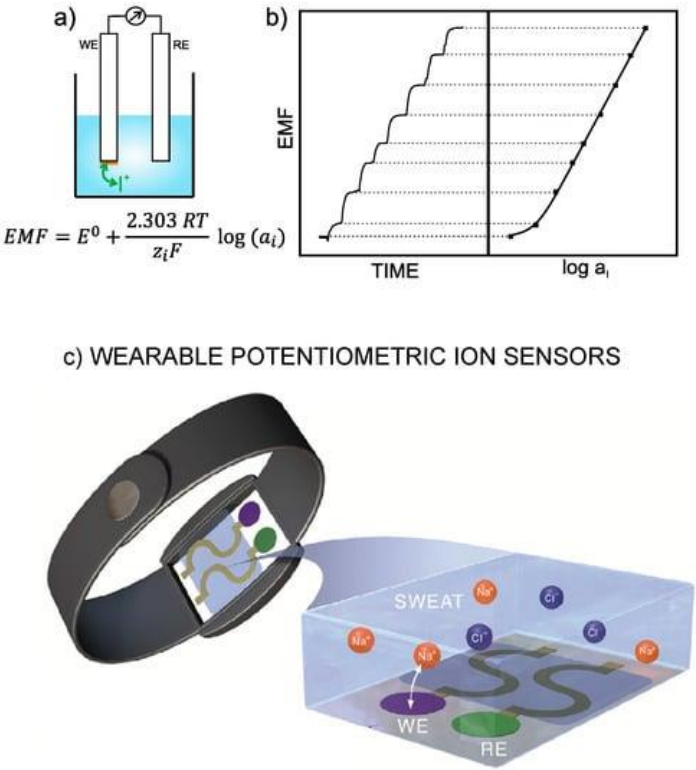

Figure 2. *(a) Illustration of a general electrochemical cell, with a potentiometric electrode (also known as a working electrode, WE, or indicator electrode) comprising an ion-selective membrane*

(drawn in orange) and a reference electrode (RE). The potential shown by WE depends on the concentration of the ion analyte in the bulk solution. In this case, I^+, represented as a cation, is the potential constant provided by RE. Electromotive force (EMF), ion selective electrode (ISE). (b) Typical traces of the dynamic potential response of the ISE for increasing ion analyte (in this case cation) concentrations, with the corresponding calibration plot (potential vs. logarithmic activity). Additional equation: Nernst equation, E_0 is the standard potential of the cell, T is the temperature, R is the gas constant, zi is the charge of the analyte and F is the Faraday constant. For the calibration curve, E_0 corresponds to the intersection and 2.303 RTziF to the slope. (c) Interaction of target ion (in this case Na^+) with sweat [45].

"Reprinted (adapted) with permission from [45] Copyright (2023) MDPI–Sensors"

2.2.Conductometric sensors

Conductometric biosensors consisting of micro-electrodes are capacitors. In conductometric biosensors, the measurement is based on the change in conductivity of the immobilized film with the binding of the analyte to the selective agent. A current proportional to the analyte concentration is generated as the conductivity of the immobilized film changes [46]. Conductometric sensors are generally bipolar [47]. It is available with different equivalent circuit systems in different combinations [48]. This situation is shown in Figure 3. As seen in Figure 3, the samples interact with the selective layer arranged in a lateral configuration. Some types of conductometric sensors are short-circuited. This is because chemicals are found in gas or non-conductive liquids, which are the application area of resistors [48], [49]. For this reason, excitation signals also stimulate while measuring in conductometric sensors [48].

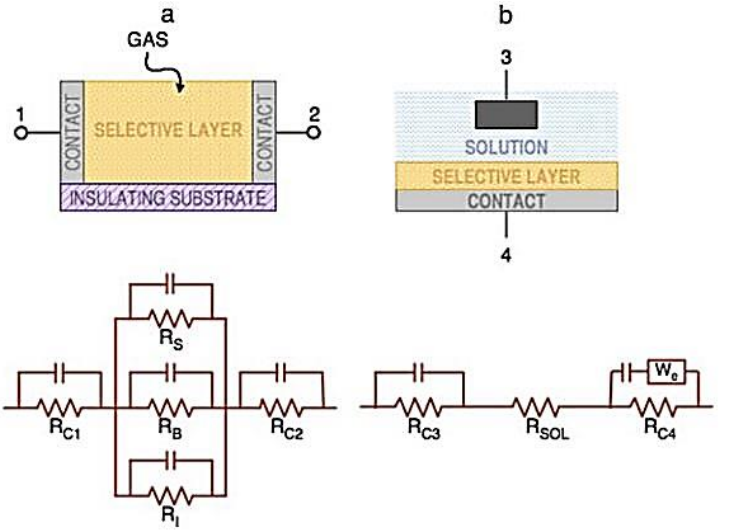

Figure 3. *General chemiresistors and the circuits that correspond to any one of the five resistances can be regulated by chemical contact in (a) lateral configuration; (b) impedimetric chemiresistor, where capacitance CB is chemically manipulated [47].*

"Reprinted (adapted) with permission from [47] Copyright (2023) Springer– Princ. Chem. Sensors"

2.3.Amperometric sensors

The applied voltage acts as a driving factor for electrocatalytic redox processes, which generate electric currents proportional to the analyte's concentration [50]. Amperometric measurements are a very accurate and precise analytical technique. For fundamental instrumentation, a regulated potential system is needed, and an electrochemical cell is formed by two electrodes submerged in an electrolyte with the appropriate composition [51]. A three-electrode cell using one electrode as the reference electrode is a more complex and more common method [51]. However, a reference electrode (such as gold/gold chloride or Hg/Hg_2Cl_2) is one that maintains a constant potential compared to a working electrode

[52]. The electrode where the desired reaction takes place is referred to as a working electrode. As an additional electrode, inert conductive materials (such platinum or graphite) are frequently utilized [50]. A supporting electrolyte is required in controlled potential investigations to avoid electromigration effects, reduce the solution's resistance, and maintain a steady ionic strength. In-depth descriptions of theoretical issues and practical strategies are provided.

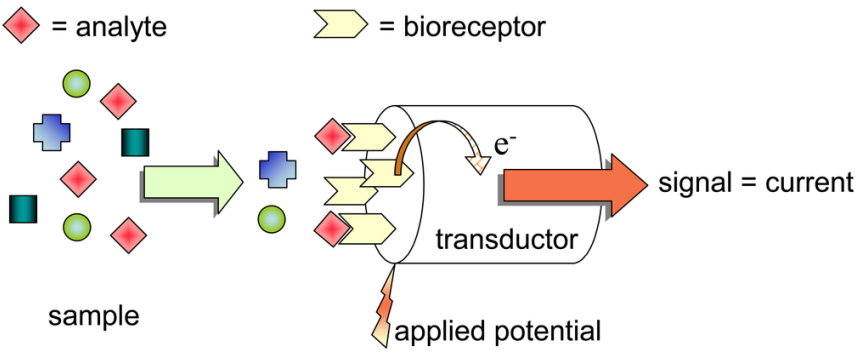

Figure 4. *A illustration showing how an amperometric biosensor mechanisms [53].*

"Reprinted (adapted) with permission from [53] Copyright (2023) MDPI – Sensors"

Using amperometric biosensors, typically the analyte is involved in or followed in a redox reaction by measuring the current in an electrochemical cell. At an electrode, the oxidation state is changed by the analyte or related species through a biochemical reaction. The electron flow is followed in proportion to the amount of electrochemically converted species at the electrode [53]. The working principles of an amperometric biosensor are shown in Figure 4.

3.Applications of electrochemical sensors

For the examination of biological, environmental, industrial, and pharmaceutical species, electrochemical sensors have long been

preferred [29]. This is because of their long-term reliability, high sensitivity and accuracy, speed, and ease of downsizing. For over two decades, numerous nanomaterials with outstanding properties have been used to improve analytical performance in electrochemical analysis, such as conductive polymers, , metal oxides, metals, and carbon-based and metal-organic nanomaterial frameworks [29], [54], [55]. This modification increases the specificity of electrochemical sensors while enabling the use of bio-inspired receptors as well as recognition molecules such as aptamers, antibodies, and enzymes. This aims to provide high electrocatalytic activity for certain electrochemical processes [29], [56]. The sensitivity of these tests can be increased by changing the surface shape and structure, increasing the electrical conductivity and surface area. Due to recent developments in single molecule detection, in vivo analysis, wearable technology, and point-of-care diagnostics, electrochemical sensors have been more widely used [56]. Electrochemical sensors have high sensitivity providing low limit of detections (LODs) and limit of quantifications (LOQs) ideal for flow analysis and warning systems due to their fast analytical response; their simplicity allows for an almost unlimited number of geometries, materials and configurations; and ease of use is an important advantage. As an added advantage, electrochemical biosensors are fast data acquisition, rapid detection of the substrate, high sensitivity, high specificity, and economy [29]. Biosensors consist of three main components: (i) biocomponent or biological detection systems (ii) transducers and (iii) signal processing systems [57]–[60]. Examples of biocomponents are DNA or RNA probes, cells, antibodies, binding molecules, and organelles. Transducers, on the other hand, are devices that convert the data obtained as a result of the interaction of the analyte with biocomponents into electrical signals [29]. The signal processing system is a detector and is the device that converts them into readable form [29], [61].

3.1.Electrochemical sensors for biomolecules

They are detected by biological or physiological electrochemical sensors to measure the biological activity of small size biomolecules such as hormones, enzymes or nucleic acids, catalyze cellular processes and transfer genetic information [60], [62]. Although it is difficult technology to create a sensing technology for biomolecules, biomolecular methods such as polymer chain reaction (PCR) and gel electrophoresis have been invented. However, despite their certainty, they have disadvantages such as large reagent requirements and laboriousness or long-term requirements [63], [64]. For this reason, the method of determining biomarkers by electrochemical sensors has been used. Figure of *Altuner et al* as seen in Fig. 5, an electrochemical aptasensor has been developed for the detection of 3.3 5.5 tetramethyl benzidine (TMB) molecules [6]. According to Figure 5, the TMB molecule is trapped in porous mesoporous nanoparticles, and its fixation is ensured by leaving the pores using agents that mimic enzymatic systems and ions such as phosphate.

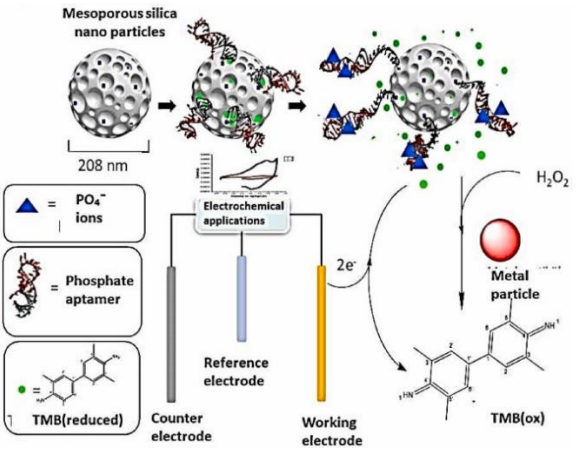

Figure 5. *TMB biyomokülünün tespitine yönelik geliştirilen bir elektrokimyasal aptamer bazlı sensör sistemi [6].*

"Reprinted (adapted) with permission from [6] Copyright (2023) ,Elsevier– Chemosphere"

3.2.Enzyme-based electrochemical sensor applications

Living organisms are organic catalytic molecules that makeup enzymes. They can accelerate biological processes by reducing the activation energy and enable substrates to be converted into products at least ten million times faster in cellular metabolism [65]. Substrate conversion via enzymes is highly specific. While some enzymes are selective for a single substrate, others might have an impact on a number of substrates that have structural similarities. An enzyme-catalyzed reaction can only start once the enzyme and its substrate have formed a complex. The procedures they catalyze do not alter or recycle enzymes. The enzyme also starts forward or backward motion[29], [65]. Enzymatic activity monitoring is very popular. Numerous analytical techniques such as mass spectrometry [66], electrochemical techniques [6], Raman spectroscopy [67] and spectrophotometry have been used to determine enzyme activity. Electrochemical procedures are cheaper and faster than other analytical techniques that may require better pretreatment, filtration and a skilled operator [68]. Enzymatic sensors that allow an enzyme to be immobilized on an electrode are then used to measure the concentration of the matched substrate. The technique of immobilization and the mediator used are the two factors that primarily distinguish enzyme-based biosensors [69].

3.3.Electrochemical (bio)sensors for health applications

The prevalence of diabetes and the use of biosensors by diabetics contribute significantly to business profitability worldwide [29]. Diagnosing diabetes preventively and quickly is becoming more popular. The development of biosensors has made it possible to determine blood sugar over a wide temperature range of various interfering substances. The detection of glucose by zinc-oxide (ZnO) nanorods is an inexpensive, safe, accurate, fast, and safe method [29], [70]. Due to increasing sensitivity and accuracy within a one-minute sample volume, as well as the widespread usage of biosensors in the field of diabetes, a significant market demand is anticipated in the next years. Due to their tremendous capacity for

monitoring, treatment, diagnosis, well-being, and well-being, portable electronic gadgets are an essential part of the whole health system [71], [72]. Users will strengthen preventative measures and obtain a better understanding of their wellbeing by integrating accessible treatment technology in hospitals and urgent care facilities [29]. The market is leading to increased use of biosensors in technological advances and various applications (Figure 6) [73]. Wearable biosensors have made people's lives easier.

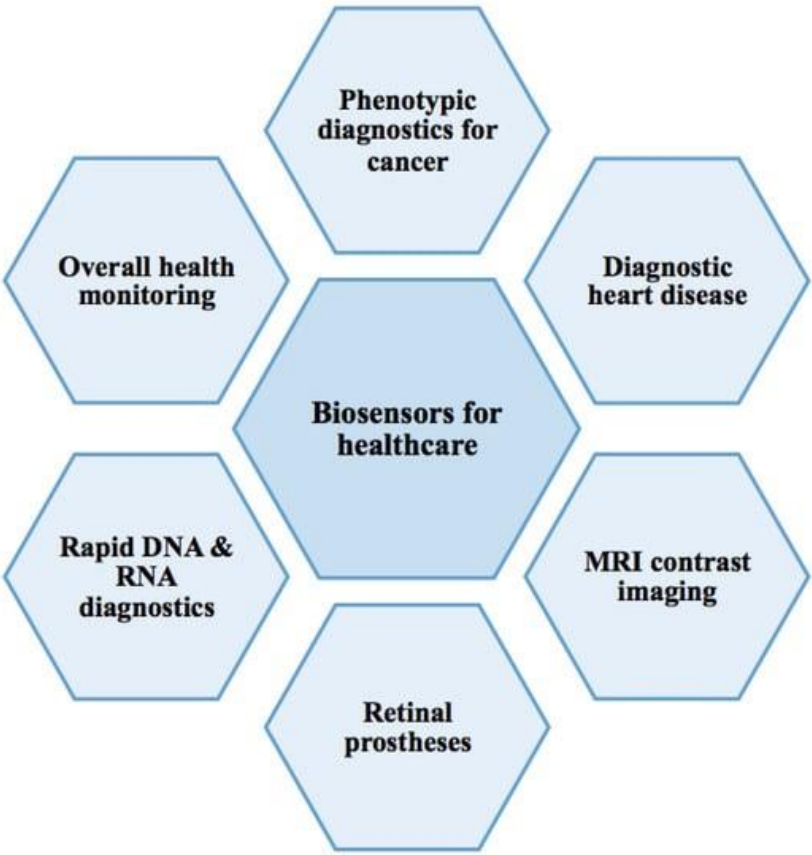

Figure 6. *The health areas of electrochemical biosensors [29].*
"Reprinted (adapted) with permission from [29] Copyright (2023) MDPI–Sensors"

3.4.Electrochemical sensors for enviromental areas

Due to stricter environmental controls, demand for more advanced chemical sensors for chemical pollutant emissions and discharges is increasing [74]. Electrochemical sensors show great promise for this task. The effect of surface adsorption of impurities is the most serious problem causing a non-repeatable response [35], [75].

Three main areas of development in technology attempting to improve the performance of these devices are discussed: advances in sensor design and measurement techniques, techniques to achieve new electrode selectivity, and the use of micro miniaturization and microelectronic fabrication techniques [74]. Recent applications for the measurement of toxic metals, organics, and gases, including volatile organic compounds (figure 7), are an important step today and will lead to more serious environmental problems in the future.

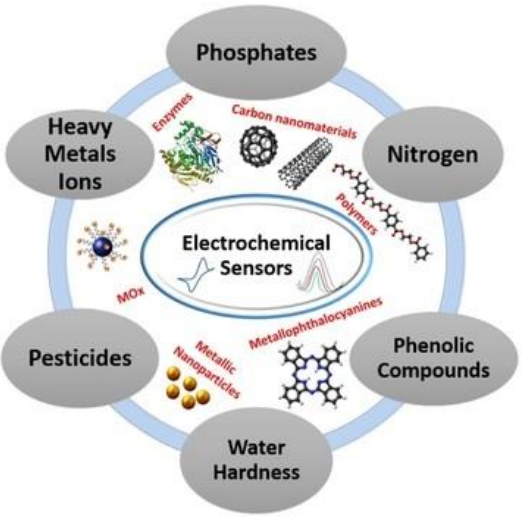

Figure 7. *Electrochemical sensor applications for enviromental areas [76]*

"Reprinted (adapted) with permission from [76] Copyright (2023) MDPI–Sensors"

3.5.Anatlytical applications of electrochemical sensors

Electrochemical approaches have been demonstrated to offer higher benefits over other analytical techniques due to their mobility and inexpensive cost. The majority of large businesses have accepted this form of analytical equipment due to its swift and concentrated evaluation. Electroanalytical sensors are anticipated to be the next generation of analytical systems because of their adaptability and simplicity [29]. Therefore, many scientists and researchers have been concentrating on the invention and manufacture of electroanalytical sensors with high selectivity and sensitivity for a variety of chemicals, including drugs, food, and environmental toxins. *Karimi-Maleh et al.* [77] recently reviewed the mechanism and several electroanalytical applications of DNA, enzymatic, and electrocatalytic approaches.

3.6.Electrochemical sensors for nanotechnology

Nanotechnology has made significant progress in the sensor sector during the past several years [1]. It is believed that the use of such technologies and the use of nanoscale materials improve sensor performance [6]. Numerous unusual and fascinating physical and chemical properties offered by nanomaterials have been found [1,6]. Low-dimensional nanometer-sized materials and systems have opened up a brand-new area of research in condensed-matter physics in recent years [78]. There are many more types of materials that can be utilized to make nanosensors in addition to the ones described above [29]. Due to its many applications, carbon is regarded as a unique element. Carbon is an intriguing element that can be found in many different materials, such as graphite, diamond, fullerenes, and graphene [79]. Previous studies have covered some of the most important and recent developments made possible by the use of carbon-based nanostructures in nanotechnology for the development of chemical and biological sensors as well as their use in the pharmaceutical and medicinal industries [29]. Nanocomposites are employed to improve the sensitivity, selectivity, and repeatability in the majority of reported biosensors. Nanocomposites are solid

materials made up of several phase domains, at least one of which possesses nanoscale characteristics. Interest has grown recently as a result of the unique and interesting characteristics of nanocomposites [29], [79]. Nanocomposites have a high surface-to-volume ratio, reactive capacity, biocompatibility, and high adsorption, which are all advantageous in the production of sensors. Biomolecule immobilization, biomolecule labeling, and an increase in electron transfer rate are all facilitated by nanocomposites. The most popular nanocomposites used to modify the electrode surface include conducting polymers, nanofibers, graphene, carbon nanotubes (CNTs), metal-organic frameworks (MOFs), and nanoparticles (Nps). MOFs can be employed as electrocatalysts for CO2 reduction reactions (CO2RR) because of their equally distributed metal centers [29]. The basic design of an electrochemical sensor based on carbon nanomaterials for identifying metabolic illness indicators is shown in Figure 6.

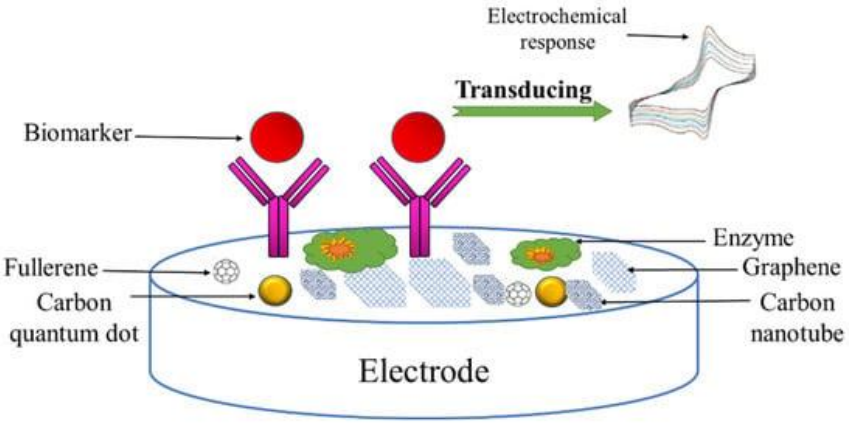

Figure 8. *An electrochemical biosensor based on nanoparticles is depicted in this schematic illustration [29].*

"Reprinted (adapted) with permission from [29] Copyright (2023) MDPI– Sensors"

4.Future prospects

A potential field of study is electrochemical sensor technology [29]. Selection continues to be at the heart of the majority of the issues in this field, and that must be acknowledged. However, when direct detection in undamaged samples is possible, electrochemical sensors' rapid analytical speed and ability to detect incredibly minute quantities without appreciably affecting the sample remain extremely desired properties [80].

Future biosensor techniques could result in the development of a cell-friendly analyte for point-of-care and precise medical diagnostics. Research into biology has substantially improved thanks to the introduction of electrochemical sensors [81], [82]. Additional advantages include sensitivity, selectivity, and processing speed, all of which will assist upcoming industries. As a result, advanced large-scale systems for disease diagnosis and monitoring may employ quick, non-destructive, and scalable electrochemical sensors. The use of arrays to monitor a wide range of organic and inorganic pollutants, the creation of diverse biological identification materials, microelectronic industrial breakthroughs, and micro- and disposable sensors are only a few examples of recent developments in this field. For monitoring a range of pollutants, flow-injection systems and online systems have also been developed. Nanomaterials research has recently made improvements that have improved sensor functionality. Building multianalyte detection systems with sensor arrays might be helpful for managing pollution as well as for therapeutic and diagnostic monitoring [29].

5.Conclusion

In this review article, after the electrochemical sensors are described in detail, the types, application areas and future role of electrochemical sensors are mentioned with references to the relevant places. Electrochemical sensors are sensors that work with electrical energy and receive a permanent signal result through electricity. It is intended for the diagnosis of various chemical

analyzes with electrical energy. Among electrochemical sensors, amperometric, potentiometric and conductometric sensors are the most known sensor types. Amperometric measurements are an analytical method with high accuracy and precision; the applied voltage acts as a driving force for electrocatalytic redox reactions that produce electric currents proportional to the concentration of the analyte. Potentiometric sensors are an electrochemical analytical technique based on ion-selective electrodes. Conductometric biosensors consisting of micro-electrodes are capacitors. In conductometric biosensors, the measurement is based on the change in conductivity of the immobilized film with the binding of the analyte to the selective agent. A current proportional to the analyte concentration is generated as the conductivity of the immobilized film changes. All sensor types have found the opportunity to work in many scientific departments due to their fast, practical, cheap and easy portability. The most widely applied applications are in the field of health and environment, nanotechnological studies, detection of biomolecules, analytical kits and enzymatic sensor studies. While sensor studies for the transfer of DNA and RNA, hormones, nucleic acids and genetic information are applied in the detection of biomolecules, sensor studies on enzymes are applied in enzymatic studies. Electrochemical sensors are used in environmental areas for the detection of toxic metals, organics, and gases, including volatile organic compounds, while in the health field, electrochemical sensors are used in applications such as the diagnosis of phenotypic diseases such as cancer, the diagnosis of pests in the body, DNA and RNA diagnostics, etc. Therefore, as technology develops and scientific studies increase, the application area of sensors will increase even more in the future

REFERENCES

1. Altuner, E. E.; Akin, M.; Bayat, R.; Bekmezci, M.; Burhan, H.; Sen, F. “Challenges in commercialization of carbon nanomaterial-based sensors,” *Carbon Nanomater. Sensors Emerg. Res. Trends Devices Appl.*, 2022, 381–392.

2. Bulut, Y. “Biyosensörlerin Tanımı ve Biyosensörlere Genel Bakış,” 2011, 16–18.

3. Blackman S. S. P. R. “Design and analysis of modern tracking systems,” 2023.

4. Hovanessian, S. A. “Introduction to sensor systems,” 2023.

5. Ng, G. W.; Ng, K. H. “Sensor management – what, why and how,” *Inf. Fusion*, 2000, 1, 2, 67–75.

6. Altuner, E. E.; Ozalp, V.C.; Yilmaz, M.D.; Sudagidan, M.; Acar, E.E.; Tasbasioglu,B; Aygun, A.; Sen, F. “Development of electrochemical aptasensors detecting phosphate ions on TMB substrate with epoxy-based mesoporous silica nanoparticles,” *Chemosphere*, 2022, 297, 134077.

7. Alizadeh, M.; Asrami, P.N.; Altuner, E.E.; Gulbagca, F.; Tiri, R.N.E.; Aygun, A.; Kaynak, I; Sen, F.; Cheraghi, S. “An ultra-sensitive rifampicin electrochemical sensor based on Fe3O4 nanoparticles anchored Multiwalled Carbon nanotube modified glassy carbon electrode,” *Chemosphere*, 2022, 136566.

8. Hassani, A.; Khoshfetrat, A . B.; Rahbarghazi, R.; Saka, S. “Collagen and nano-hydroxyapatite interactions in alginate-based microcapsule provide an appropriate osteogenic microenvironment for modular bone tissue formation,” *Carbohydr. Polym.*, 2022, 277, 118807.

9. Wu, Y.; Feng, J.; Hu, G.; Zhang, E.; Yu, H. H.; “Colorimetric Sensors for Chemical and Biological Sensing Applications,” *Sensors*, 2023, *23*, 5, 2749.

10. Qin, M.; Li, J.; Song, Y. “Toward High Sensitivity: Perspective on Colorimetric Photonic Crystal Sensors,” *Anal. Chem.*, 2022, 94, 27, 9497–9507.

11. Bahreyni, A.; Yazdian-Robati, R.; Ramezani, M.; Abnous, K.; Taghdisi, S. M.; “Fluorometric aptasensing of the neonicotinoid insecticide acetamiprid by using multiple complementary strands and gold nanoparticles,” *Microchim. Acta*, 2018, 185, 5, 1–7.

12. Hernandez, F. J.; Ozalp, V. C.; “Graphene and Other Nanomaterial-Based Electrochemical Aptasensors,” *Biosensors*, 2012, 2, 1, 1–14.

13. Bayramoglu G.; Ozalp, V. C.; Oztekin, M.; Arica, M. Y. “Rapid and label-free detection of Brucella melitensis in milk and milk products using an aptasensor,” *Talanta*, 2019, 200, 263–271.

14. Saratale, R. G.; Karuppusamy, I.; Dattatraya, G.; Saratale, G.D.; Pugazhendhi, A.; Kumar, G.; Park, Y.; Ghodake, G.S.; Bharagava, R.N.; Banu, J.R.; Shin, H.S. “A comprehensive review on green nanomaterials using biological systems: Recent perception and their future applications,” *Colloids and Surfaces B: Biointerfaces*, 2018, 170, 20–35.

15. Chu, N.; Liang, Q.; Hao, W.; Jiang, Y.; Liang, P.; Zeng, R. J. “Microbial electrochemical sensor for water biotoxicity monitoring,” *Chem. Eng. J.*, 2021, 404, 127053.

16. Ozalp, V. C.; Karabiyik, G.; Bayrac, A. T.; Guvenc Tuna, B. “Graphene-Based Electrochemical Aptasensors,” in *Handbook of Graphene, Biosensors and Advanced Sensor*, 2019,University of Warsaw, 6, 465.

17. Dunkelberger, K. A. “Hypothesis-driven distributed sensor management,” 19942232, 79–90.

18. Zia, A.I.; Mohd Syaifudin, A.R.; Mukhopadyay, S.C.; Yu, P.L.; Al-Bahadly,I.H.; Gooneratne, C.P.; Kosel, J.; Liao, T.-S. “Electrochemical impedance spectroscopy based MEMS

sensors for phthalates detection in water and juices," *J. Phys. Conf. Ser.*, 2013, 439, 012026.

19. Sofen, L. E.; Furst, A. L. "Perspective—Electrochemical Sensors to Monitor Endocrine Disrupting Pollutants," *J. Electrochem. Soc.*, 2020, 167, 3, 037524.

20. Gao, L.; Zhou, M.; Zheng, Y.; Gu, H.; Chen, H.; Guo, L. "Effect of zinc oxide on yttria doped ceria," *J. Power Sources*, 2010, 195, 10, 3130–3134.

21. Rey, J. F. Q.; Muccillo, E. N. S. "Lattice parameters of yttria-doped ceria solid electrolytes," *J. Eur. Ceram. Soc.*, 2004, 24, 6, 1287–1290.

22. Okuyama, Y.; Nagamine, S.; Nakajima, A.; Sakai, G.; Matsunaga, N.; Tahahashi, F.; Kimata, K.; Oshima, T.; Tsuneyoshi, K. "Proton-conducting oxide with redox protonation and its application to a hydrogen sensor with a self-standard electrode," *RSC Adv.*, 2016, 6, 40, 34019–34026.

23. Zhang, Y.; Liu, S.; Wang, L.; Qin, X.; Tian,J.; Lu, W.; Chang, G.; Sun, X. "One-pot green synthesis of Ag nanoparticles - graphene nanocomposites and their applications in SERS , H 2 O 2 , and glucose sensing," *RSC Adv.*, 2011, 2, 2, 538–545.

24. Dutta, A. K.; Maji, S.K.; Sritastawa, D.N.; Mondal, A.; Biswas, P.; Paul, P.; Adhikary, P. "Synthesis of FeS and FeSe nanoparticles from a single source precursor: A study of their photocatalytic activity, peroxidase-like behavior, and electrochemical sensing of H 2O 2," *ACS Appl. Mater. Interfaces*, 2012, 4, 4, 1919–1927.

25. Xu, J.; Wang, Y.; Hu, S. "Nanocomposites of graphene and graphene oxides: Synthesis, molecular functionalization and application in electrochemical sensors and biosensors. A review," *Microchim. Acta*, 2016, 1841, 184, 1, 1–44.00604-016-2007-0.

26. Pejcic, B.; De Marco, R. “Impedance spectroscopy: Over 35 years of electrochemical sensor optimization,” *Electrochim. Acta*, 2006, 51, 28, 6217–6229.

27. Naveen, M. H.; Gurudatt, N. G.; Shim, Y. B. “Applications of conducting polymer composites to electrochemical sensors: A review,” *Appl. Mater. Today*, 2017, 9, 419–433.

28. Lee, C. W.; Suh, J . M.; Jang, H. W. “Chemical Sensors Based on Two-Dimensional (2D) Materials for Selective Detection of Ions and Molecules in Liquid,” *Front. Chem.*, 2019, 7, 490901.

29. Baranwal, J.; Barse, B.; Gatto, G.; Broncova, G.; Kumar, A., “Electrochemical Sensors and Their Applications: A Review,” *Chemosens.* 2022,. 10, 363.

30. Chadha U.; Bhardwaj, P.; Rawat, P.; Agarwal, R.; Gupta, I.; Panwaji, M.; Singh, S.; Aguja, C.; Selvaraj, S.K.; Banavoth, M.; Sonar, P.; Badoni, M.; Chakrovorty, A. “Recent progress and growth in biosensors technology: A critical review,” *J. Ind. Eng. Chem.*, 2022 109, 21–51.

31. Nguyen, T. H.; Hilton, J. P.; Lin, Q. “Emerging applications of aptamers to micro- and nanoscale biosensing,” *Microfluid. Nanofluidics*, 2009, 6, 3, 347–362.

32. Hierlemann, A.; Gutierrez-Osuna, R. “Higher-order chemical sensing,” *Chem. Rev.*, 108, 2, 563–613.

33. Cardoso, R. M.; Pereira, T.S.; Facure, M.H.M.; Dos Santos, D.M.; Mercenta, L.A.; Mattoso, L.H.C.; Correa, D.S. “Current progress in plant pathogen detection enabled by nanomaterials-based (bio)sensors,” *Sensors and Actuators Reports*, 2022, 4, 100068.

34. Wei, D.; Bailey, M. J. A.; Andrew, P.; Ryhänen, T. “Electrochemical biosensors at the nanoscale,” *Lab Chip*, 2009, 9, 15, 2123–2131.

35. Naresh, V.; Lee, N. “A Review on Biosensors and Recent Development of Nanostructured Materials-Enabled Biosensors,” *Sensors,* 2021, 21, 1109.

36. Ahmad, R.; Griffete, N.; Lamouri, A.; Felidj, N.; Chehimi, M. M.; and Mangeney, C. “Nanocomposites of Gold Nanoparticles@Molecularly Imprinted Polymers: Chemistry, Processing, and Applications in Sensors,” *Chem. Mater.,* 2015, 27, 16, 5464–5478.

37. Mohan, C.; Kumar, V.; “Ion-selective Electrodes Based on PVC Membranes for Potentiometric Sensor Applications: A Review,” *Int. J. Membr. Sci. Technol.*, 2021, 8, 2, 76–84.

38. Hu, J.; Stein, A.; Bühlmann, P. “Rational design of all-solid-state ion-selective electrodes and reference electrodes,” *TrAC Trends Anal. Chem.*, 2016, 76, 102–114.

39. Gamazo-Real, J. C.; Vázquez-Sánchez, E.; Gómez-Gil, J. “Position and Speed Control of Brushless DC Motors Using Sensorless Techniques and Application Trends,” *Sensors,* 2010, 10, *6901-6947*.

40. Grieshaber, D.; MacKenzie, R.; Vörös, J.; Reimhult, E. “Electrochemical Biosensors - Sensor Principles and Architectures,” *Sensors* 2008, 8, 1400-1458.

41. Kraikaew, P.; Soda, Y.; Nussbaum, R.; Jeanneret, S.; Bakker, E. “Portable instrument and current polarization limitations of high sensitivity constant-potential capacitive readout with polymeric ion-selective membranes,” *Sensors Actuators B Chem.*, 2023, 379, 133220.

42. Bakker, E.; Bühlmann, P.; Pretsch, E. “Carrier-based ion-selective electrodes and bulk optodes. 1. General characteristics,” *Chem. Rev.*, 1997, 97, 8, 3083–3132.

43. Ceresa, A.; Bakker, E.; Hattendorf, B.; Günther, D .; Pretsch, E. “Potentiometric Polymeric Membrane Electrodes for Measurement of Environmental Samples at Trace Levels: New

Requirements for Selectivities and Measuring Protocols, and Comparison with ICPMS," *Anal. Chem.*, 2000, 73, 2.

44. Salvador, J. P.; Adrian, J.; Galve, R.; Pinacho, D.G.; Kreuzer, M.; Sanchez-Baeza, F.; Marco, M.P. "Chapter 2.8 Application of bioassays/biosensors for the analysis of pharmaceuticals in environmental samples," *Compr. Anal. Chem.*, 2007, 50, 279–334.

45. Cuartero, M.; Parrilla, M.; Crespo, G. A. "Wearable Potentiometric Sensors for Medical Applications," *Sensors*, 2019, 19, 363.

46. Altun, A. "İletken polimer tabanlı amperometrik biyosensörlerin geliştirilmesi," 2019.

47. Korotcenkov, G.; Cho, B. K. "Engineering approaches to improvement of conductometric gas sensor parameters. Part 2: Decrease of dissipated (consumable) power and improvement stability and reliability," *Sensors Actuators B Chem.*, 2014, 198, 316–341.

48. Janata, J. "Conductometric Sensors," *Princ. Chem. Sensors*, 2009, 241–266.

49. Buvailo, A. I.; Xing, Y.; Hines, J.; Dollahon, N . Borguet, E. "TiO 2/LiCl-based nanostructured thin film for humidity sensor applications," *ACS Appl. Mater. Interfaces*, 2011, 3, 2, 528–533.

50. Ronkainen N. J.; Halsall, H. B.; Heineman, W. R. "Electrochemical biosensors," *Chem. Soc. Rev.*, 2010, 39, 5, 1747–1763.

51. Ramakrishnan, S.; Shannon, C. "Display of solid-state materials using bipolar electrochemistry," *Langmuir*, 2010, 26, 7, 4602–4606.

52. Weber, S. "Manufacturing of Gold Nanoelectrode Ensembles for Intracellular Recording on Living Cells," 2018.

53. Belluzo, M . S.; Ribone, M. É.; Lagier, C. M. “Assembling Amperometric Biosensors for Clinical Diagnostics,” *Sensors* 2008, 8, 1366-1399.

54. Sinha, A.; Dhanjai; Tan, B.; Huang, Y.; Zhao, H.; Dang, X.; Chen, J.; Jain, R. “MoS2 nanostructures for electrochemical sensing of multidisciplinary targets: A review,” *TrAC Trends Anal. Chem.*, 2018, 102, 75–90.

55. Mehrvar, M.; Abdi, M. “Recent Developments, Characteristics, and Potential Applications of Electrochemical Biosensors,” *Anal. Sci.* 2004, 208, 20, 8, 1113–1126.

56. Zhou, Y.; Kubota, L. T.; Zhou, Y. L.; Kubota, L. T. “Trends in Electrochemical Sensing,” *ChemElectroChem*, vol. 7, no. 18, pp. 3684–3685, Sep. 2020, doi: 10.1002/CELC.202001025.

57. Castillo, J.; Gaspar, S.; Leth, S.; Niculescu, M.; Mortari, A.; Bontidean, I.; Soukharev, V.; Dorneanu, S.A.; Ryabov, A.D.; Csöregi, C., “Biosensors for life quality: Design, development and applications,” *Sensors Actuators B Chem.*, 2004, 102, 2, 179–194.

58. Chaubey, A.; Malhotra, B. D. “Mediated biosensors,” *Biosens. Bioelectron.*, 2002, 17, 6–7, 441–456.

59. Llorent-Martínez, E. J. P; Ortega-Barrales; Fernández-de Córdova, M. L.; Ruiz-Medina, A. “Trends in flow-based analytical methods applied to pesticide detection: A review,” *Anal. Chim. Acta*, 2011, 684, 1–2, 30–39.

60. Knutson, S. D.; Sanford, A. A.; Swenson, C. S.; Korn, M. M.; Manuel, B. A.; Heemstra, J. M. “Thermoreversible Control of Nucleic Acid Structure and Function with Glyoxal Caging,” *J. Am. Chem. Soc.*, 2020, 142, 41, 17766–17781. O

61. Böck, S.; Korzeniowski, F.; Schlüter, J ., Krebs, F.; Widmer, G. “Madmom: A new python audio and music signal processing library,” *MM 2016 - Proc. ACM Multimed. Conf.*, 2016, 1174–1178.

62. Hannocks, M. J.; Zhang, X.; Gerwien, H.; Chashchina, A.; Burneister, M.; Korpos, E.; Song, J.; Sorokin, L. "The gelatinases, MMP-2 and MMP-9, as fine tuners of neuroinflammatory processes," *Matrix Biol.*, 2019, 75–76, 102–113.

63. Wang, C. F.; Sun, X. Y.; Su, M.; Wang, Y. P.; Lv, Y. K. "Electrochemical biosensors based on antibody, nucleic acid and enzyme functionalized graphene for the detection of disease-related biomolecules," *Analyst*, 2020, 145, 5, 1550–1562.

64. Asal, M .; Özen, Ö.; Şahinler, M.; Polatoğlu, I. "Recent Developments in Enzyme, DNA and Immuno-Based Biosensors," *Sensors*, 2018, 18, 1924.

65. Aledo, J. C.; Lobo, C.; Del Valle, A. E. "Energy diagrams for enzyme-catalyzed reactions: Concepts and misconcepts," *Biochem. Mol. Biol. Educ.*, 2003, 31, 4, 234–236.

66. Mohammed, A. M.; Rahim, R.A.; Ibraheem, I.J.; Loong, F.K.; Hisham, H.; Hashim, U.; Al-Douri, Y. , "Application of gold nanoparticles for electrochemical DNA biosensor," *J. Nanomater.*, 2014.

67. Moldovan, R.; Vareshchagina, R.; Milenko, K.; Iakob, B.-C.; Bodoki, A.E.; Falamas, A.; Tosa, N.; Muntean, C.M.; Farcau, C.; Bodoki, E. "Review on combining surface-enhanced Raman spectroscopy and electrochemistry for analytical applications," *Anal. Chim. Acta*, 2022, 1209, 339250.

68. Kavita V, "DNA Biosensors-A Review," *J. Bioeng. Sci.*, 2017, 7, 2.

69. Ashrafi, A. M.; Sys, M.; Sedlackova, E.; Farag, A.S.; Adam, V.; Pribyl, J.; Richtera, L. "Application of the Enzymatic Electrochemical Biosensors for Monitoring Non-Competitive Inhibition of Enzyme Activity by Heavy Metals," *Sensors*, 2019, 19, 2939.

70. Marie, M.; Mandal, S.; Manasreh, O. “An Electrochemical Glucose Sensor Based on Zinc Oxide Nanorods,” *Sensors,* 2015, *15, 18714-18723*.

71. Dervisevic, M.; Alba, M.; Prieto-Simon, B.; Voelcker, N. H. “Skin in the diagnostics game: Wearable biosensor nano- and microsystems for medical diagnostics,” *Nano Today*, 2020, 30, 100828.,

72. Borberg, E.; Granot, E.; Patolsky, F.; “Ultrafast one-minute electronic detection of SARS-CoV-2 infection by 3CLpro enzymatic activity in untreated saliva samples,” *Nat. Commun.* 2022, 131, 13, 1–11.

73. Haleem, A.; Javaid, M.; Singh, R. P.; Suman, R.; Rab, S. “Biosensors applications in medical field: A brief review,” *Sensors Int.*, 2021, 2, 100100.

74. Fleet, B.; Gunasingham, H. “Electrochemical sensors for monitoring environmental pollutants,” *Talanta*, 1992, 39, 11,. 1449–1457.

75. Stradiotto, N . R.; Yamanaka, H.; Zanoni, M. V. B. “Electrochemical sensors: a powerful tool in analytical chemistry,” *J. Braz. Chem. Soc.*, 2003, 14, 2, 159–173.

76. O. Kanoun; Lazerevic-Pasti, T.; Pasti, I.; Nasraoui, S.; Talb, M.; Brahem, A.; Adiraju, A.; Sheremet, E.; Rodriguez, R.D.; Ben Ali, B.M.; Al-Hammry, A. “A Review of Nanocomposite-Modified Electrochemical Sensors for Water Quality Monitoring,” *Sensors*, 2021, 21, 4131, .

77. Karimi-Maleh, H.; Karimi, F.; Alizadeh, M.; Sanati, A. L. “Electrochemical Sensors, a Bright Future in the Fabrication of Portable Kits in Analytical Systems,” *Chem. Rec.*, 2020, 20, 7, 682–692.

78. Deng, K.; Li, L. “CdS Nanoscale Photodetectors,” *Adv. Mater.*, 2014, 26, 17, 2619–2635.

79. Georgakilas, V.; Perman, J. A.; Tucek, J.; Zboril, R. “Broad Family of Carbon Nanoallotropes: Classification, Chemistry, and Applications of Fullerenes, Carbon Dots, Nanotubes, Graphene, Nanodiamonds, and Combined Superstructures,” *Chem. Rev.*, 2015, 115, 11, 4744–4822.

80. Yew, Y. P.; Shameli, K.; Miyake, M.; Kuwano, N.; Bt Ahmad Bharudin, N.B.; Bt Mohamad, S.E.; Lee, K.X. “Green Synthesis of Magnetite (Fe3O4) Nanoparticles Using Seaweed (Kappaphycus alvarezii) Extract,” *Nanoscale Res. Lett.*, 2016, 11, 1.

81. Arikan, K.; Burhan, H.; Bayat, R.; Sen, F. “Glucose nano biosensor with non-enzymatic excellent sensitivity prepared with nickel–cobalt nanocomposites on f-MWCNT,” *Chemosphere*, 2021, 132720.

82. Altuner, E. E.; Akin, M.; Bayat, R.; Bekmezci, M.; Burhan, H.; Sen, F. “Challenges in commercialization of carbon nanomaterial-based sensors,” *Carbon Nanomater. Sensors*, 2022, 381–392.

CHAPTER VII

Hydrogen Production from Solar Water Splitting Using Photocatalytic and Photoelectrochemical Technologies

Fatih ARLI[1]
Hakan DUMRUL[2]
Edip TAŞKESEN[3]

Introduction

Global energy consumption is increasing daily, producing environmental issues caused by overusing fossil fuels. Approximately 80% of today's energy demands are provided by fossil fuels (Hassan et al., 2023; Ishaq et al., 2022; Razi & Dincer, 2022). The utilization of fossil fuels causes the release of greenhouse

[1] Dr.Öğr.Üyesi, Şırnak Üniversitesi, Orcıd: 0000-0002-0899-3460
[2] Dr.Öğr.Üyesi, Şırnak Üniversitesi, Orcıd: 0000-0003-1122-3886
[3] Dr.Öğr.Üyesi, Şırnak Üniversitesi, Orcıd: 0000-0002-3052-9883

gases, especially carbon dioxide, into the atmosphere and climate change. Moreover, using these non-renewable energy resources also causes air and water pollution. The world's demand for energy is expected to increase and double by 2050 and triple by the end of the 21st century (Falciani & Chiavazzo, 2023). To restrict global warming to 1.5 degrees Celsius, carbon neutrality becomes mandatory by the middle of the 21st century. The need for clean and renewable energy resources must be urgently solved without wasting more time. Solar energy is an abundant and environmentally friendly resource. Therefore, among all renewable energy sources (geothermal, marine, wind, biomass, etc.), it plays a crucial role in alleviating the energy crisis and reducing environmental concerns (Chi et al., 2022; Dharmarajan et al., 2023; Oh et al., 2018). Hydrogen is considered a pivotal energy system for the future, serving as a clean, renewable energy storage and carrier. Therefore, converting solar energy into a usable and storable form such as hydrogen has become a highly desirable goal not only from an economic point of view but also from an environmental point of view (Akyüz et al., 2020; Kabir et al., 2018). Three primary technologies are often used in the industrial generation of hydrogen: water electrolysis, coal gasification, and steam methane reforming (Figure 1). However, as can be seen from the figure given, current hydrogen production is still based on fossil fuels. This highlights the need to focus more on sustainable energy sources and green methods of hydrogen production, given the fact that fossil fuels are a limited and non-renewable resource (Akyüz et al., 2019; Kabir et al., 2018). Water electrolysis holds great promise among these hydrogen production methods, as water is considered renewable. However, although water electrolysis is a crucial technique in hydrogen generation technology, it has high costs when considered from a practical perspective.

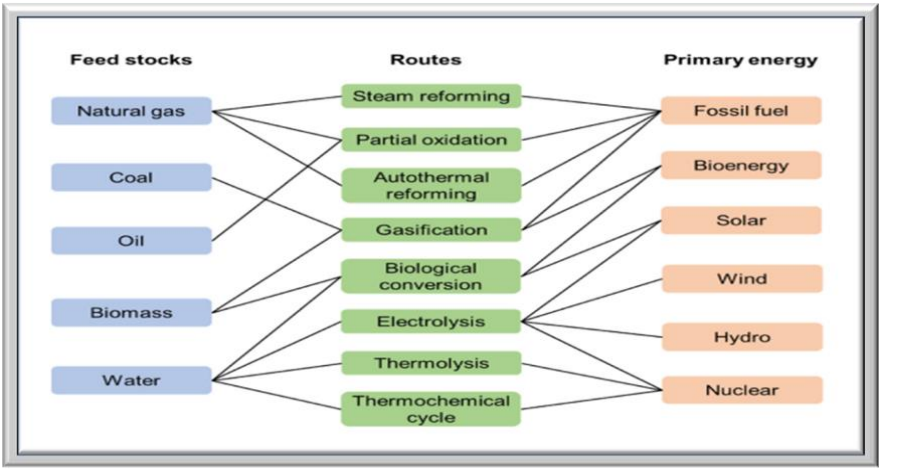

Figure 1. *Fundamental energy sources, materials, and routes for hydrogen production (M. Ji & Wang, 2021).*

Solar energy may generally be converted or stored in chemical bonds by water splitting (WS) based on photocatalytic (PC) or photoelectrochemical (PEC) technologies. After the 1972 study on PC WS methods by Fujishima and Honda, research on the topic increased considerably (S. Chen et al., 2020; X. Zhang et al., 2010). PC and PEC WS using solar energy has been considered an exciting solution in recent years to solve the limitations of water electrolysis mentioned above. Figure 2 (A and B) shows the publication numbers of studies reported in PC and PEC WS between the years (2014-2023 October included).

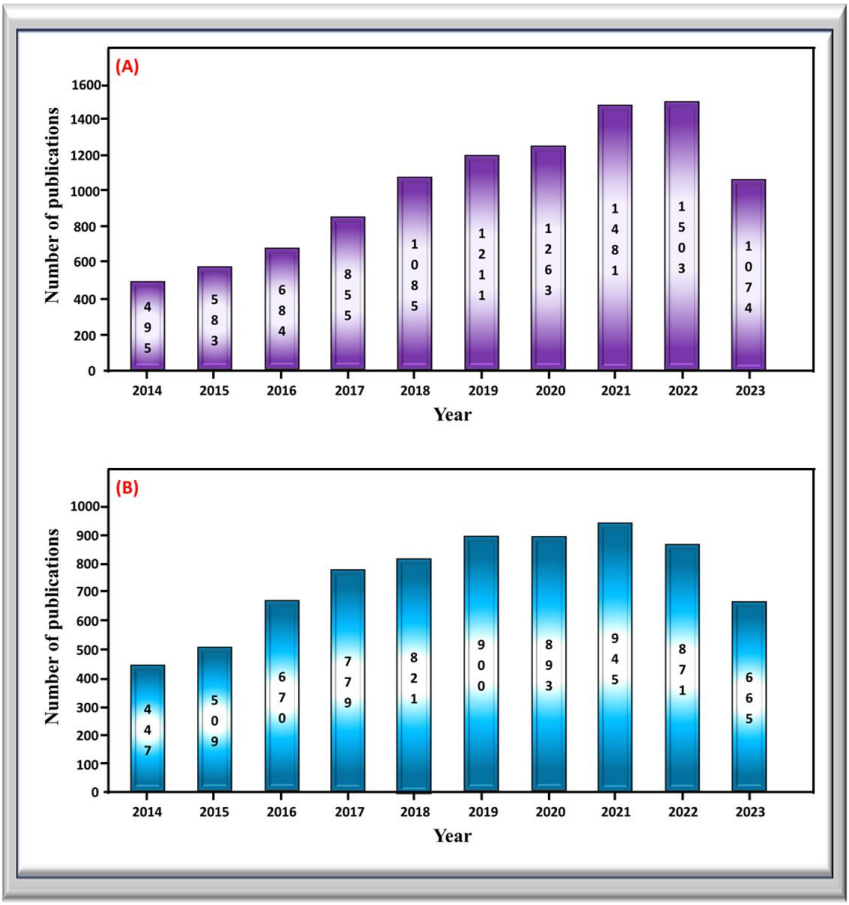

Figure 2. *Number of publications on PC and PEC WS technologies reported by Web of Science in November 2023: (A) PC and (B) PEC WS.*

This chapter will discuss PC and PEC WS technologies in detail. The basic concepts used in both PC and PEC WS technologies, their similarities and differences, which calculations are used, and the research carried out by these technologies in the last three years are reported in detail. In the conclusion section, inferences, and information about what needs to be done in the future are given.

Solar powered water section (PC and PEC WS)

Solar WS is a system that converts solar energy into chemical energy based on the photosynthesis of green plants (Qi et al., 2018). From a thermodynamic perspective, the overall WS reaction is an uphill reaction requiring a minimum Gibbs free energy (GE) of ΔG^0 = + 237 kJ/mol. According to the Nernst equation, this value corresponds to ΔE^0 = 1.23 V. This is explained as the semiconductor's (SC) capability to absorb light with photon energy greater than 1.23eV (λ~1000 nm and shorter) to initiate the WS reaction (Maeda, 2011; Pattanayak et al., 2022; X. Zhang & Jiang, 2022). Equation (1) represents the general WS process.

$$2H_2O \rightarrow 2H_2 + O_2 \quad \textbf{(1)}$$

Oxidation and reduction reactions in an acidic electrolyte can be written as in equations (2) and (3):

$$2H_2O + 4h^+ \rightleftharpoons O_2 + 4H^+ \quad E^0_{ox} = -1.299 \text{ V vs NHE} \quad \textbf{(2)}$$

$$2H^+ + 4e^- \rightleftharpoons H_2 \quad E^0_{red} = +0.000 \text{ V vs NHE} \quad \textbf{(3)}$$

For an alkaline electrode, oxidation and reduction reactions can be written as in equations (4) and (5):

$$4OH^- + 4h^+ \rightleftharpoons 2H_2O + O_2 \quad E^0_{ox} = -0.401 \text{ V vs NHE} \quad \textbf{(4)}$$

$$4H_2O + 4e^- \rightleftharpoons 2H_2 + 4OH^- \quad E^0_{red} = -0.828 \text{ V vs NHE} \quad \textbf{(5)}$$

Basic principles of PC WS

The PC WS system converts water into hydrogen and oxygen using semiconductor catalysts to produce environmentally friendly and sustainable hydrogen fuel. This process aims to obtain an environmentally friendly, clean, and renewable energy source by converting water into hydrogen and oxygen using solar energy (Ahmad et al., 2015; Wu et al., 2020). At the same time, PC WS is considered artificial photosynthesis, like solar-powered photosynthesis in green plants (Fajrina & Tahir, 2019; Shi et al., 2014). The PC WS process triggered by light can be created by a

facile technology using semiconductor materials as photocatalysts. During this process, light energy is converted into chemical energy. Simultaneously, the WS reaction is accelerated to produce GE (Fajrina & Tahir, 2019). PC WS is schematically reported in the literature, as displayed in Figure 3 (A and B) (Song et al., 2022; Y. Y. Wang et al., 2022).

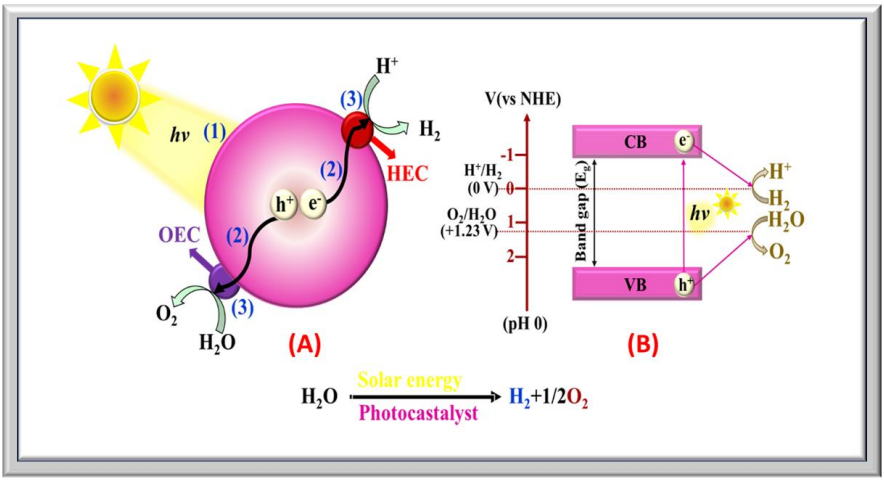

Figure 3. *The mechanism of PC WS ; (A) semiconductor photocatalyst (B) one-step excitation (Y. Y. Wang et al., 2022).*

In the first step of PC WS technology, the photon with the desired energy, hv, hits the surface of the photocatalytic semiconductor and is absorbed by it.. Then, the electrons in the semiconductor migrate from the occupied valence band (E_{VB}) to the empty conduction band (E_{CB}). As a result, electrons (e^-) and holes (h^+) are generated. An example reaction is shown in equation (6).

$$\text{Semiconductor} + \text{hv} \rightarrow e^-_{(CB)} + h^+_{(VB)} \qquad \textbf{(6)}$$

In the second step, electrons and holes excited by the photon begin to circulate freely on the surface of the semiconductor and gather in the active regions on the surface. Finally, the successfully separated electrons and holes react with protons (H^+) to produce

Hydrogen gas (H_2) and with water (H_2O) to produce Oxygen gas (O_2), respectively.

The reactions during PC WS are also given in equations (7-9) (Gupta, 2017; Y. Y. Wang et al., 2022).

$$\text{Reduction: } 2H^+ + 2e^- \rightarrow H_2 \quad \textbf{(7)}$$

$$\text{Oxidation: } H_2O + h^+ \rightarrow 2H^+ + \frac{1}{2}O_2 \quad \textbf{(8)}$$

$$\text{Overall reaction: } H_2O \rightarrow H_2 + \frac{1}{2}O_2 \quad \textbf{(9)}$$

Basic principles of PEC WS

PEC WS has become an environmentally friendly and promising technology to convert solar energy into hydrogen fuel compared with traditional and other advanced techniques (Ayodhya, 2023; Chi et al., 2022; Tijent et al., 2023). A primary PEC mechanism is shown in Figure 4. This mechanism contains a container filled with an aqueous electrolyte and two electrodes.

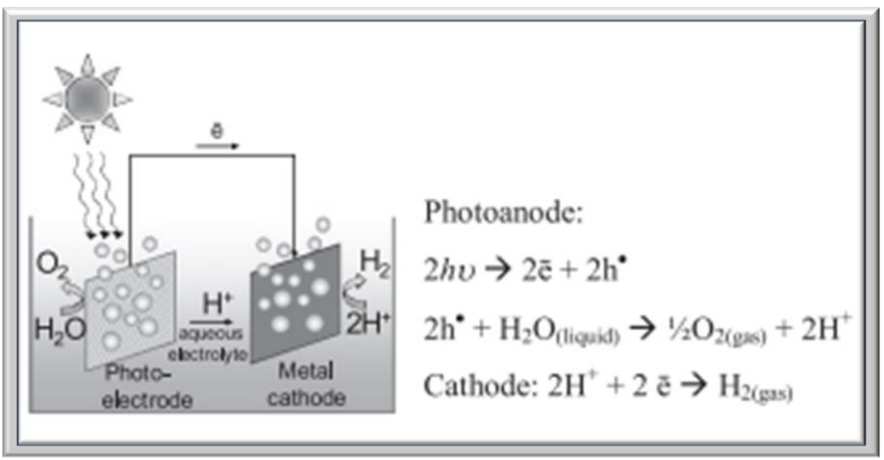

Figure 4. *Schematic of PEC WS (Abouelela et al., 2021).*

One or both electrodes are sensitive to light and are called photoactive. The aqueous electrolyte container has a transparent or optical window to allow light to reach the photoelectrode (PE) or

photoactive electrode. PEC WS occurs when energy requirements are met, as shown in Table 1 (Minggu et al., 2010).

Table 1. *PEC WS requirements (Minggu et al., 2010).*

Conditions	Main requirements
PEC water splitting	$H_2O_{(liquid)} + 2h\nu \longrightarrow \frac{1}{2} O_2(gas) + H_{2\,(gas)}$
Minimum potential required	$E^O_C\,(25\ ^OC)_{min} = 1.229$ eV
Practical potential (+ overpotential & losses)	$E^O_{H2O}\,(25\ ^OC)_{prac} = 1.229$ eV $E_{bandgap} > E^O_{H2O}$
For efficient utilization of sunlight	UV> $h\nu$ (Vis) > IR $h\nu \geq E_{bandgap}$
Band edge requirement	$C_{bandedge} < E^O_{H2/H+}$ $V_{bandedge} > E^O_{O2/H2O}$

Figure 5 (A-E) shows the PC and PEC WS energy diagrams. When a semiconductor is exposed to light, the following steps take place;

- Electrons in the E_{VB} are excited to the E_{CB} when they absorb photons with energies higher than the energy of the band gap (E_g).
- E_{CB} and E_{VB} excited electrons and holes are produced, respectively.
- These photogenerated carriers can drive reduction and oxidation reactions if charge injections into the reactants are thermodynamically favorable.

Figure 5 (A) shows the E_g semiconductor to achieve PC WS using a single photocatalyst. The phenomenon here should be between the reduction and oxidation potentials of water, which are +0 and +1.23 V, respectively, compared to the normal hydrogen electrode (NHE) when the reactant solution is at pH 0 (Hisatomi et al., 2014; Li et al., 2021). Figure 5 (B) displays an alternative system,

the "Z-scheme", which is similar to photosynthesis in green plants. In this technology, two semiconductors are connected in series with reversible redox shuttles, and the reduction and oxidation of water to hydrogen occur in one photocatalyst and the simultaneous reduction of oxidized redox mediators and oxidation of water to oxygen in the other photocatalyst. So, the Z-scheme is a system in which reactions such as WS and oxygen and hydrogen evolution co-occur with two different photocatalysts. This process can proceed by inter-particle electron transfer and, in some cases, can operate efficiently despite the absence of reversible redox shuttles (Hisatomi et al., 2014; Li et al., 2021). The PEC WS system generally uses three types of cells, including an n-type semiconductor photoanode, a p-type semiconductor photocathode, and a tandem system consisting of an n-type photoanode and a p-type photocathode. Electrons generated by photogeneration at the n-type photoanode transfer to the opposite electrode (cathode), producing an anodic photocurrent and reducing H^+ ions to H_2 at the cathode (Figure 5 (C)). In contrast, the holes formed by photogeneration in the p-type photocathode transfer to the counter electrode (anode), produce a cathodic photocurrent, and oxidize water to O_2 and H^+ ions (Figure 5(D)). In the tandem cell, both the n-type photoanode and the p-type photocathode absorb light energy, oxidizing water to O_2 and reducing H^+ ions to H_2, respectively (Figure 5 (E)) (Ayodhya, 2023; Liu et al., 2023). As shown in Figure 6, TiO_2 is a common n-type semiconductor widely used as the photoanode in n-type PEC cells.

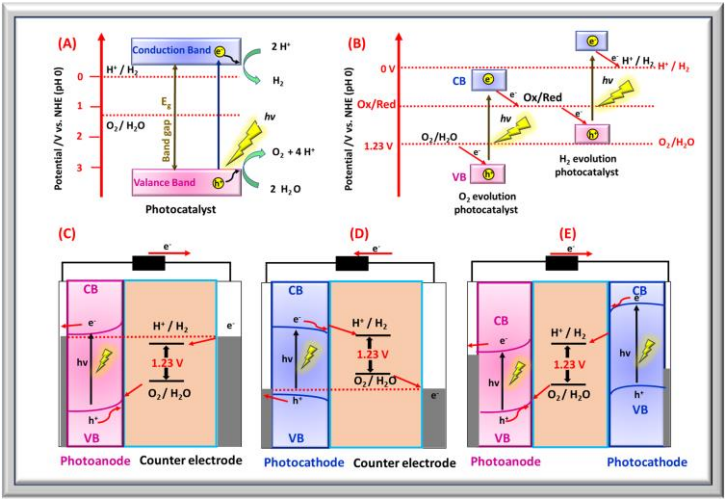

Figure 5. *PC WS energy graphs using (A) one-step excitation and (B) two-step excitation (Z-scheme); and PEC WS utilizing (C) a photoanode, (D) a photocathode, and (E) tandem configuration (Ayodhya, 2023; Hisatomi et al., 2014).*

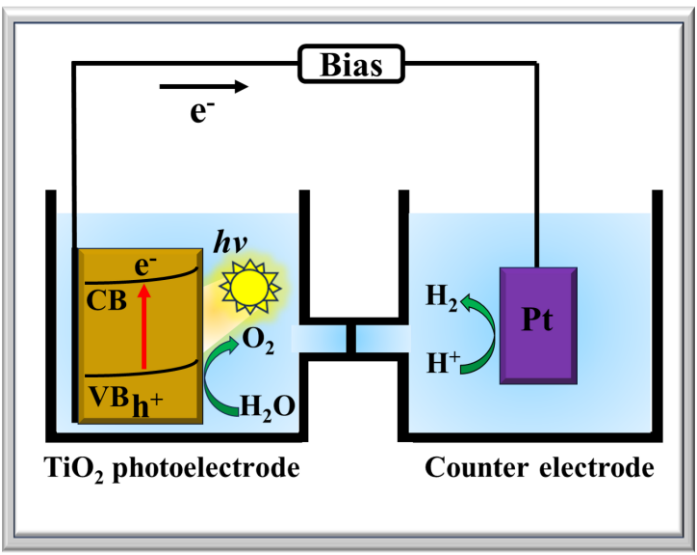

Figure 6. *PEC WS using a TiO_2 photoanode (Abouelela et al., 2021).*

Requirements of a photocatalyst

An ideal photocatalyst absorbs light energy, excites electrons from the E_{VB} to the E_{CB}, and simultaneously creates holes. These excited electrons and holes move toward the photocatalyst surface. Photo-excited holes and electrons trigger the oxidation and splitting of water into oxygen and hydrogen gas (Figure 7). As long as there is light, the process continues. In line with this goal, various basic needs can be determined for materials to efficiently carry out the WS reaction (Figure 8). First, the photocatalyst must have the optimal band structure to benefit from solar energy at the maximum level. This band structure must be higher than 1.23 eV and is compatible with the energy of photons in the visible region (2.0-2.4 eV). The thermodynamic energy required for WS requires a band gap higher than 1.23 eV, but the energy of a photon in the visible light spectrum is between 2.0-2.4 eV. However, it should be noted that the minimum band gap should be higher in an ideal photocatalyst. This minimizes energy losses due to thermodynamic losses, entropy change, recombination of electron-hole pairs, kinetic losses, etc. For optimal performance, the photocatalyst must be designed to consider these various factors (Ayodhya, 2023; Jafari et al., 2016).

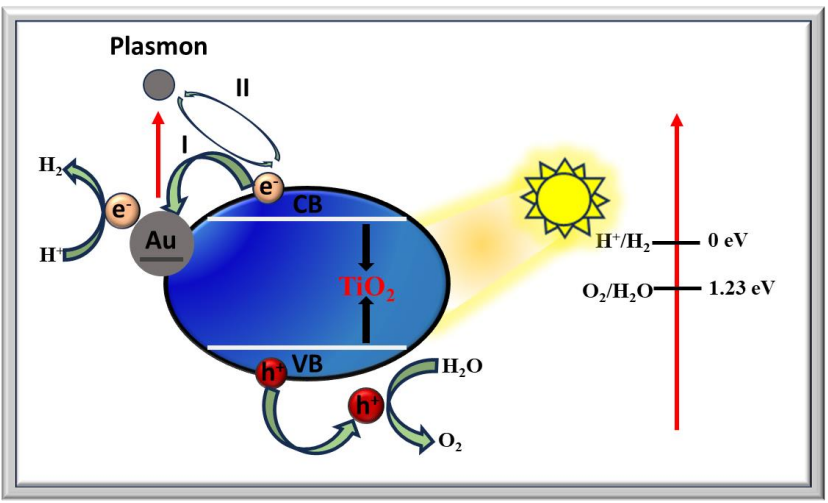

Figure 7. *TiO_2 Band Gap (Ayodhya, 2023; Jafari et al., 2016).*

An energy loss of about 0.8 eV can be allowed in natural systems. Secondly, the lower level of the E_{CB} of the photocatalyst should be more harmful than the reduction potential of H^+/H_2. In contrast, the upper level of the E_{VB} should be more favorable than the oxidation potential of O_2/H_2O. This allows efficient transport of carriers (electrons and holes) for the reduction of H_2 and oxidation of O_2. Thirdly, to efficiently transport the photocatalyst through the photocatalyst to the surface, the photo-induced electron-hole separation must be favorable in terms of efficiency, and the carrier mobility must be high. Since the recombination of carriers in the photocatalyst negatively affects the efficiency, the crystallinity of the materials must be high.

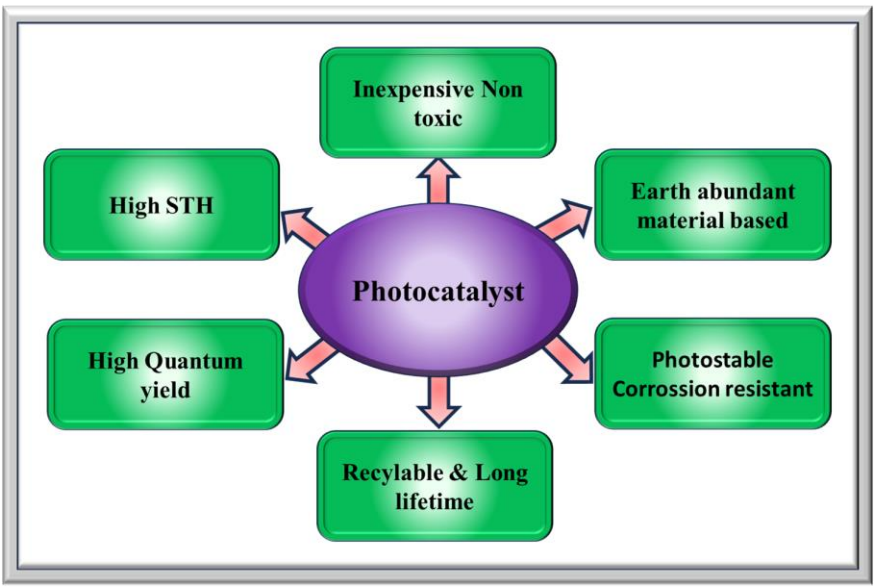

Figure 8. *Properties of commercially desirable photocatalysts for H_2 production (Saddique et al., 2023; Tentu & Basu, 2017).*

Fourth, photocatalysts in photocatalytic reactions must often operate stably in extreme environments such as high temperatures and acidic/alkaline conditions. The stability of photocatalysts under these conditions is crucial for reaction efficiency and long-term use.

For an ideal general water-splitting semiconductor, the E_{VB} and E_{CB} edge positions should lie between the water oxidation and reduction potentials (*i.e.*, $E_{CB} > E_{red, water}$, and $E_{VB} < E_{ox, water}$). Figure 9 shows various semiconductor photocatalysts' band gap and band edge positions (band edge according to water redox potentials) (Tamirat et al., 2016). For example, certain photocatalysts such as GaP, TaON, and CdS have suitable semiconductor properties for solar WS. However, they exhibit instability by oxidizing anions more efficiently than water. As a result, the photocatalysts degrade rapidly and do not perform stably in the long term. Lastly, the photocatalyst must have a high surface activity and a large area of surface. The large surface area allows water molecules to contact the catalyst effectively. High activity on the surface boosts the catalyst's capacity to split water into protons and hydroxyl anions. Additionally, as the particle size of photocatalysts decreases (increases the surface area), the probability of the charge carrier reaching the surface increases. The last two basic requirements should be considered when determining suitable candidates for photocatalyst design. Then, the electronic structures of the materials should be designed to meet the first three requirements. Additionally, candidate materials must have a high surface area and be readily obtainable (Ayodhya, 2023).

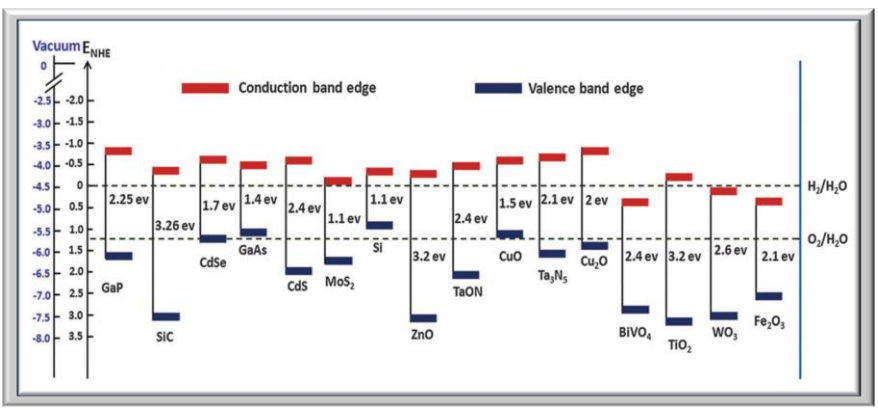

Figure 9. *SC photocatalyst band structures and redox potentials (Li et al., 2021; Tamirat et al., 2016).*

PC and PEC WS similarities and differences

PC and PEC technologies can be used as the two main methods for solar WS. The similarity between these two systems is that they use a photoactive semiconductor as the active component (Wu et al., 2020). The main difference between these two technologies is that PEC uses electrical energy in addition to photon energy. Current PEC systems report STH rates between 2% and 3%, which refers to the efficiency of STH conversion. On the other hand, STH efficiency in PC systems is as low as 0.1% due to lower light harvesting capacity (Tentu & Basu, 2017; Zhou et al., 2016).

While conventional PC WS methods use heterogeneous powder semiconductors, the PEC WS method has the following advantages. These advantages are:

- An externally or automatically applied voltage can inhibit the recombination of charge carriers resulting from photogeneration, improving the separation and transfer of excited electron–hole pairs of photocatalysts.
- Separation is simple because the hydrogen and the oxygen can be easily collected on different types of photoelectrodes.
- Semiconductor films can be coated on conductive substrates, making them easier to scale up for industrial application in the future.
- Finally, because it does not require mixing, powdered PC consumes less energy than WS systems (Adamopoulos et al., 2019; Minggu et al., 2010).

The distinction between PC and PEC systems is detailed in Table 2.

Tablo 2. *Comparison of PC and PEC technology (Y. Y. Wang et al., 2022).*

Experimental details	PC Water Splitting	PEC water splitting
Catalysts from	Powder (majority)	Thin film
İncident light	All directions	Vertical direction on the catalyst
Energy input	Solar energy	Solar energy and external electricity
Cost	Low	Relatively high
Gases collecting	Seperating process required	Directed collected from seperated electrodes
Efficiency benchmark	STH	STH/IPCE/others
Efficiency	Low	Relatively high
Recycle of catalysts	Complex and time consuming	Simple and effective

PC and PEC WS efficiency

STH is frequently used to indicate the H_2 production efficiency of a PC WS, and the calculation method in the literature is given in equation 10 (Y. Y. Wang et al., 2022; W. Yang & Prabhakar, 2019).

$$\text{STH} = \left[\frac{\left(\frac{mmolH_2}{s}\right) * \left(\frac{237kj}{mol}\right)}{P_{total}\,(mW/cm^2) * Area(cm^2)}\right] \text{AM1.5G} \qquad (\mathbf{10})$$

The PEC WS STH conversion efficiency is calculated as follows in equation (11) (Y. Y. Wang et al., 2022; W. Yang & Prabhakar, 2019).

$$\text{STH} = \left[\frac{\text{I}J_{\text{SC}}\,(\text{mA/cm}^2) * (1.23\text{V})\text{I} * \eta_{\text{F}}}{P_{\text{total}}\,(\text{mW/cm}^2)}\right] \text{AM1.5G} \qquad (\mathbf{11})$$

Where:

J_{SC}: is the short-circuit photocurrent density.

$P_{total:}$ is incident illumination power density.

η_F: is the Faradic efficiency for hydrogen evolution.

To understand the contribution of different wavelengths of light to STH performance, the National Renewable Energy Laboratory standard AM1.5G solar spectrum is shown in Figure 10.

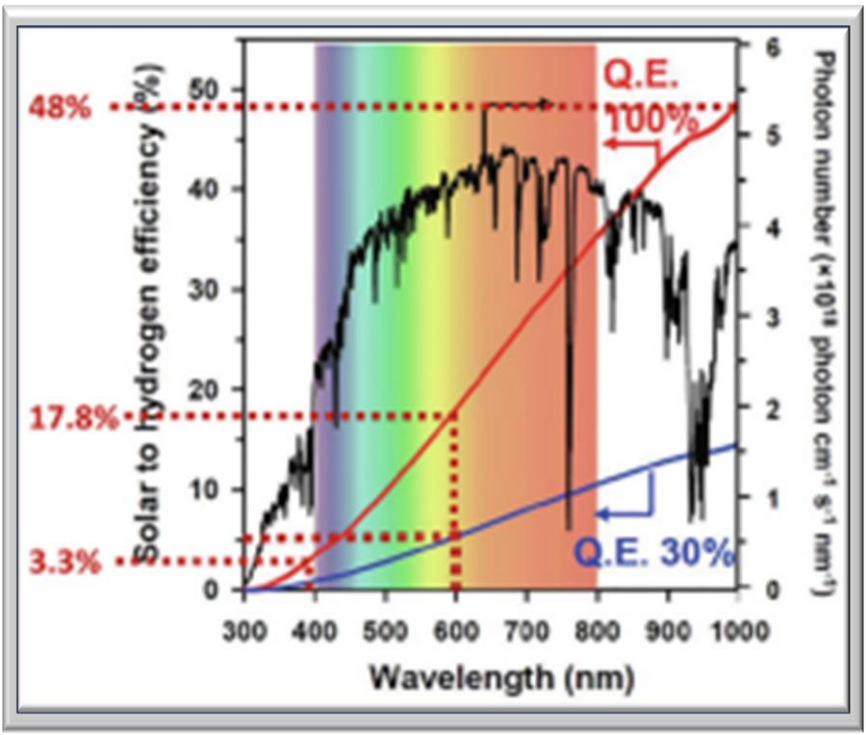

Figure 10. *Theoretical efficiency for STH integrated from a low wavelength to corresponding wavelength with QEs of 100 and 30% (Takanabe & Domen, 2011).*

All UV photons contribute to a maximum theoretical STH performance of only 3.3%, with 100% quantum efficiency. Light at 600 nm (2.07 eV) gives an efficiency of 17.8%. Using light up to

1000 nm (1.23 eV), a single semiconductor's calculated STH efficiency is ~48%. This fact demonstrates that visible light contributes significantly to the STH yield, indicating that it is essential to increase the visible light activity of photocatalysts. IPCE is the ratio of the received photocurrent to the incident photon flux and be expressed equation 12 (Jiang et al., 2017).

$$\text{IPCE}\ (\lambda) = \frac{\text{electrons}/cm^2/\text{s}}{\text{photons}/cm^2/\text{s}} = \frac{J_{\text{ph}}\ (\text{mA}/\text{cm}^2) * (1239.8\ (\text{V} * nm)}{P_{mono}\ (\text{mW}/\text{cm}^2)\ * \lambda\ (nm)} \quad (\mathbf{12})$$

In this equation,

1239.8 V * nm: is the product of h (Planck's constant)

c: speed of light and,

P_{mono}: represents the calibrated illumination power density of monochromatic light.

PC and PEC WS performance comparison

Hydrogen and oxygen evolution efficiencies obtained from studies reported in the literature on PC and PEC WE are presented. Zuo et al. integrated ultrathin TiO_2 nanosheets by hydrothermal and solvothermal methods into the growth of $ZnIn_2S_4$ to produce TiO_2-$ZnIn_2S_4$ heterostructure nanoflowers and investigated the PC WS performance under 300 W Xenon light illumination. They reported the optimized DZH nanoflowers as enhanced PC WS activity (214.9 μmol g^{-1} sa^{-1} for H_2 formation and 81.7 μmol g^{-1} sa^{-1} for O_2 formation without any co-catalyst and sacrificial agent) (Zuo et al., 2021). Velusamy et al. synthesized the FCN/BiO nano heterostructure using the solvothermal method and investigated the PEC WS performance under AM 1.5 G light illumination. FCN/BiOI nano heterostructure showed photocurrent density ten times higher than BCN nanostructure and 3.8 times higher than FCN. As a result, FCN/BiOI reported a high induced photocurrent density (20.17 mA/cm^2) and H2 evolution rate (3762 μmol h^{-1} cm^{-2}) under sunlight

illumination ($\lambda \geq 420$ nm) compared to the other (Velusamy et al., 2023). Another research reported Xu et al. first fabricated novel Fe-MOF derivatives α-Fe_2O_3 and FeP-PC using the solvothermal method to facilitate the separation and utilization efficiency of charge carriers and to activate the overall WS performance of ketamine-based TpPa-1-COF. They investigated the PC WS performance under 300 W Xenon light illumination. As a result, they reported a hydrogen and oxygen production performance of 97.45 μmol $g^{-1}h^{-1}$ / 48.68 μmol $g^{-1}h^{-1}$, respectively (M. L. Xu et al., 2022). Some of the studies conducted between 2021 and 2023 for PC and PEC WS technologies are selected, and their detailed analysis, characteristics, and hydrogen production performances are listed in Table 3.

Table 3. *Detailed analysis of investigations reported between 2021-2023 on PC and PEC WS technologies.*

Photocatalyst &Aplica.	Bandgap (eV)	Synthesis method	Electrolyte	H_2&O_2 evolution	Current density	Light source	Ref.
g-C_3N_4 (BCN-HT100) &PC	-	Hydrotermal method	Na_2SO_4	- & 816 $\mu molh^{-1}g^{-1}$	-	300 W Xe lamp	(Cheng et al., 2023)
(RGO)-$Cd_{0.60}Zn_{0.40}S$-Pt &PC and PEC Hybrid	2.28	Solvothermal method	Na_2S & Na_2SO_3	196$\mu molh^{-1}$ & -	1.41 mA/cm^2	300 W Xe lamp	(Uğuz & Koca, 2021)
$CaTiO_3$/Cu/TiO_2 method Na_2SO_4	3.37	Hydrothermal $\mu molh^{-1}g^{-1}$	0.5 M Xe lamp	23.550 & -	-	300 W	(J. Yang et al., 2022) &PC
Ce-doped TNTAs &PC	2.61	Two-step anodization	-	43.07 $\mu molh^{-1}cm^{-2}$ & -	-	AM 1.5G	(Tong et al., 2023)
CoCi/NiFeOOH/$BiVO_4$ &PEC	-	İmpregnation method	0.5 M Na_2SO_4	170 µmol & -	-	AM 1.5G Xe lamp	(Hu et al., 2022)
NiCo LDH (Pc-NiCo LDH/ Ni_3S_2/Co_9S_8) &PEC	-	Hydrothermal method	0.1 M KOH	6.4 μLs^{-1} & 3.1 μLs^{-1}	-	Simulated Xe lamp	(Zheng et al., 2023)
NiFe-MOF/TiO_2 &PEC	2.98	Hydrothermal method	0.5 M Na_2SO_4	- & -	0.77 $mAcm^2$	300 W Xe lamp	(Cui et al., 2020)
20LieCdS/TiO_2 & PEC	2.53	-	0.35 M Na_2SO_3	38.61mL g/h	2.1 mA/cm^2	35 m W/cm^2	(Ghoti et al., 2023)

			0.25 M Na_2S	- & -	Xe lamp	
FCN/BiOI &PEC	1.97	Solvothermal method	0.5 M Na_2SO_4	3762 $\mu molh^{-1}cm^{-2}$ & -	20 mA/cm^2	AM 1.5G (Velusamy et al., 2023)
α-Fe_2O_3/TpPa-1-COF /FeP &PC	2.0& 2.02& 1.35	Solvothermal method	0.5 M Na_2SO_4	97.45 $\mu molh^{-1}g^{-1}$ & 48.68 $\mu molh^{-1}g^{-1}$	16.20 mA/cm^2	300 W Xe lamp (M. L. Xu et al., 2022)
N-TiO_2/Ti (CN) /N-C-10 &PEC	1.85	Solvothermal method	0.5 M Na_2SO_4	- & -	458.6 $\mu A/cm^2$	300 W Xe lamp (Y. Wang et al., 2023)
$BiVO_4$/NiO/rGO &PEC	2.40 & 3.25	Hummers method	0.5 M Na_2SO_4	- & -	1.52 mA/cm^2	AM 1.5 G (Bai et al., 2022)
NiO/RP &PEC	3.29 & 1.99	Hydrothermal method	1 M KOH	171.8 $\mu molh^{-1}g^{-1}$ & -	-	AM 1.5 G (N. Chen et al., 2021)
ZnO@PDA/CeO_2 &PEC	3.0 & 3.01	Hydrohermal method	0.1 M Na_2SO_4	-& -	0.25 mA/cm^2	30 mW cm^2 LED (Celebi et al., 2021)
$ZnSnO_3$@$ZnIn_2S_4$ &PC	3.23 & 2.46	Solvothermal method	-	16340.18 $\mu molh^{-1}g^{-1}$ & -	-	300 W Xe lamp (Guo et al., 2021)
Al-dopedSrTiO &PC	2.21	Polymerizable complexation	1.0 M K_2SO_4	1.256 $mmolh^{-1}$	-	300 W Xe lamp (Su et al., 2022)

/solid phase & griding method				0.692 mmolh^{-1}			

Table 3. continued

Photocatalyst &Aplica.	Bandgap (eV)	Synthesis method	Electrolyte	H_2&O_2 evolution	Current density	Light source	Ref.
In_2O_{3-x}-1 & PEC	2.62	Hydrothermal method	1 M NaOH	- & -	0.97 mA cm^{-2}	300 W Xe lamp	(H. Xu et al., 2022)
FICM (α-Fe_2O_3 -In_2O_3 -Co (OH)x -Mn_3O_4 &PEC	1.99	Hydrothermal method	Na_2SO_4	- & -	6.5 mA cm^{-2}	AM 1.5 G	(M. H. Ji et al., 2023)
Ti_3C_2/Ti-ZnO &PEC	3.12	-	0.1 M KOH -	- & -	4.5x10^{-5} A cm^{-2}	1 Sun 100 mW/cm^2	(Sreedhar et al., 2022)
H/C-CdS &PC	2.32 & 2.37	-	0.5 M Na_2SO_4	3.190 mmol g^{-1} h^{-1}	-	LED lamp	(M. Zhang et al., 2021)
TiO_2–$ZnIn_2S_4$ TNZIS-50 &PC	3.12 & 2.33 &	Hydrothermal solvothermal method	0.5 M Na_2SO_4	214.9 μmol g^{-1} h^{-1} & 81.7 μmol g^{-1} h^{-1}	-	300 W Xe lamp	(Zuo et al., 2021)

Ni_4P_2-CQDs@CdS & PC	2.51 & 2.41	Hydrothermal method	0.5 M Na_2SO_4	145 μmol g^{-1} h^{-1} & -	-	100 Mw LED lamp	(Dong et al., 2021)
CeO_2/Fe_2O_3/Ver &PC	1.97 1.94	Precipitation method	-	3.1 mol g^{-1} & - 2.4 mol g^{-1} & - 4.7 mol g^{-1} & -	-	8 W Hg lamp	(Reli et al., 2021)
CoS/g-C_3N_4/NiS &PC	1.53 2.82	Hydrothermal physical stirring method	-	1.93 mmol mmol g^{-1} h^{-1} & -	-	300 W Xe lamp	(Bi et al., 2022)
STO:La/RhHoMS -BVO&PC	-	-	-	46.2μmol &22.3g^{-1} h^{-1}		300 W Xe lamp	(Wei et al., 2021)

Conclusion

This work provides detailed information on the fundamental aspects of PC and PEC WS, calculation methods, comparisons, and recently reported work in this field. Hydrogen is seen as an essential element in supporting future sustainable development and in shaping the energy landscape. In addition, the fact that hydrogen can be utilized as an energy carrier and raw material, which is accepted as one of the basic principles of energy transition, makes it an essential position in the energy field. The cost of hydrogen produced by petrochemical methods derived from fossil fuels may be low, but this production method is not renewable. Hydrogen production with (PC) and (PEC) systems, the two main methods for splitting water with solar energy, is promising for the future. Solar energy to chemical energy conversion applications are being developed in parallel with PC and PEC technologies. While photoactive semiconductors are the main components of these systems, several standard methodologies have been developed and implemented to increase their performance. The primary distinction between these two methods is that PEC utilizes more electrical energy than photon energy. Current PC and PEC WS report STH ratios of <2% and ~10%, respectively. Although PEC WS currently appears to be more efficient between the two systems, the following issues should be taken into consideration in future investigations to meet commercial expectations.

- Must design durable and highly efficient photoelectrodes made of new materials.
- Optimizing the use of light.
- Increase PEC cell panel size with simple design criteria.
- Techno-economic evaluations should be made, and the device's lifetime should be at least ten years.

Ultimately, we should remember that fossil fuel prices, political policies, geographical locations, cost, and other factors will determine the future road map of H_2 production with solar energy.

However, H_2 production with solar energy will undoubtedly play a vital role in a safe, economical, and clean energy future.

REFERENCES

Abouelela, M. M., Kawamura, G., & Matsuda, A. (2021). A review on plasmonic nanoparticle-semiconductor photocatalysts for water splitting. *Journal of Cleaner Production*, *294*. https://doi.org/10.1016/j.jclepro.2021.126200

Adamopoulos, P. M., Papagiannis, I., Raptis, D., & Lianos, P. (2019). Photoelectrocatalytic hydrogen production using a TiO2/WO3 bilayer photocatalyst in the presence of ethanol as a fuel. *Catalysts*, *9*(12), 1–12. https://doi.org/10.3390/catal9120976

Ahmad, H., Kamarudin, S. K., Minggu, L. J., & Kassim, M. (2015). Hydrogen from photo-catalytic water splitting process: A review. *Renewable and Sustainable Energy Reviews*, *43*, 599–610. https://doi.org/10.1016/j.rser.2014.10.101

Akyüz, D., Rıza Özkaya, A., & Koca, A. (2020). Photocatalytic and photoelectrochemical performances of Mo, Ni and Cu decorated metal chalcogenides. *Materials Science in Semiconductor Processing*, *116*(March). https://doi.org/10.1016/j.mssp.2020.105127

Akyüz, D., Zunain Ayaz, R. M., Yılmaz, S., Uğuz, Ö., Sarıoğlu, C., Karaca, F., Özkaya, A. R., & Koca, A. (2019). Metal chalcogenide based photocatalysts decorated with heteroatom doped reduced graphene oxide for photocatalytic and photoelectrochemical hydrogen production. *International Journal of Hydrogen Energy*, *44*(34), 18836–18847. https://doi.org/10.1016/j.ijhydene.2019.04.049

Ayodhya, D. (2023). Semiconductors-based Z-scheme materials for photoelectrochemical water splitting: A review. *Electrochimica Acta*, *448*(December 2022), 142118. https://doi.org/10.1016/j.electacta.2023.142118

Bai, S., Han, J., Zhang, K., Zhao, Y., Luo, R., Li, D., & Chen, A. (2022). rGO decorated semiconductor heterojunction of BiVO4/NiO to enhance PEC water splitting efficiency. *International*

Journal of Hydrogen Energy, *47*(7), 4375–4385. https://doi.org/10.1016/j.ijhydene.2021.11.122

Bi, Z. xu, Guo, R. tang, Ji, X. yin, Hu, X., Wang, J., Chen, X., & Pan, W. guo. (2022). Direct Z-scheme CoS/g-C3N4 heterojunction with NiS co-catalyst for efficient photocatalytic hydrogen generation. *International Journal of Hydrogen Energy*, *47*(81), 34430–34443. https://doi.org/10.1016/j.ijhydene.2022.08.028

Celebi, N., Arlı, F., Soysal, F., & Salimi, K. (2021). Z-scheme ZnO@PDA/CeO2 heterojunctions using polydopamine as electron transfer layer for enhanced photoelectrochemical H2 generation. *Materials Today Energy*, *21*, 100765. https://doi.org/10.1016/j.mtener.2021.100765

Chen, N., Cao, J., Guo, M., Liu, C., Lin, H., & Chen, S. (2021). Novel NiO/RP composite with remarkably enhanced photocatalytic activity for H2 evolution from water. *International Journal of Hydrogen Energy*, *46*(37), 19363–19372. https://doi.org/10.1016/j.ijhydene.2021.03.091

Chen, S., Huang, D., Xu, P., Xue, W., Lei, L., Cheng, M., Wang, R., Liu, X., & Deng, R. (2020). Semiconductor-based photocatalysts for photocatalytic and photoelectrochemical water splitting: Will we stop with photocorrosion? In *Journal of Materials Chemistry A* (Vol. 8, Issue 5). Royal Society of Chemistry. https://doi.org/10.1039/c9ta12799b

Cheng, C., Shi, J., Mao, L., Dong, C. L., Huang, Y. C., Zong, S., Liu, J., Shen, S., & Guo, L. (2023). Ultrathin porous graphitic carbon nitride from recrystallized precursor toward significantly enhanced photocatalytic water splitting. *Journal of Colloid and Interface Science*, *637*, 271–282. https://doi.org/10.1016/j.jcis.2023.01.098

Chi, J., Jiang, Z., Yan, J., Larimi, A., Wang, Z., Wang, L., & Shangguan, W. (2022). Recent advancements in bismuth vanadate photoanodes for photoelectrochemical water splitting. *Materials*

Today Chemistry, *26*, 101060. https://doi.org/10.1016/j.mtchem.2022.101060

Cui, W., Bai, H., Shang, J., Wang, F., Xu, D., Ding, J., Fan, W., & Shi, W. (2020). Organic-inorganic hybrid-photoanode built from NiFe-MOF and TiO2 for efficient PEC water splitting. *Electrochimica Acta*, *349*, 136383. https://doi.org/10.1016/j.electacta.2020.136383

Dharmarajan, N. P., Vidyasagar, D., Yang, J., Talapaneni, S. N., Lee, J., Ramadass, K., Singh, G., Fawaz, M., Kumar, P., & Vinu, A. (2023). Bio-inspired Supramolecular Self-assembled Carbon Nitride Nanostructures for Photocatalytic Water Splitting. *Advanced Materials*. https://doi.org/10.1002/adma.202306895

Dong, Y., Han, Q., Hu, Q., Xu, C., Dong, C., Peng, Y., Ding, Y., & Lan, Y. (2021). Carbon quantum dots enriching molecular nickel polyoxometalate over CdS semiconductor for photocatalytic water splitting. *Applied Catalysis B: Environmental*, *293*(April), 120214. https://doi.org/10.1016/j.apcatb.2021.120214

Fajrina, N., & Tahir, M. (2019). A critical review in strategies to improve photocatalytic water splitting towards hydrogen production. *International Journal of Hydrogen Energy*, *44*(2), 540–577. https://doi.org/10.1016/j.ijhydene.2018.10.200

Falciani, G., & Chiavazzo, E. (2023). An overview on modelling approaches for photochemical and photoelectrochemical solar fuels processes and technologies. *Energy Conversion and Management*, *292*(June), 117366. https://doi.org/10.1016/j.enconman.2023.117366

Ghoti, A. N., Patil, A. B., & Pardeshi, S. K. (2023). Li sensitized CdS/TiO2 nanocomposite photoanode for solar water splitting, hydrogen generation and photoelectrochemical (PEC) performance. *International Journal of Hydrogen Energy*, *xxxx*. https://doi.org/10.1016/j.ijhydene.2023.08.025

Guo, F., Huang, X., Chen, Z., Shi, Y., Sun, H., Cheng, X., Shi, W., & Chen, L. (2021). Formation of unique hollow ZnSnO3@ZnIn2S4 core-shell heterojunction to boost visible-light-driven photocatalytic water splitting for hydrogen production. *Journal of Colloid and Interface Science*, *602*, 889–897. https://doi.org/10.1016/j.jcis.2021.06.074

Gupta, N. M. (2017). Factors affecting the efficiency of a water splitting photocatalyst: A perspective. *Renewable and Sustainable Energy Reviews*, *71*(November 2016), 585–601. https://doi.org/10.1016/j.rser.2016.12.086

Hassan, I. U., Naikoo, G. A., Salim, H., Awan, T., Tabook, M. A., Pedram, M. Z., Mustaqeem, M., Sohani, A., Hoseinzadeh, S., & Saleh, T. A. (2023). Advances in photochemical splitting of seawater over semiconductor nano-catalysts for hydrogen production: A critical review. *Journal of Industrial and Engineering Chemistry*, *121*, 1–14. https://doi.org/10.1016/j.jiec.2023.01.006

Hisatomi, T., Kubota, J., & Domen, K. (2014). Recent advances in semiconductors for photocatalytic and photoelectrochemical water splitting. *Chemical Society Reviews*, *43*(22), 7520–7535. https://doi.org/10.1039/c3cs60378d

Hu, X., Li, Y., Wei, X., Wang, L., She, H., Huang, J., & Wang, Q. (2022). Preparation of double-layered Co−Ci/NiFeOOH co-catalyst for highly meliorated PEC performance in water splitting. *Advanced Powder Materials*, *1*(3), 100024. https://doi.org/10.1016/j.apmate.2021.11.010

Ishaq, H., Dincer, I., & Crawford, C. (2022). A review on hydrogen production and utilization: Challenges and opportunities. *International Journal of Hydrogen Energy*, *47*(62), 26238–26264. https://doi.org/10.1016/j.ijhydene.2021.11.149

Jafari, T., Moharreri, E., Amin, A. S., Miao, R., Song, W., & Suib, S. L. (2016). Photocatalytic water splitting - The untamed dream: A review of recent advances. *Molecules*, *21*(7). https://doi.org/10.3390/molecules21070900

Ji, M. H., Chen, Y. X., Chen, R., Li, K. X., Zhao, H. P., Shi, H. Y., Wang, H. L., Jiang, X., & Lu, C. Z. (2023). A novel α-Fe2O3 photoanode with multilayered In2O3/Co–Mn nanostructure for efficient photoelectrochemical water splitting. *International Journal of Hydrogen Energy*, *xxxx*. https://doi.org/10.1016/j.ijhydene.2023.08.061

Ji, M., & Wang, J. (2021). Review and comparison of various hydrogen production methods based on costs and life cycle impact assessment indicators. *International Journal of Hydrogen Energy*, *46*(78), 38612–38635. https://doi.org/10.1016/j.ijhydene.2021.09.142

Jiang, C., Moniz, S. J. A., Wang, A., Zhang, T., & Tang, J. (2017). Photoelectrochemical devices for solar water splitting-materials and challenges. *Chemical Society Reviews*, *46*(15), 4645–4660. https://doi.org/10.1039/c6cs00306k

Kabir, E., Kumar, P., Kumar, S., Adelodun, A. A., & Kim, K. H. (2018). Solar energy: Potential and future prospects. *Renewable and Sustainable Energy Reviews*, *82*(September 2017), 894–900. https://doi.org/10.1016/j.rser.2017.09.094

Li, X., Garlisi, C., Guan, Q., Anwer, S., Al-Ali, K., Palmisano, G., & Zheng, L. (2021). A review of material aspects in developing direct Z-scheme photocatalysts. *Materials Today*, *47*(xx), 75–107. https://doi.org/10.1016/j.mattod.2021.02.017

Liu, H., Fan, X., Li, Y., Guo, H., Jiang, W., & Liu, G. (2023). Hematite-based photoanodes for photoelectrochemical water splitting: Performance, understanding, and possibilities. *Journal of Environmental Chemical Engineering*, *11*(1), 109224. https://doi.org/10.1016/j.jece.2022.109224

Maeda, K. (2011). Photocatalytic water splitting using semiconductor particles: History and recent developments. *Journal of Photochemistry and Photobiology C: Photochemistry Reviews*, *12*(4), 237–268. https://doi.org/10.1016/j.jphotochemrev.2011.07.001

Minggu, L. J., Wan Daud, W. R., & Kassim, M. B. (2010). An overview of photocells and photoreactors for photoelectrochemical water splitting. *International Journal of Hydrogen Energy*, *35*(11), 5233–5244. https://doi.org/10.1016/j.ijhydene.2010.02.133

Oh, T. H., Hasanuzzaman, M., Selvaraj, J., Teo, S. C., & Chua, S. C. (2018). Energy policy and alternative energy in Malaysia: Issues and challenges for sustainable growth – An update. *Renewable and Sustainable Energy Reviews*, *81*(July 2017), 3021–3031. https://doi.org/10.1016/j.rser.2017.06.112

Pattanayak, P., Singh, P., Bansal, N. K., Paul, M., Dixit, H., Porwal, S., Mishra, S., & Singh, T. (2022). Recent progress in perovskite transition metal oxide-based photocatalyst and photoelectrode materials for solar-driven water splitting. *Journal of Environmental Chemical Engineering*, *10*(5), 108429. https://doi.org/10.1016/j.jece.2022.108429

Qi, J., Zhang, W., & Cao, R. (2018). Solar-to-Hydrogen Energy Conversion Based on Water Splitting. *Advanced Energy Materials*, *8*(5), 1–16. https://doi.org/10.1002/aenm.201701620

Razi, F., & Dincer, I. (2022). Renewable energy development and hydrogen economy in MENA region: A review. *Renewable and Sustainable Energy Reviews*, *168*(July), 112763. https://doi.org/10.1016/j.rser.2022.112763

Reli, M., Ambrožová, N., Valášková, M., Edelmannová, M., Čapek, L., Schimpf, C., Motylenko, M., Rafaja, D., & Kočí, K. (2021). Photocatalytic water splitting over CeO2/Fe2O3/Ver photocatalysts. *Energy Conversion and Management*, *238*. https://doi.org/10.1016/j.enconman.2021.114156

Saddique, Z., Imran, M., Javaid, A., Kanwal, F., Latif, S., Santos, J. C. S. dos, Kim, T. H., & Boczkaj, G. (2023). Bismuth-based nanomaterials-assisted photocatalytic water splitting for sustainable hydrogen production. *International Journal of Hydrogen Energy*, *xxxx*. https://doi.org/10.1016/j.ijhydene.2023.05.047

Shi, N., Li, X., Fan, T., Zhou, H., Zhang, D., & Zhu, H. (2014). Artificial chloroplast: Au/chloroplast-morph-TiO2 with fast electron transfer and enhanced photocatalytic activity. *International Journal of Hydrogen Energy*, *39*(11), 5617–5624. https://doi.org/10.1016/j.ijhydene.2014.01.187

Song, H., Luo, S., Huang, H., Deng, B., & Ye, J. (2022). Solar-Driven Hydrogen Production: Recent Advances, Challenges, and Future Perspectives. *ACS Energy Letters*, *7*(3), 1043–1065. https://doi.org/10.1021/acsenergylett.1c02591

Sreedhar, A., Ta, Q. T. H., & Noh, J. S. (2022). Rational engineering of morphology modulated Ti-ZnO thin films coupled monolayer Ti3C2 MXene for efficient visible light PEC water splitting activity. *Journal of Electroanalytical Chemistry*, *921*(March), 116703. https://doi.org/10.1016/j.jelechem.2022.116703

Su, Z., Fang, F., Li, X., Han, W., Liu, X., & Chang, K. (2022). Synergistic surface oxygen defect and bulk Ti3+ defect engineering on SrTiO3 for enhancing photocatalytic overall water splitting. *Journal of Colloid and Interface Science*, *626*, 662–673. https://doi.org/10.1016/j.jcis.2022.06.109

Takanabe, K., & Domen, K. (2011). Toward visible light response: Overall water splitting using heterogeneous photocatalysts. *Green*, *1*(5–6), 313–322. https://doi.org/10.1515/GREEN.2011.030

Tamirat, A. G., Rick, J., Dubale, A. A., Su, W. N., & Hwang, B. J. (2016). Using hematite for photoelectrochemical water splitting: A review of current progress and challenges. *Nanoscale Horizons*, *1*(4), 243–267. https://doi.org/10.1039/c5nh00098j

Tentu, R. D., & Basu, S. (2017). Photocatalytic water splitting for hydrogen production. *Current Opinion in Electrochemistry*, *5*(1), 56–62. https://doi.org/10.1016/j.coelec.2017.10.019

Tijent, F. Z., Voss, P., & Faqir, M. (2023). Recent advances in InGaN nanowires for hydrogen production using photoelectrochemical water splitting. *Materials Today Energy*, *33*, 101275. https://doi.org/10.1016/j.mtener.2023.101275

Tong, M. H., Chen, Y. X., Lin, S. W., Zhao, H. P., Chen, R., Jiang, X., Shi, H. Y., Zhu, M. L., Zhou, Q. Q., & Lu, C. Z. (2023). Synchronous electrochemical anodization: A novel strategy for preparing cerium doped TiO2 nanotube arrays toward visible-light PEC water splitting. *Electrochimica Acta*, *463*(February), 1–12. https://doi.org/10.1016/j.electacta.2023.142793

Uğuz, Ö., & Koca, A. (2021). Hybrid <scp>photoelectrochemical–photocatalytic</scp> hydrogen evolution reaction with reduced graphene oxide–binary metal chalcogenide composites. *International Journal of Energy Research*, *45*(13), 19303–19315. https://doi.org/10.1002/er.7027

Velusamy, P., Liu, X., Sathiya, M., Alsaiari, N. S., Alzahrani, F. M., Nazir, M. T., Elamurugu, E., Pandian, M. S., & Zhang, F. (2023). Investigate the suitability of g-C3N4 nanosheets ornamented with BiOI nanoflowers for photocatalytic dye degradation and PEC water splitting. *Chemosphere*, *321*(January), 138007. https://doi.org/10.1016/j.chemosphere.2023.138007

Wang, Y. Y., Chen, Y. X., Barakat, T., Zeng, Y. J., Liu, J., Siffert, S., & Su, B. L. (2022). Recent advances in non-metal doped titania for solar-driven photocatalytic/photoelectrochemical water-splitting. *Journal of Energy Chemistry*, *66*, 529–559. https://doi.org/10.1016/j.jechem.2021.08.038

Wang, Y., Zhao, Y., Zhu, P., Wu, X., Koshayeva, A., Ding, L., Wei, G., & Su, Y. (2023). A promising one-step carbothermal reduction nitridation strategy for enhancing photoelectrochemical performance of TiO2 nanowire array-based catalysts with stable nitrogen doping and desired core-double shell structure. *Applied Surface Science*, *639*(June), 158261. https://doi.org/10.1016/j.apsusc.2023.158261

Wei, Y., Wan, J., Wang, J., Zhang, X., Yu, R., Yang, N., & Wang, D. (2021). Hollow Multishelled Structured SrTiO3 with La/Rh Co-Doping for Enhanced Photocatalytic Water Splitting under Visible Light. *Small*, *17*(22), 1–7. https://doi.org/10.1002/smll.202005345

Wu, H., Tan, H. L., Toe, C. Y., Scott, J., Wang, L., Amal, R., & Ng, Y. H. (2020). Photocatalytic and Photoelectrochemical Systems: Similarities and Differences. *Advanced Materials*, *32*(18), 1–21. https://doi.org/10.1002/adma.201904717

Xu, H., Chen, S., Wang, K., & Wang, X. (2022). Enhancing the PEC water splitting performance of In2O3 nanorods by a wet chemical reduction. *International Journal of Hydrogen Energy*, *47*(90), 38219–38228. https://doi.org/10.1016/j.ijhydene.2022.08.305

Xu, M. L., Li, J. R., Wu, X. M., Yu, T., Qin, G. Y., Wang, F. J., Zhang, L. N., Li, K., & Cheng, X. (2022). The excellent photocatalytic overall water splitting activity of TpPa-1-COF excited via MOF derived FeP-PC and α-Fe2O3 dual cocatalysts. *Applied Surface Science*, *602*(July), 154371. https://doi.org/10.1016/j.apsusc.2022.154371

Yang, J., Shi, C., Dong, Y., Su, H., Sun, H., Guo, Y., & Yin, S. (2022). Efficient hydrogen generation of vector Z-scheme CaTiO3/Cu/TiO2 photocatalyst assisted by cocatalyst Cu nanoparticles. *Journal of Colloid and Interface Science*, *605*, 373–384. https://doi.org/10.1016/j.jcis.2021.07.106

Yang, W., & Prabhakar, R. (2019). *Chem Soc Rev photovoltage , and stability of photoelectrodes*. https://doi.org/10.1039/c8cs00997j

Zhang, M., Nie, S., Cheng, T., Feng, Y., Zhang, C., Zheng, L., Wu, L., Hao, W., & Ding, Y. (2021). Enhancing the macroscopic polarization of CdS for piezo-photocatalytic water splitting. *Nano Energy*, *90*(September). https://doi.org/10.1016/j.nanoen.2021.106635

Zhang, X., & Jiang, S. P. (2022). Layered g-C3N4/TiO2 nanocomposites for efficient photocatalytic water splitting and CO2 reduction: a review. *Materials Today Energy*, *23*. https://doi.org/10.1016/j.mtener.2021.100904

Zhang, X., Jing, D., & Guo, L. (2010). Effects of anions on the photocatalytic H2 production performance of hydrothermally synthesized Ni-doped Cd0.1Zn 0.9S photocatalysts. *International Journal of Hydrogen Energy*, *35*(13), 7051–7057. https://doi.org/10.1016/j.ijhydene.2009.12.132

Zheng, Y., Wang, L., Pang, J., Sun, K., Hou, J., Wang, G., Guo, W., & Chen, L. (2023). Ni3S2/Co9S8 embedded poor crystallinity NiCo layered double hydroxides hierarchical nanostructures for efficient overall water splitting. *Journal of Colloid and Interface Science*, *637*, 85–93. https://doi.org/10.1016/j.jcis.2023.01.074

Zhou, H., Yan, R., Zhang, D., & Fan, T. (2016). Challenges and Perspectives in Designing Artificial Photosynthetic Systems. *Chemistry - A European Journal*, *22*(29), 9870–9885. https://doi.org/10.1002/chem.201600289

Zuo, G., Wang, Y., Teo, W. L., Xian, Q., & Zhao, Y. (2021). Direct Z-scheme TiO2–ZnIn2S4 nanoflowers for cocatalyst-free photocatalytic water splitting. *Applied Catalysis B: Environmental*, *291*(February), 120126. https://doi.org/10.1016/j.apcatb.2021.120126

CHAPTER VIII

Polysaccharides gums: Gum tragacanth-based hydrogel for the removal of pollutants

F. Fulya TAKTAK [1]

Introduction

Polysaccharide gums are important biodegradable industrial raw materials that are abundant in nature. Polysaccharide gums are biopolymers derived from various natural sources (see Figure 1) (Parhi, Sahoo & Das, 2023; Mohammed, Naveed & Jost, 2021). Some plant gums are a product of the natural protective mechanism of the plant against pathological conditions such as fungal attack, high temperatures or physical impact (Amiri et al., 2021; Muruganantham et al., 2022). Such gums are called exudate gums (Barak, Mudgil & Taneja, 2020).

[1] Doç. Dr., Uşak University, fulya.taktak@usak.edu.tr

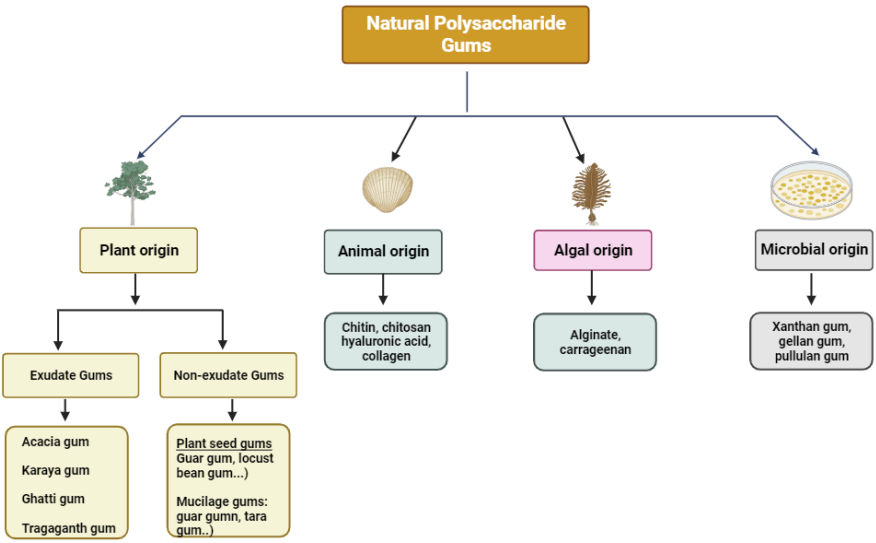

Figure 1: Classification of polysaccharides gums according to their source.

Gums are heterogeneous carbohydrates formed by O-glycosidic bonds between different sugars such as arabinose, glucose, and galactose (Shobana et al., 2022). Gums obtained by extraction from different sources are called non-exudates. Gums extracted from plants and animals can be produced in large quantities. The wide variety of structural properties of polysaccharides results from differences in monosaccharide composition, linkage types and patterns, and chain shapes which determines their physical properties, including degree of polymerization, solubility, flow behavior, gelling potential, and/or surface and interfacial properties (Izydorczyk & Wang, 2005; Gomez, Malinconico & Laurienzo, 2008).

Exudate gums are among the oldest natural gums. The four most important exudate gums—karaya gum, acacia gum, Ghati gum, gum Arabic, and tragacanth gum—have been used by people for centuries as food and as a remedy for various diseases.

Gum Tragacanth

The plant species Astragalus grows in the mountainous regions of Turkey and Iran (Yıldırım & Cansaran, 2010). It is the most species-rich genus of the Fabaceae family, and more than 400 different species of this genus, which includes more than 2000 species worldwide, grow naturally in our country, and more than half of them are endemic species that grow only in Turkey. Tragacanth gum is a dried exudate obtained from the stems and stalks of various Astragalus species (A. gummifer, A. parrowianus, A. fluccosus, A. rahensis, A. gossypinus, A. microcephalus and A. compactus.), with Astragalus microcephalus and Astragalus gummifer being the main sources (Gavlighi, 2013). A gum called tragacanth is extracted from the stems of these species. It is a yellow, sticky, whitish, valuable gum extracted from the cracks in the stem (Prasad et al., 2022). Tragacanth gum is a highly branched anionic polysaccharide and one of the most cost-effective natural biopolymers available. It is a biocompatible, highly viscous, odorless, tasteless, polyhydroxylated, and very hydrophilic polysaccharide with a molecular weight of ~850 kDa.

As summarized in Figure 2, gum tragacanth is mainly composed of water-insoluble bassorin (BIW) and water-soluble gum tragacanth (TGSW), but the composition of gum tragacanth in different Astragalus species varies (Taghavizadeh et al., 2021; Boamah et al., 2023; Balaghi, Mohammadifar & Zargaraan, 2010).

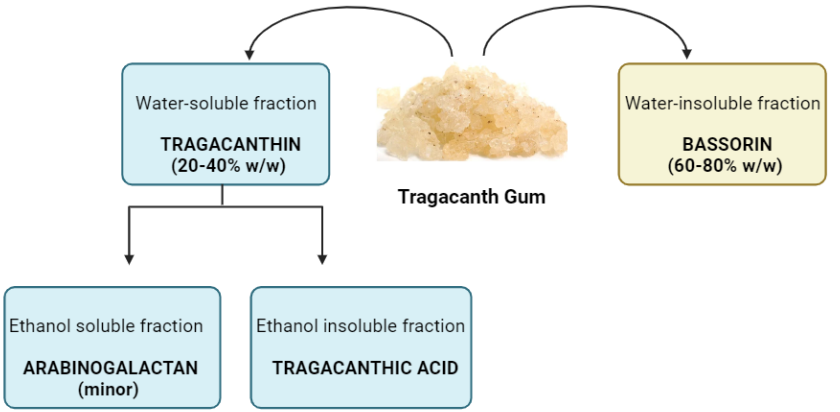

Figure 2: Gum tragacanth fractions

Figure 2 shows that the percentage of tragacanthin and bassorin fractions of gum tragacanth varies over a wide range. This is due to the fact that the different Astra gallus species yield very different proportions of water-soluble and water-insoluble fractions (Andeson & Grant, 1988).

The different composition of the gum tragacanth obtained, depending on the Astragallus species used, therefore leads to differences in many physicochemical properties of the product, such as solubility, gelling capacity, surface/interface properties, and viscosity.

Application of gum tragacanth in industrial water treatment

Wastewater treatment has become the focus of research and technology worldwide. Over the last quarter of a century, the use of chemicals has increased considerably, mainly due to growing consumer habits and industrial development. Due to the lack of pre-treatment in industry, dyes, pesticides, heavy metals, and organic compounds are released from the source into receiving waters, with extremely dangerous consequences for humans, animals, and plants (Berradi et al., 2019; Zhou et al., 2018; Lellis et al., 2019; Patil et al.,

2022). Intensive efforts are being made worldwide, particularly in science, to treat wastewater. Adsorption is one of these methods, that is expected to be easy to handle, time-saving, and cost-saving (Rashid et al., 2021; Nassar, 2010; Abdelfattah, 2016). In this context, the production of inexpensive and abundant adsorbents, which may contain different functional groups, is very important for the removal of various pollutants from industrial wastewater by adsorption.

Cross-linked hydrogels are produced by the cross-linking of polymer chains during the polymerization of monomers with hydrophilic side groups such as OH and NH_2Hydrogels are known as superadsorbents which can adsorb hundreds of times their own mass in water. The diversity of their functional groups enables them to interact with many heavy metals or organic impurities in water. Chemically crosslinked hydrogels are prepared by adding chemical crosslinkers such as glutaraldehyde (An et al., 1995), N, N′-methylene-bis-acrylamide (Taktak & Özyaranlar, 2022). divinyl sulfone (Sannino et al., 2004), and epichlorohydrin (Garnica-Palafox et al., 2014) to the polymerization medium. These chemically cross-linked hydrogels, which are mechanically reinforced, can withstand harsh conditions such as pH, ionic strength, and heat in water. On the other hand, regeneration is possible. Furthermore, the desired physico-chemical and biochemical properties of hydrogels are usually imparted to polymer matrices by using fillers such as clay, metal oxides or carbon nanoparticles (Gonzalez & Alvarez, 2019; Xing & Tang, 2022).

In recent years, gum-based hydrogels produced by graft copolymerization of various monomers with different polysaccharide gums have shown very successful results in the removal of pollutants from wastewater. The fact that polysaccharide gums are naturally and abundantly available paves the way for their use in this field.

Table 1: List of articles on hydrogels based on tragacanth gum (GT) synthesized for the removal of pollutants from wastewater, found by Scopus search for all years.

Hydrogel	**Reactants**	**Pollutants**	**Adsorption capacity**	**Reference**
TG-***cl***-GA/CC	GT, glutaraldehyde (GA), $CaCO_3$ (CC)	methylene blue	1401 - 2145 mg/g,	(Mallakpour & Tabesh, 2021).
GumT-cl-HEMA)	GT, 2-hydroxyethyl methacrylate (HEMA)	malachite green	88.57	(Sharma et al., 2021)
GumT-cl-HEMA/TiO_2	GT, 2-hydroxyethyl methacrylate (HEMA), TiO_2	malachite green	103.09	(Sharma et al., 2021)
TG-***cl***-PAA/Fe_3O_4	GT, acrylic acid (AA), Fe_3O_4	malachite green thioflavin T rhodamine B	642.9 552.6 413.6	(Jaymand, 2023)
CF@SS@PTG	GT, $CoFe_2O_4$ (*CF*), silica-shell (SS), poly (methacrylic acid) (PTG)	methyl orange methyl red	336 387	(Moghaddam et al., 2020)
Poly (AMPS)-g-GT/GO	GT, 2-acrylamido-2-methylpropanesulfonic acid (AMPS), graphene oxide	Pb (II) Cd (II) Ag (I)	142.50 112.50 132.12	(Sahraei, Pour & Ghaemy, 2017)
Poly (AMPS-co-VI g-GT/PVA/GO/Fe_3	GT, 1-vinylimidazole (VI), 2-acrylamido-2-methyl-1-propanesulfonic acid (AMPS), poly (vinyl alcohol) (PVA), graphene oxide (GO), Fe_3O_4	crystal violet Congo red Pb (II) Cu (II)	81.78 69.67 94.0 101.74	(Sahraei & Ghaemy, 2017)

Poly (AMPS-***g***-GT)/PVA/GO/Ag^0	GT, 2-acrylamido-2-methyl-1-propanesulfonic acid (AMPS), poly (vinyl alcohol), graphene oxide (GO), Ag	Ca^{2+} Mg^{2+}	114.18 162.46	(Mohammadian, Sahraei & Ghaemy, 2019).
Fe_3O_4/P(MMA)-***g***-TG	TG, poly (methyl methacrylate, Fe_3O_4	Cr (VI)	7.64	(Sadeghi, Rad, & Moghaddam, 2014).
GT/TMSQA	GT, quaternary ammonium salt (TMSQA)	NO^{3-}	19.95	(Shojaipour, Ghaemy & Amininasab, 2020)
GA-GT/PAAm	GT, glutamic acid (GA), polyacrylamide (PAAm)	U(VI)	384.6	(Moghaddam et al., 2019)
TG-*g*-PANI	GT, aniline (ANI)	U(VI)	26	(Sadeghi & Asadi, 2023).
PPAC/TG	GT, pomegranate peels (PPAC)	crystal violet	455.61	(Thamer, Al-aizari, & Abdo, 2023).
TG/VCFCNT	GT, vitamin C-functionalized carbon nanotube (VCFCNT)	methylene blue	863	(Tabesh & Mallakpour, 2023).
GT-PVA/TA	GT, poly (vinyl alcohol) (PVA), tannin (TA)	methyl violet	35.21	(Parsaeian et al., 2023)

The presence of numerous OH and COOH groups in the structure of GT makes it possible to modify it with many functional organic or inorganic compounds, making it suitable for the production of new materials. Hydrogels based on gum tragacanth (TG) used in wastewater treatment are listed in Table 2. Scopus was

searched in all years to find all articles in this field. A total of 15 research papers on tragacanth-based hydrogel adsorbents for wastewater treatment were published, with the number increasing over the years. The oldest article dates back to 2014, and it seems that tragacanth-based adsorbents are a relatively new field for future wastewater treatment studies. As can be seen from the results, the synthesis of tragacanth-based adsorbents has increased significantly in 2023. These adsorbents have been used to adsorb heavy metals such as Pb and Cr, as well as dyes such as methylene blue and Congo red, which are among the main pollutants in wastewater. In recent years, water pollution has become one of the most important problems for the whole world, in parallel with increasing environmental pollution. The interest in low-cost adsorbents with high adsorption capacity is due to growing environmental awareness.

Conclusion

This study includes an analysis of scientific publications on tragacanth-based hydrogel adsorbents used in wastewater treatment. The data comes from the Scopus® database and covers all years. The number of publications in 2023 in this field is the highest at 4. The researchers mainly focused on the removal of dyes and heavy metals from wastewater, which are known to have negative effects on humans and other living organisms and can be toxic, mutagenic, or carcinogenic. Tragacanth gum is a new focus for future research, and it is certain that it will be included in the composition of adsorbents in more and more studies.

References

Abdelfattah, I., Ismail, A. A., Al Sayed, F., Almedolab, A., & Aboelghait, K. M. (2016). Biosorption of heavy metals ions in real industrial wastewater using peanut husk as efficient and cost effective adsorbent. *Environmental Nanotechnology, Monitoring & management.* https://doi.org/10.1016/j.enmm.2016.10.007

Amiri, M. S., Mohammadzadeh, V., Yazdi, M. E. T., Barani, M., Rahdar, A., & Kyzas, G. Z. (2021). Plant-based gums and mucilages applications in pharmacology and nanomedicine: a review. *Molecules*, *26*(6), 1770. https://doi.org/10.1016/j.enmm.2016.10.007

An, Y., Koyama, T., Hanabusa, K., Shirai, H., Ikeda, J., Yoneno, H., & Itoh, T. (1995). Preparation and properties of highly phosphorylated poly (vinyl alcohol) hydrogels chemically crosslinked by glutaraldehyde. *Polymer*, *36*(11), 2297-2301. https://doi.org/10.1016/0032-3861(95)95310-W

Anderson, D. M. W.& Grant, D. A. D. (1988). The chemical characterization of some Astragalus gum exudates. *Food Hydrocolloids*, *2*(5), 417-423. https://doi.org/10.1016/S0268-005X(88)80006-7

Balaghi, S., Mohammadifar, M., & Zargaraan, A. (2010). Physicochemical and rheological characterization of gum tragacanth exudates from six species of Iranian *Astragalus*. *Food Biophysics*, 5, 59-71. https://doi.org/10.1007/s11483-009-9144-5

Barak, S., Mudgil, D., & Taneja, S. (2020). Exudate gums: chemistry, properties and food applications–a review. *Journal of the Science of Food and Agriculture*, *100*(7), 2828-2835. https://doi.org/10.1002/jsfa.10302

Berradi, M., Hsissou, R., Khudhair, M., Assouag, M., Cherkaoui, O., El Bachiri, A., & El Harfi, A. (2019). Textile finishing dyes and their impact on aquatic environs. *Heliyon*, *5*(11), e02711. https://doi.org/10.1016/j.heliyon.2019.e02711.

Boamah, P. O., Afoakwah, N. A., Onumah, J., Osei, E. D., & Mahunu, G. K. (2023). Physicochemical properties, biological properties and applications of gum tragacanth-A review. *Carbohydrate Polymer Technologies and Applications*, 100288. https://doi.org/10.1016/j.carpta.2023.100288

Garnica-Palafox, I. M., Sánchez-Arévalo, F. M., Velasquillo, C., García-Carvajal, Z. Y., García-López, J., Ortega-Sánchez, C., ... & Solís-Arrieta, L. P. M. I. D. (2014). Mechanical and structural response of a hybrid hydrogel based on chitosan and poly (vinyl alcohol) cross-linked with epichlorohydrin for potential use in tissue engineering. *Journal of Biomaterials Science, Polymer Edition*, *25*(1), 32-50. https://doi.org/10.1080/09205063.2013.833441

Gavlighi, H. A., Meyer, A. S., Zaidel, D. N., Mohammadifar, M. A., & Mikkelsen, J. D. (2013). Stabilization of emulsions by gum tragacanth (Astragalus spp.) correlates to the galacturonic acid content and methoxylation degree of the gum. *Food Hydrocolloids*, *31*(1), 5-14. https://doi.org/10.1016/j.foodhyd.2012.09.004

Gomez d'Ayala, G., Malinconico, M., & Laurienzo, P. (2008). Marine derived polysaccharides for biomedical applications: chemical modification approaches. *Molecules*, *13*(9), 2069-2106. https://doi.org/10.3390/molecules13092069

Gonzalez, J. S., & Alvarez, V. A. (2019). Different fillers in PVA composite hydrogels: Their influence on the final properties.

Izydorczyk, M., Cui, S. W., & Wang, Q. (2005). Polysaccharide gums: structures, functional properties, and applications. *Food carbohydrates: Chemistry, physical properties, and applications*, *293*, 299.

Jaymand, M., (2023) Biosorptive removal of cationic dyes from ternary system using a magnetic nanocomposite hydrogel based on modified tragacanth gum. *Carbohydrate Polymer*

Technologies and Applications, 100403. https://doi.org/10.1016/j.carpta.2023.100403

Lellis, B., Fávaro-Polonio, C. Z., Pamphile, J. A., & Polonio, J. C. (2019). Effects of textile dyes on health and the environment and bioremediation potential of living organisms. *Biotechnology Research and Innovation*, *3*(2), 275-290. https://doi.org/10.1016/j.biori.2019.09.001

Mallakpour, S., & Tabesh, F. (2021). Effective adsorption of methylene blue dye from water solution using renewable natural hydrogel bionanocomposite based on tragacanth gum: Linear-nonlinear calculations. *International Journal of Biological Macromolecules*, *187*, 319-324. https://doi.org/10.1016/j.ijbiomac.2021.07.105

Mohammadian, M., Sahraei, R., & Ghaemy, M. (2019). Synthesis and fabrication of antibacterial hydrogel beads based on modified-gum tragacanth/poly (vinyl alcohol)/Ag0 highly efficient sorbent for hard water softening. *Chemosphere*, *225*, 259-269. https://doi.org/10.1016/j.chemosphere.2019.03.040

Moghaddam, R. H., Dadfarnia, S., Shabani, A. M. H., & Tavakol, M. (2019). Synthesis of composite hydrogel of glutamic acid, gum tragacanth, and anionic polyacrylamide by electron beam irradiation for uranium (VI) removal from aqueous samples: Equilibrium, kinetics, and thermodynamic studies. *Carbohydrate polymers*, *206*, 352-361. https://doi.org/10.1016/j.carbpol.2018.10.030

Moghaddam, A. Z., Jazi, M. E., Allahrasani, A., Ganjali, M. R., & Badiei, A. (2020). Removal of acid dyes from aqueous solutions using a new eco-friendly nanocomposite of $CoFe_2O_4$ modified with Tragacanth gum. *Journal of Applied Polymer Science*, *137*(17), 48605. https://doi.org/10.1002/app.48605

Mohammed, A. S. A., Naveed, M., & Jost, N. (2021). Polysaccharides; classification, chemical properties, and future perspective applications in fields of pharmacology and biological

medicine (a review of current applications and upcoming potentialities). *Journal of Polymers and the Environment*, *29*, 2359-2371. https://doi.org/10.1007/s10924-021-02052-2

Muruganantham, S., Krishnaswami, V., Anitha Manikandan, D., Aravindaraj, N., Suresh, J., Murugesan, M., & Kandasamy, R. (2022). Gums as Pharmaceutical Excipients: An Overview. *Gums, Resins and Latexes of Plant Origin: Chemistry, Biological Activities and Uses*, 145-189.

Nassar, N. N. (2010). Rapid removal and recovery of Pb (II) from wastewater by magnetic nanoadsorbents. *Journal of hazardous materials*, *184*(1-3), 538-546. https://doi.org/10.1016/j.jhazmat.2010.08.069.

Parhi, R., Sahoo, S. K., & Das, A. (2023). Applications of polysaccharides in topical and transdermal drug delivery: A recent update of literature. *Brazilian Journal of Pharmaceutical Sciences, 58*. https://doi.org/10.1590/s2175-97902022e20802

Parsaeian, M. R., Haji Shabani, A. M., Dadfarnia, S., & Hafezi Moghaddam, R. (2023). Synthesis of tragacanth composite hydrogels, polyvinyl alcohol and tannins by electron beam irradiation and its application for methyl violet removal from aqueous media. *Polymer Bulletin*, 1-17. https://doi.org/10.1007/s00289-023-04880-9

Patil, R., Zahid, M., Govindwar, S., Khandare, R., Vyavahare, G., Gurav, R., ... & Jadhav, J., Desai, N., Pandit, S., Jadhav, J. (2022). Constructed wetland: a promising technology for the treatment of hazardous textile dyes and effluent. In *Development in Wastewater Treatment Research and Processes* (pp. 173-198). Elsevier. https://doi.org/10.1016/B978-0-323-85583-9.00016-8

Prasad, N., Thombare, N., Sharma, S. C., & Kumar, S. (2022). Production, processing, properties and applications of karaya (Sterculia species) gum. *Industrial Crops and Products*, *177*, 114467. https://doi.org/10.1016/j.indcrop.2021.114467

Rashid, R., Shafiq, I., Akhter, P., Iqbal, M. J., & Hussain, M. (2021). A state-of-the-art review on wastewater treatment techniques: the effectiveness of adsorption method. *Environmental Science and Pollution Research*, *28*, 9050-9066. https://doi.org/10.1007/s11356-021-12395-x.

Sadeghi, S., Rad, F. A., & Moghaddam, A. Z. (2014). A highly selective sorbent for removal of Cr (VI) from aqueous solutions based on Fe_3O_4/poly (methyl methacrylate) grafted Tragacanth gum nanocomposite: optimization by experimental design. *Materials Science and Engineering: C*, *45*, 136-145. https://doi.org/10.1016/j.msec.2014.08.063

Sadeghi, S., & Asadi, E. (2023). Tragacanth gum grafted polyaniline hydrogel as a biodegradable adsorbent for the removal of uranyl ions from water samples. *Polymer Bulletin*, 1-20. https://doi.org/10.1007/s00289-023-05065-0

Sahraei, R., & Ghaemy, M. (2017). Synthesis of modified gum tragacanth/graphene oxide composite hydrogel for heavy metal ions removal and preparation of silver nanocomposite for antibacterial activity. *Carbohydrate polymers*, *157*, 823-833. https://doi.org/10.1016/j.carbpol.2016.10.059

Sahraei, R., Pour, Z. S., & Ghaemy, M. (2017). Novel magnetic bio-sorbent hydrogel beads based on modified gum tragacanth/graphene oxide: Removal of heavy metals and dyes from water. *Journal of cleaner production*, *142*, 2973-2984. https://doi.org/10.1016/j.jclepro.2016.10.170

Sannino, A., Madaghiele, M., Conversano, F., Mele, G., Maffezzoli, A., Netti, P. A., Ambrosio, L. & Nicolais, L. (2004). Cellulose derivative− hyaluronic acid-based microporous hydrogels cross-linked through divinyl sulfone (DVS) to modulate equilibrium sorption capacity and network stability. *Biomacromolecules*, *5*(1), 92-96. https://doi.org/10.1021/bm0341881

Shobana, N., Prakash, P., Samrot, A. V., Jane Cypriyana, P. J., Kajal, P., Sathiyasree, M., Saigeetha, S., Dhas, T. S., Anand, D.

A., Sabesan, G. S., Muthuvenkatachalam, B. S, Mohanty, B. K. & Visvanathan, S. (2022). Purification and characterization of gum-derived polysaccharides of Moringa oleifera and Azadirachta indica and their applications as plant stimulants and bio-pesticidal agents. *Molecules*, *27*(12), 3720. https://doi.org/10.3390/molecules27123720

Sharma, B., Thakur, S., Mamba, G., Gupta, R. K., Gupta, V. K., & Thakur, V. K. (2021). Titania modified gum tragacanth based hydrogel nanocomposite for water remediation. *Journal of Environmental Chemical Engineering*, *9*(1), 104608. https://doi.org/10.1016/j.jece.2020.104608

Shojaipour, M., Ghaemy, M., & Amininasab, S. M. (2020). Removal of NO3− ions from water using bioadsorbent based on gum tragacanth carbohydrate biopolymer. *Carbohydrate polymers*, *227*, 115367. https://doi.org/10.1016/j.carbpol.2019.115367

Tabesh, F., & Mallakpour, S. (2023). Removal of the environmental pollutant methylene blue using bio-nanohydrogel nanocomposite containing tragacanth gum and vitamin C-functionalized carbon nanotube. *Polymer Bulletin*, 1-15. https://doi.org/10.1007/s00289-023-04781-x

Taghavizadeh Yazdi, M. E., Nazarnezhad, S., Mousavi, S. H., Sadegh Amiri, M., Darroudi, M., Baino, F., & Kargozar, S. (2021). Gum tragacanth (GT): a versatile biocompatible material beyond borders. *Molecules*, *26*(6), 1510. https://doi.org/10.3390/molecules26061510

Taktak, F. F., & Özyaranlar, E. (2022). Semi-interpenetrating network based on xanthan gum-cl-2-(N-morpholinoethyl methacrylate)/titanium oxide for the single and binary removal of cationic dyes from water. *International Journal of Biological Macromolecules*, *221*, 238-255. https://doi.org/10.1016/j.ijbiomac.2022.08.139

Thamer, B. M., Al-aizari, F. A., & Abdo, H. S. (2023). Activated Carbon-Incorporated Tragacanth Gum Hydrogel

Biocomposite: A Promising Adsorbent for Crystal Violet Dye Removal from Aqueous Solutions. *Gels*, *9*(12), 959. https://doi.org/10.3390/gels9120959

Xing, W., & Tang, Y. (2022). On mechanical properties of nanocomposite hydrogels: Searching for superior properties. *Nano Materials Science*, *4*(2), 83-96. https://doi.org/10.1016/j.nanoms.2021.07.004

Yıldırım, C. & Cansaran, A. (2010). A study on the floristical, phytosociological and phytoecological structure of Turkish Astragalus angustifolius subsp. angustifolius associations. *Kastamonu University Journal of Forestry Faculty*, *10*(2), 164-171.

Zhou, Q., Zhang, J., Fu, J., Shi, J., & Jiang, G. (2008). Biomonitoring: an appealing tool for assessment of metal pollution in the aquatic ecosystem. *Analytica chimica acta*, *606*(2), 135-150. https://doi.org/10.1016/j.aca.2007.11.018.

CHAPTER IX

Aromatic Substances With Antıbıotıc Effect

Elgiz SHARIFOV[1]
Hülya ÇELİK[2]

Introduction

An antibiotic is a type of antimicrobial agent used against bacteria or microorganisms that kills them or prevents them from multiplying. Antibiotics are used to treat or prevent bacterial infections. These substances often exert a special effect against microorganisms and interfere with pathogenic bacteria without harm to human health. Antibiotic aromatic substances are components that are usually found naturally in plants and have antibacterial properties.

[1] Ağrı Ibrahim Cecen University, Faculty of Pharmacy
[2] Doç.Dr, Ağrı Ibrahim Cecen University, Faculty of Pharmacy Basic Pharmaceutical Sciences Department / Fundamental Sciences of Pharmacy 04100 Agri/TURKEY

Antibiotic aromatic substances are components that are usually found in plants and have antimicrobial properties. These substances can inhibit or kill the growth of bacteria, fungi, or other microorganisms. While primary metabolites do not show specific properties in living things but are found in every living thing, secondary metabolites evaluated specifically may lead to different pharmacological activities. There are many parameters that affect the pharmacological activity of drogs. Although they do not have a single pharmacological activity, the various alkaloids, flavonoids, aromatic substances, etc. they contain significantly affect this activity. One of these effects is that they are antibiotic. Certain aromatic substances activate this activity.

The majority of plants synthesize aromatic substances in the form of phenols (Geissman 1963). These substances are most often used as a defense mechanism against microorganisms, insects and herbivores. Some of these, such as terpenoids, give plants their smell; Many compounds determine the taste of the plant, while some compounds play a role in the use of plants for medicinal purposes. (Altuner, 2008)

When antibiotics first appeared, there were no resistance problems yet, and therefore they were used successfully. Today, the increasing number of resistant pathogens all over the world has increased the need for new antimicrobials. The problem of resistance has ceased to be a problem of some pathogenic strains or some hospital departments and has become seen in almost all major bacterial pathogens and treatment units such as emergency care and intensive care units, and even community-acquired infections.

With the increasing development of new antibiotics, antibiotics such as kinupristin/dalfopristin, linezolid, daptomycin and tigecycline have been put into clinical use against gram-positive pathogens with multiple antibiotic resistance. In addition, new glycopeptides such as dalbavansin, oritavansin, telavansin, and new anti MRSA β-lactams such as ceftobiprol and ceftarolin have been used in treatment.

In order to cope with the treatment difficulties, while the search for new antibacterials continues, the more effective use of existing antibiotics and the evaluation of interactions between antibiotics have come to the fore. The problem of resistance, which arose shortly after the discovery of antibiotics, required the search for solutions in those ages as well (Silver 2011).

General information

Primary metabolites are considered essential for almost all living organisms and derive from primary metabolic reactions. These include carbohydrates, nucleotides, proteins, tricarboxylic acid cycle intermediates, lipids, common pigments of photosynthetic processes, and lignin. The primary metabolism of bryophytes is very similar to that of vascular plants. In its cell walls it contains essential compounds such as cellulose, chlorophyll a, chlorophyll b, major carotenoids, starch, nucleic acids, sugars, and some lipids. In studies with bryophytes, lignin-like aromatic compounds, carbohydrates and amino acids are encountered.

There are many aromatic substances and phytochemical compounds that show antimicrobial activity. These compounds can inhibit or kill the growth of microorganisms. Here are examples of aromatic substances and phytochemicals that exhibit some antimicrobial activity:

Allicin: Garlic contains a phytochemical called allicin. Allicin exerts an antimicrobial effect on many microorganisms, including bacteria, fungi and viruses.

Eugenol (Black Pepper and Cellar Oil): Eugenol is a compound found abundantly in black pepper and cellar oil. Due to its antimicrobial properties, it is traditionally used to treat toothache.

Thymol (Thyme): Thyme contains an aromatic compound that contains thymol. Thymol exerts a strong antimicrobial effect on bacteria and fungi and is traditionally used for wound cleansing.

Carvacrol (Thyme and Thyme Oil): Carvacrol is an aromatic compound found in oregano and oregano oil. Carvacrol is an antimicrobial agent that acts on bacteria and fungi.

Tea Tree Oil: Tea tree oil has a strong antimicrobial effect against various microorganisms. It is used to treat skin problems and prevent infections.

Berberine (Golden Seal and Oregon Stirrup)*:* Berberine is an alkaloid found in many plant species. Berberine is effective against bacteria and parasites and is used in the treatment of infections of the digestive tract.

Globaceae (mother-of-pearl): Globaceae is a phytochemical found in the mother-of-pearl plant. Globaceae has the ability to kill microorganisms or inhibit their growth and is used in the treatment of skin problems.

Curcumin (Turmeric): Curcumin, the main active ingredient in turmeric, has antimicrobial and anti-inflammatory properties. It is used to relieve digestive problems and reduce inflammation.

Cineole (Peppermint Oil): Peppermint oil contains a compound called cineole. Cineole is mainly used in the treatment of respiratory infections.

Rosmarinic Acid**:** Rosmarinic acid is a phytochemical compound found in rosemary and has antimicrobial properties. Rosemary oil is used to alleviate skin problems and support hair health.These compounds have evolved evolutionarily as a natural defense mechanism of plants in fighting disease.

These antimicrobial compounds evolved evolutionarily as part of plants' natural defense mechanisms and have been used by humans for medicinal purposes. However, caution should be exercised when using plant extracts or oils that contain these compounds because misuse or overdose can cause some adverse effects.

Recently, one of the problems that have emerged in health sciences is the resistance of pathogenic microorganisms to antibiotic drugs. Therefore, many antibiotics currently used have almost lost their effectiveness against microorganisms. For this reason, new antibiotic drugs, most of which are synthetic, have been introduced to the markets. On the other hand, it is well known that most of the microorganisms on Earth are still unknown, so their antimicrobial potential is also unknown. (Başkaya, 2018)

Sulfonamides are the first group of drugs to be systematically used in the treatment of bacterial infections in humans; They act bacteriostatically (inhibits the growth of bacteria). In general, they show a wide range of antimicrobial activity against both Gram-negative and Gram-positive bacteria. It was discovered that it could be used as a diuretic in the 1940s and as an antidiabetic in the 1950s. The importance of sulfonamides did not decrease in part with the invention of penicillin and other antibiotics, but in the mid-1970s their importance increased again with the use of drug mixtures (such as trimethoprim, trimethamine, etc.), and they are still widely used in the treatment of specific infections. (Karadeniz, Palabıyık, Çakır and Çalış, 2011).

Some aromatic substances, phytochemicals that show antimicrobial activity can be exemplified in Phenolics such as Coumarins, Tannins, Simple Phenols and Phenolic Acids, Quinones, Flavonoids, Flavins, Flavonols.

Phenols

Coumarins

Coumarin derivatives are sold commercially as oral anticoagulants. In addition to their anticoagulant effects, coumarins are used in many biological and pharmaceutical studies due to the physiological, biological, antibiotic and anticancer effects of base coumarin derivatives. Recently, studies on coumarin-based prodrug synthesis have been carried out. Some coumarin derivatives have a

strong medicinal effect as antibacterial and antifungal. It is known that base coumarin derivatives also show antituberculosis activity, and their bases have insecticidal (insecticidal drug) properties. Due to the fact that it has an important bioactivity power, new types of coumarin derivatives with effective pharmacological value have been synthesized in recent years.

Tannins

In general, compounds containing a group of polymeric phenolic substances are called tannins. They are found in almost all structures of plants (Scalbert 1991). They can be obtained from the condensation of flavone derivatives and the polymerization of quinones (Geissman 1963).

Tannin-containing compounds play a role in the prevention and treatment of diseases. They are also involved in many physiological activities, such as stimulation of phagocytic cells and stimulation of anti-infective actions (Haslam 1996). One of its molecular effects is that it forms covalent bonds with proteins, as well as hydrophobic effects and complexes with hydrogen bonds (Haslam 1996, Stern et al. 1996). In plants, tannins inhibit insect growth (Schultz 1988).

Studies have found that tannins are toxic to yeasts, bacteria and filamentous fungi (Scalbert 1991). Tannins have been observed to bind to the cell wall of bacteria, thereby inhibiting the growth and protease activity of bacteria (Jones et al. 1994).

Simple Phenols and Phenolic Acids

Some of the simple bioactive phytochemicals are composed of a single phenolic ring. Cinnamic and caffeic acids are common examples of oxidized phenylpropane-derived compounds. Hydroxylated phenols such as Catechol and Pirogallol have toxic effects against microorganisms.

Catekol has two -OH groups while pyrogallol contains three -OH groups. The number of OH in the phenolic group was thought to be associated with toxic effects against microorganisms, and studies showed that the toxic effect increased with the increase in -OH groups (Geismann 1963).

Phenolic substances cause enzyme inhibition in microorganisms. In addition, researchers have found that oxidized phenols exert greater inhibitory effects (Urs and Dunleavy 1975, Scalbert 1991). Compounds with a C3 side chain and without oxygen are classified as essential oils. Eugenol, which is a class of essential oils, has been found to have a bacteriostatic effect against fungi and bacteria (Duke 1985).

Kinons

Quinones have an aromatic ring structure containing two ketone structures and are colored, highly reactive and widely found in nature. They cause blackening of cut or injured fruits and vegetables. They are responsible for a moderate pathway of melanin synthesis in human skin (Schmidt 1988).

In addition to being a stable source of free radicals, quinones cause loss of function in proteins because they irreversibly complex with nucleophilic amino acids in proteins (Stern et al. 1996). Possible targets in microbial cells include surface adhesins, cell wall polypeptides, and membrane-bound enzymes.

flavonoids, flavinles, flavonolles

Flavonoids, flavins, and flavonols are natural compounds and can exert antibiotic effects, but these effects are usually not as strong as a direct antibiotic. Instead, these compounds can often affect the growth or reproduction of microorganisms or support the immune system. Here is some information about the antibiotic-like effects of flavonoids, flavins, and flavonols:

Antimicrobial Effects: Some flavonoids and flavonols may have mild antimicrobial effects against bacteria and fungi. For example, quercetin, a flavonoid, can inhibit the growth of some types of bacteria.

Antioxidant Effects: Many flavonoids have powerful antioxidant properties. Antioxidants can reduce cellular damage and support the immune system by neutralizing free radicals. Therefore, foods and drinks containing flavonoids can be used to protect the body against infections.

Anti-inflammatory Effects: Some flavonoids and flavonols have anti-inflammatory properties that can reduce inflammation. This can limit the spread of infections throughout the body.

Immune System Support: Flavonoids and flavonols can increase the activity of immune system cells and strengthen immune responses. This can create a better defense mechanism against infections.

Viral Infections: Some flavonoids and flavonols may have antiviral effects, especially against viral infections such as influenza (flu).

However, flavonoids, like antibiotics, are limited in their ability to directly kill microorganisms and may be ineffective against some bacteria. Furthermore, the effects of flavonoids can vary depending on their type and amount, target microorganisms, and immune system responses.

More scientific research is needed to learn more about the health benefits of flavonoids and similar compounds. Therefore, it is important to consult with a healthcare professional before using flavonoids and similar natural compounds for therapeutic purposes.

Flavonoids are synthesized by plants against microorganisms (Dixon et al. 1983). Studies have shown that flavonoids, which have the ability to form complexes with both extracellular and soluble proteins and the cell wall of bacteria, are effective antimicrobial

agents against many microorganisms. Many lipophilic flavonoids have also been found to cause disruption of microbial membranes (Tsuchiya et al. 1996).

Catechins are flavonoid compounds with the most C3 unit reduced. These compounds have been found to be found in vitro to detect Vibrio cholerae O1 (Borris 1996), Streptococcus mutans (Batista et al. 1994; Sakanaka et al. 1989; Tsuchiya et al. 1994), Shigella (Vijaya et al. 1995) and other bacteria. Catechins have been found to inactivate cholera toxins in Vibrio (Borris 1996) and inhibit bacterial glycosyltransferase isolation of S. mutans (Nakahara et al. 1993).

Flavoniod compounds also have an inhibitory effect against many viruses. Studies have found that flavonoids such as swertifrancheside, glycyrrhizin and chrysin are effective against HIV (Pengsuparp et al. 1995, Watanbe et al. 1996, Critchfield et al. 1996). In addition, flavone derivatives have been found to inhibit respiratory syncytial virus (RSV) (Kaul et al. 1985, Barnard et al. 1993)

The source of odor of plants is basic oil fractions and these oils are secondary metabolites in isoprene structure. They can be in the form of diterpenes, triterpene and tetraterpenes, as well as hemi-terpene and sesquiterpene structure. These compounds are often called terpenoids because they contain other elements such as oxygen. Terpenoids are synthesized from acetate units and have the same roots as fatty acids, but are distinguished from fatty acids by their extensive branching.

Chaurasia and Vyas (1977) stated that 60% of the main oil derivatives examined inhibited fungi and 30% inhibited bacteria. Although the mechanisms of action of terpenes are not fully understood, they are known to cause membrane disruption in combination with lipophilic compounds.

Capsaicin, a terpenoid compound, is known to have a wide range of biological activity in humans. Its effect on the nervous

system, cardiovascular and digestive systems (Virus and Gebhart 1979) is as effective as its use as an analgesic (Cordell and Araujo 1993). Capsaicin has bacteriocidal action against Helicobacter pylori (Jones et al. 1997)

Heterocyclic nitrogen compounds are called alkaloids. One of the most important alkaloids for its medicinal use is morphine, which was isolated from poppy in 1805 (Fessenden and Fessenden 1982). The name morphine comes from the Greek dream god Morpheus, and codeine and heroin are derivatives of morphine.

Diterpenoid alkaloids have generally been isolated from plants of the Ranunculaceae family (Atta-your-Rahman and Coudhary 1995) and have been found to have antimicrobial properties (Omulokoli et al. 1997).

In addition to the effects of alkaloids on microorganisms, their anti-diarrheal effects have also been determined (Ghoshal et al. 1996)

Peptides that inhibit microorganisms were first identified in 1942 (Balls et al. 1942). They act by the formation of ion channels in microbial membranes or by competitive inhibition of the binding of microbial proteins to host polysaccharide receptors (Terras et al. 1993, Zhang and Lewis 1997).

It has long been known that bacteria and fungi are inhibited by these substances (De Bolle et al. 1996).

Thionins are peptides commonly found in barley and wheat and are toxic to gram-negative and gram-positive bacteria (Fernandes de Caleya et al. 1972)

Let's examine the mechanism of antibiotic action in the moss plant. As noted by Richardson (1981), bacteria are not known to play a significant role in the decay of many moss species. The reason for this is the antibiotic produced by mosses. Studies have shown that some species (e.g. species belonging to the genus Sphagnum) have high antibiotic activity, while some species, such as Funaria

hygrometreca, do not show activity against the bacterial and fungal species tested. This is thought to be related to the habitat in which the species lives. The F. hygrometreca species settles in areas open to development after a fire. It is thought that it does not have the ability to synthesize antibiotics because there are very few creatures to compete with in these areas.

Mosses (Lichen) are an example of plants that can exert antibiotic effects. Mosses show their mechanism of antibiotic action through a common symbiotic relationship of bacteria and fungi.

Mosses are formed by the combination of a fungus (fungus) and an algae (usually green algae) or cyanobacteria (blue-green algae). This symbiotic relationship is a form of symbiosis in which both the fungus and the algae or cyanobacteria support each other.

The mechanism of antibiotic action works as follows:

Protective Role of the Fungus: The fungus forms the main body and structures of the moss. This structure can grow in humid environments and acts as a protective shell.

Photosynthesis of Algae or Cyanobacteria: Algae or cyanobacteria make up the green part of the moss. These algae, or cyanobacteria, produce energy by photosynthesis. This energy is necessary for the survival of both themselves and the fungus.

Antibiotic Production: Some species of mosses aid in the production of antibiotics produced by their fungi. These antibiotics protect against bacterial and fungal infections on the surface of the mushroom's moss. Fungi maintain the health of the moss by maintaining the production of these antibiotics.

Antibiotic Effect: The antibiotics produced can inhibit or kill the growth of microorganisms on the surface of the moss. This increases the resistance of the moss plant to bacterial and fungal infections.

This symbiotic relationship involves the moss plant's ability to produce a natural antibiotic and therefore inhibit the growth of

certain microorganisms. However, this mechanism can vary depending on the type of moss plant and the environmental conditions in which it lives. In addition, the antibiotic potential of mosses has been the subject of research, and some species are known to contain antimicrobial components.

Considering that mosses have been used for centuries in the treatment of some diseases and wounds, it will be very important to analyze the algae species with antimicrobial activity, to purify the substances that cause antimicrobial activity, and to design drugs using these substances.

For this, first of all, extractions should be prepared using as many algae species as possible, and the antimicrobial effect of these extractions should be tested on a wide range of different strains.

In moss species with antimicrobial effects, the purification of the active ingredient that causes antimicrobial activity and the subsequent detection of this substance will be very important for the continuation of the studies. Elucidating the mechanism of activity of the purified active substance will also be one of the important steps for drug design.

Secondary compounds found in the structure of mosses include aromatic compounds, terpenoids and fatty acids. Next to terpenoids, aromatic compounds are the most important secondary products of bryophytes.

Aromatic compounds found in bryophytes include benzoic and cinnamic acid derivatives, phenolethers, alkylphenols, phenylglycosides, bisbibenzyls, bisbibenzyl dimers, stilbenes, phenanthrenes, naphthalenes, acetophenones, lignans, flavonoids, coumarins, iscoumarins, comestanes, benzonaphthoxanthanones.

Flavonoids are the most commonly observed phenolics in bryophytes, although not known in hornworts. The types of flavonoids found in bryophytes can be listed as flavone aglycones and glycosides, flavonol aglycones and glycosides, anthocyanins

and their derivatives, aurons, biflavonoids, flavanones, dihydrochalcones, dihydroflavonols, isoflavones, triflavones.

For the study of antimicrobial activity, strains of microorganisms known to be sensitive to antimicrobial agents are used. The selection and use of a specific and sensitive test microorganism is the first and most important stage of these tests. The most commonly used test microorganisms are Salmonella typhosa, S. aureus, Bacillus stearothermophilus, Bacillus mesentericus and Streptococcus thermophilus strains. With these tests, the effect of an antimicrobial substance on a particular test microorganism can be determined as "minimal inhibitory concentration (MIC)" or "minimal lethal concentration (MLC)", as well as the sensitivity of any microorganism strain to a certain antimicrobial substance. On the other hand, by using these tests, the presence of antimicrobial substances in any environment (a surface, a food, etc.) can be revealed qualitatively or quantitatively. It can use many methods to test antimicrobial activity. However, the "tube dilution method" and the "agar diffusion method" are the most common methods used for this purpose.

In the tube dilution method, the dilution of the microorganisms to be counted is done in a suitable dilution solution. The number of living cells in the material is estimated by evaluating the tubes that are added to the liquid medium from the dilutions and microorganism growth is seen at the end of incubation. With the tube dilution method, it is tried to determine the MIC and/or MLK values of antimicrobial substances (AMM). MIC value: It is the lowest concentration of AMM that inhibits (inhibits) reproduction (increase in the number of live cells present) under test conditions in the test microorganism suspension (culture fluid containing a certain number of live microorganisms) under test conditions. Minimum concentration of inhibition (MIC) refers to the lowest concentration that can visibly inhibit the development of a microorganism during incubation. MIC was made to observe the resistance of mo to the antimicrobial agent and to observe the activity of the new antimicrobial agent.

The minimum bactericide concentration (MBC) is the lowest antibiotic concentration required to kill a microorganism MBC is performed immediately after the MIC test and samples are taken from tubes where no growth is observed in MIC and added to solid medium. The first concentration at which there is no reproduction is expressed as the minimum bactericide concentration. The lowest concentration of antifungals required to kill a fungus is called the minimum fungicide concentration (MFC).

In the agar diffusion method, the effectiveness of many AMMs (especially antibiotics and disinfectants) can be demonstrated easily and in a short time with this method. Using this method, the sensitivity of the microorganism to be tested to AMM/AMMs or the presence of an AMM in any environment can also be determined. Method; It is based on the principle of determining whether the AMM (or the sample suspected of containing AMM), which is appropriately added to a suitable agar medium in the petri dish inoculated with the test microorganism, diffuses in the medium and prevents the development of the test microorganism in the area where it is diffused. The agar diffusion method can be applied in several ways. However, the most common form of application is 'paper disc agar diffusion' and 'hole agar diffusion' methods.

The agar diffusion method is divided into two. In paper disc agar diffusion, the selected test microorganism is inoculated with the previously prepared liquid culture bulk plate method and surface spreading method. The method of spreading to the surface is carried out directly with a sterile swab immersed in a liquid culture or by spreading on agar with Drigalski's extract. In this method, the cooled medium is mixed with sterile petri dishes from the sample. It is a method made by counting the live colonies in the incubation as a result of leaving the solidified agar medium to incubation and determining the number of live microorganisms.

In the hole agar diffusion method, it is acted exactly as in the paper disc agar diffusion method. However, in the hole agar

diffusion method, AMM-impregnated paper discs are not placed in the agar medium inoculated with the test microorganism, instead, a certain number of holes are drilled in the medium at appropriate intervals and the AMM solution to be tested is poured into each of these holes.

Another example that can be examined is propolis. Propolis has a variety of therapeutic effects, including antibacterial, anti-inflammatory, healing, anesthetic, anticaries, antifungal, antiprotozoal and antiviral activities. Its in vitro antibacterial activity was confirmed against many Gram-positive and Gram-negative bacteria, resulting mainly through the synergistic action of pinocembrin and galangin flavonoids, which are components of propolis. Other flavonoids such as chrysin and kaempferol have been shown to have an antiviral effect by reducing intracellular proliferation of viruses such as herpes simplex (Ghisalberti, 1979; Park et al., 1998; Marcucci, 1995).

This study was prepared from the Research Project Thesis of my student Elgiz SHARIFOV, Faculty of Pharmacy of Ağrı İbrahim Çeçen University.

References

Altuner, E. M. (2008). Bazı karayosunu türlerinin antimikrobiyal aktivitesinin belirlenmesi.

Atta-ur-Rahman, M. (1995). Diterpenoid and steroidal alkaloids. *Natural product reports*, *12*(4), 361.

Başkaya, Y. (2015). *Bazı patojen mikroorganizmalar üzerinde etkili antimikrobiyal maddeler üretebilen mikroorganizmaların topraktan izolasyonu* (Master's thesis, Karamanoğlu Mehmetbey Üniversitesi).

Batista, O., Duarte, A., Nascimento, J., Simões, M. F., de la Torre, M. C., & Rodríguez, B. (1994). Structure and antimicrobial activity of diterpenes from the roots of Plectranthus hereroensis. *Journal of natural products*, *57*(6), 858-861.

Baytop, T. (1984). Turkiye' de Bitkiler ile Tedavi. *Istanbul Univ. Yay*, (2355).

Elsevier, A. B. B. (1978). Preliminary report on warfarin for the treatment of herpes simplex. *Irish Coll Phys Surg*, *22*.

Borris, R. P. (1996). Natural products research: perspectives from a major pharmaceutical company. *Journal of ethnopharmacology*, *51*(1-3), 29-38.

Bown, D. (1995). *The Royal Horticultural Society encyclopedia of herbs & their uses*. Dorling Kindersley Limited.

Cordell, G. A., & Araujo, O. E. (1993). Capsaicin: identification, nomenclature, and pharmacotherapy. *Annals of Pharmacotherapy*, *27*(3), 330-336.

Cowan, M. M. (1999). Plant products as antimicrobial agents. *Clinical microbiology reviews*, *12*(4), 564-582.

De Bolle, M. F., Osborn, R. W., Goderis, I. J., Noe, L., Acland, D., Hart, C. A., ... & Broekaert, W. F. (1996). Antimicrobial peptides from Mirabilis jalapa and Amaranthus caudatus:

expression, processing, localization and biological activity in transgenic tobacco. *Plant molecular biology*, *31*, 993-1008.

Dixon, R. A., Dey, P. M., & Lamb, C. J. (1983). Phytoalexins: enzymology and molecular biology. *Advances in enzymology and related areas of molecular biology*, *55*(1), 69.

Dolaz, M., Gölcü, A., Dağcı, E. K., & Serin, S. (2002). Antimicrobial Activities of Silician Sumach (Rhus coriaria). *Proceedings of ICNP, Trabzon*, 79-82.

Duke, J. A. (2002). *Handbook of medicinal herbs*. CRC press.

Duke, J. A., & Ayensu, E. S. (1985). Medicinal plants of China. *(No Title)*.

De Caleya, R. F., Gonzalez-Pascual, B., García-Olmedo, F., & Carbonero, P. (1972). Susceptibility of phytopathogenic bacteria to wheat purothionins in vitro. *Applied microbiology*, *23*(5), 998-1000.

Fessenden, R. J., & Fessenden, J. S. (1982). Boston, MA Willard Grant Press. *Organic Chemistry*, *139*.

FLORKIN, M. (1963). *COMPREHENSIVE BIOCHEMISTRY. VOL. 09. PYRROLE PIGMENTS, ISOPRENOID COMPOUNDS AND PHENOLIC PLANT CONSTITUENTS*. Elsevier Publishing Company

Geissman, T. A. (1963). Flavonoid compounds, tannins, lignins and, related compounds. In *Comprehensive biochemistry* (Vol. 9, pp. 213-250). Elsevier.

Ghoshal, S., Prasad, B. K., & Lakshmi, V. (1996). Antiamoebic activity of Piper longum fruits against Entamoeba histolytica in vitro and in vivo. *Journal of ethnopharmacology*, *50*(3), 167-170.

Jones, G. A., McAllister, T. A., Muir, A. D., & Cheng, K. J. (1994). Effects of sainfoin (Onobrychis viciifolia Scop.) condensed

tannins on growth and proteolysis by four strains of ruminal bacteria. *Applied and environmental microbiology*, *60*(4), 1374-1378.

Jones, N. L., Shabib, S., & Sherman, P. M. (1997). Capsaicin as an inhibitor of the growth of the gastric pathogen Helicobacter pylori. *FEMS Microbiology Letters*, *146*(2), 223-227.

Kang, S. J., Kim, S. H., Liu, P., Jovel, E., & Towers, G. H. N. (2007). Antibacterial activities of some mosses including Hylocomium splendens from South Western British Columbia. *Fitoterapia*, *78*(5), 373-376.

Kostova, I. N., Simeonov, M. F., Todorova, D. I., & Petkova, P. L. (1998). Two acylated monoterpene glucosides from Paeonia peregina. *Phytochemistry*, *48*(3), 511-514.

Kowalczyk, B., & Olechnowicz-Stepien, W. (1988). Study of Fraxinus excelsior L. leaves. I. Phenolic acids and flavonoids. *Herba Pol*, *34*, 7-13.

Omulokoli, E., Khan, B., & Chhabra, S. C. (1997). Antiplasmodial activity of four Kenyan medicinal plants. *Journal of ethnopharmacology*, *56*(2), 133-137.

Özden, A. (2014). Helicobacter pylori enfeksiyonu tedavisinde alternatif tıp. *Güncel Gastroloji*, *18*, 219-225.

Richardson, D. H. S. (1981). The Biology of Mosses, xii+ 220 pp.

Sneader, W. (1985). Drug discovery: the evolution of modern medicines. *(No Title)*.

Silver, L. L. (2011). Challenges of antibacterial discovery. *Clinical microbiology reviews*, *24*(1), 71-109.

Şahin, G. (2007). *Türkiye'den toplanan bazı Paeonia türlerinin antibakteriyel etkisi* (Master's thesis, Fen Bilimleri Enstitüsü).

Tsuchiya, H., Sato, M., Miyazaki, T., Fujiwara, S., Tanigaki, S., Ohyama, M., ... & Iinuma, M. (1996). Comparative study on the antibacterial activity of phytochemical flavanones against methicillin-resistant Staphylococcus aureus. *Journal of ethnopharmacology*, *50*(1), 27-34.

Ulubelen, A., Kutney, J. P., Dimitriadis, E., Hewitt, G. M., & Singh, M. (1969). 2a-HYDROXYMICROMERIC ACID, A PENTACYCLIC TRITERPENE FROM. *Tetrahedron Letters*, *21*, 1683.

Urs, N. R. R., & Dunleavy, J. M. (1975). Enhancement of the bactericidal activity of a peroxidase system by phenolic compounds [Xanthomonas phaseoli sojensis, soybeans, bacterial diseases]. *Phytopathology*.

Usher, G. (1974). *A dictionary of plants used by man*. Constable and Company Ltd..

Vijaya, K., Ananthan, S., & Nalini, R. (1995). Antibacterial effect of theaflavin, polyphenon 60 (Camellia sinensis) and Euphorbia hirta on Shigella spp.—a cell culture study. *Journal of ethnopharmacology*, *49*(2), 115-118.

Virus, R. M., & Gebhart, G. F. (1979). Pharmacologic actions of capsaicin: apparent involvement of substance P and serotonin. *Life sciences*, *25*(15), 1273-1283.

Zhang, Y., & Lewis, K. (1997). Fabatins: new antimicrobial plant peptides. *FEMS microbiology letters*, *149*(1), 59-64.

Zhu, Y. P. (1998). *Chinese materia medica: chemistry, pharmacology and applications*. CRC press.

Watanbe, H., Miyaji, C., Makino, M., & Abo, T. (1996). Therapeutic effects of glycyrrhizin in mice infected with LP-BM5 murine retrovirus and mechanisms involved in the prevention of disease progression. *Biotherapy*, *9*, 209-220.

CHAPTER X

Melatonin and its Functions in Metabolism

Ebru COTELI[1]

Introduction

The hormone secreted from the pineal gland in the dark and involved in many biological events such as reproduction, sleep, immunity, and circadian rhythm is called melatonin (Yazıcı & Köse, 2004). Melatonin is synthesized from tryptophan by activating beta-adrenergic receptors in the pineal gland. The production and release of this hormone begin in a dark environment and stop in a light environment. The prolongation of the light period stops the production of the melatonin hormone. For this reason, melatonin is called the "biochemical identifier of darkness" (Nal, 2018). Melatonin release in humans begins immediately after darkness falls (20:00–23:00). It reaches peak levels, especially in the middle part

[1] Assist. Prof., Kirsehir Ahi Evran University Vocational School of Health Services, Medical Services and Techniques, Kirşehir/TURKEY, Orcıd: 0000-0002-9473-0914

of the night (02:00–04:00), and ends in the morning hours (07:00–09:00). The level of the melatonin hormone varies depending on age. With aging, the melatonin hormone secretion decreases (Gupta, Riedel & Frick, 1983; Waldhauser & et al., 1988).

The melatonin hormone was first discovered by Lerner in 1958. He obtained this hormone from the pituitary and named it "melatonin" by combining the Latin words "melas," meaning black, and "tosos," meaning work, because it lightens the skin color (Hilton, 2002; Beyer, Steketee & Saphier, 1998). Another name for the melatonin hormone is N-acetyl 5-methoxy tryptamine. It is a natural neurotransmitter, as it takes part in many biological and physiological events in the body. The main function of this hormone is to adjust the human biorhythm by maintaining the body's biological clock. In addition, the best-known function of this hormone is that it makes important contributions to the immune system through cell renewal (Claustrat, Brun & Chazot, 2005; Macchi & Bruce, 2004). Melatonin is a hormone synthesized and released by the pineal gland, bone marrow, lens, ovarian cells, bile, and gastrointestinal tract in mammals (Üstündağ, Şentürk & Gül, 2020) (Figure 1).

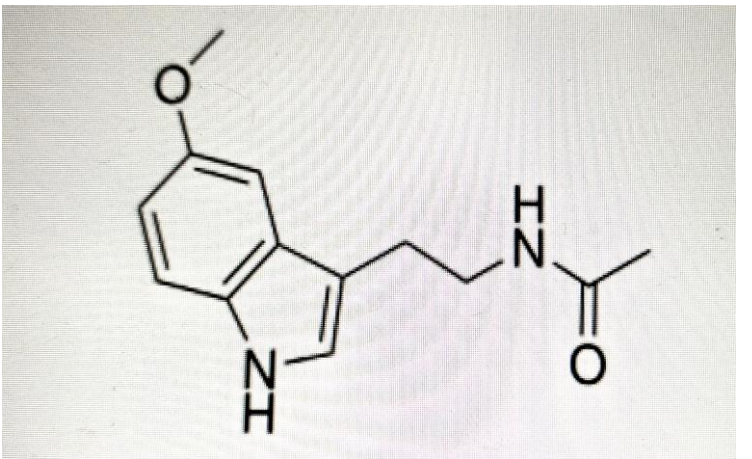

Figure 1. Melatonin (N-acetyl-5-methoxytryptamine)

Synthesis of Melatonin

Melatonin is a hormone secreted from the pineal gland. This hormone is also called the "dark hormone" because it is secreted in response to darkness (Srinivasan & et al., 2009). Melatonin hormone is synthesized from tryptophan in pinealocytes. The main ingredient of the melatonin hormone is the amino acid tryptophan. Tryptophan first turns into serotonin. Tryptophan is converted into 5-hydroxytryptophan by the enzyme tryptophan hydroxylase. 5-hydroxytryptophan is converted to serotonin by the amino acid decorboxylase enzyme; serotonin is converted into N-acetyl serotonin by the N-acetyl transferase enzyme. Then, N-acetyl serotonin is converted into melatonin via the methyltransferase enzyme (Beyer, Steketee & Saphier, 1998) (Figure 2).

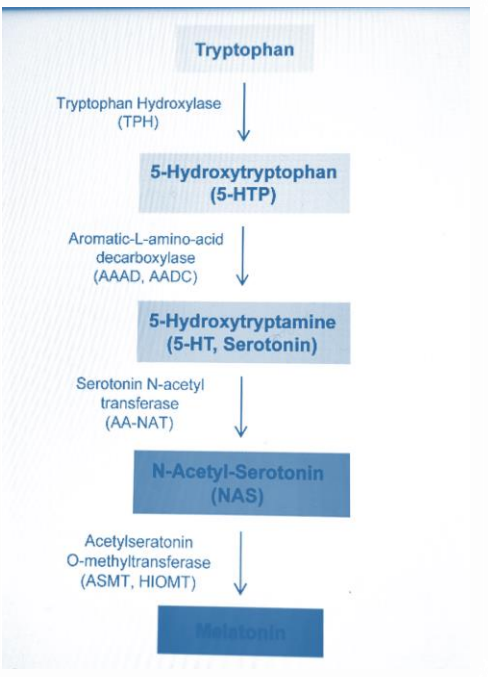

Figure 2. Melatonin synthesis scheme

Factors Affecting the Synthesis and Release of Melatonin

Many factors affect the synthesis and release of melatonin. The most important of these factors is light. Melatonin regulates synthesis and release in light and dark, day and night environments. This mechanism is called “photoneuroendocrine control." Light is a factor that controls and suppresses melatonin synthesis. The more intense the light, the greater its power to suppress melatonin (Reiter & et al., 2007; Özcelik & et al., 2013; Scheer & Czeisler, 2005).

Serum melatonin levels change with age. It has been reported that blood melatonin levels are low, especially in newborn babies. Studies have reported that babies' melatonin levels begin to increase starting in the third month. It has been reported that melatonin, in particular, passes into breast milk. It has been observed that the melatonin circadian rhythms of breastfed babies are more regular. Additionally, studies have shown that sleeping on a full stomach, alcohol, coffee, cigarettes, tea, depression, sleeping pills, and sound factors reduce melatonin release (Gomes & Soares-da-Silva, 1999; Reiter & et al., 2007; Özcelik & et al., 2013; Scheer & Czeisler, 2005; Şener, 2010; Ferguson, Rajaratnam & Dawson, 2010).

Functions of the Melatonin Hormone

Antioxidant Effect of Melatonin

Antioxidants perform many functions by interacting with free radicals, such as reducing their activity, converting them into weaker molecules, and trapping them. Melatonin has antioxidant properties due to the pyrrole ring found in its structure. The melatonin hormone prevents oxidative stress caused by toxins that cause tissue damage in metabolism. In particular, due to its structure, melatonin does not need any receptors or binding sites to scavenge free radicals (Reiter, 1996).

Melatonin is soluble in water and in the lipid phase. For this reason, it easily passes into all intracellular components. It especially protects the nucleus, cell membrane, and organelles from the damage of free radicals. Melatonin acts as an antioxidant in a way different

from normal antioxidants such as vitamins C, E, and B-carotene. In particular, it does not participate in radical-producing mechanisms. Normal antioxidants turn into oxidant substances after performing their antioxidant duties. Melatonin, in particular, inhibits pro-oxidant enzymes. Thus, it fulfills its antioxidant function by reducing the formation of free radicals (Pandi-Perumal & et al., 2008). Since melatonin easily crosses the placenta and blood-brain barrier, it can easily reach all intracellular components (Emet & et al., 2016; Çetin, 2005). Therefore, melatonin effectively protects the nucleus, cell membrane and organelles from radical damage. In particular, melatonin prevents free radicals from reaching the cell membrane by clinging to the outer surface of the phospholipid layer of the cell membrane.

This hormone can reach the cell nucleus. Therefore, melatonin functions effectively in protecting DNA against oxidative damage. Since melatonin has both lipophilic and hydrophilic properties, it is not stored in the body. It quickly mixes with body fluids and blood (Ianas, Olivescu & Badescu, 1991). Safrole substances cause cancer because they create free radicals. In particular, safrole causes DNA damage. Melatonin inhibits this damage very strongly. Studies show that melatonin slows down the development and progression of cancer. In the case of aging, antioxidant defense decreases as the functions of the pineal gland and melatonin levels decrease. Therefore, an increase in diseases related to aging is observed (Vriend & Reiter, 2015; Hardeland, 2012). Melatonin levels of people exposed to light, especially at night.

It has been reported that the risk of breast cancer is low and the risk of breast cancer is high. Breast cancer is also associated with cortisol. The risk of breast cancer is high in people with high cortisol levels, especially during the day and evening hours (Hill & et al., 2015). One of the most important functions of melatonin is to suppress tumor development. Melatonin performs this task by helping the programmed death of cells in the body called apoptosis and increasing the body's antioxidant capacity (Özçelik & et al.,

2013). Melatonin destroys free radicals and activates antioxidant enzymes through specific melatonin receptors. It fulfills its antioxidant function especially by inhibiting pro-oxidative enzymes (Şahna, Deniz & Aksulu, 2006) (Figure 3).

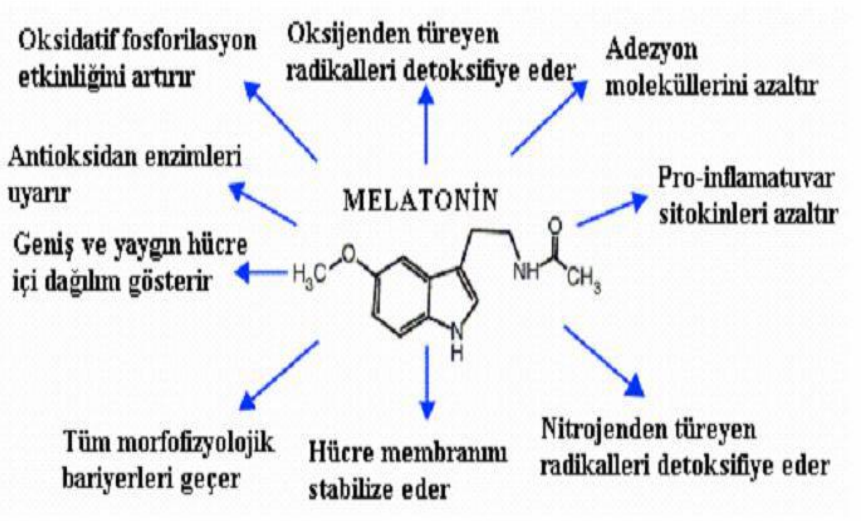

Figure 3. Functions of melatonin (Ballı, 2003).

The antioxidant properties of melatonin;

1. Increase the effectiveness of oxidative phosphorylation

2. Stimulates antioxidant enzymes

3. It shows wide and widespread intracellular distribution

4. Passes all morphological barriers

5. Stabilizes the cell membrane

6. Reduces pro-inflammatory cytokines

7. Reduces adhesion molecules

8. It neutralizes radicals derived from oxygen (Durkan & Ülkü, 2009).

Effects of Melatonin on the Immune System

Research has shown that there are few studies on the effects of melatonin on cells and tissues in the immune system (Hotchkiss & Nelson, 2002). Especially bacterial diseases, viral diseases, stress and immune deficiencies that occur during corticosteroid use or drug treatment can be prevented with melatonin (Maestroni, 2001). After hemorrhagic shock and trauma events occurring in the body, the immune system is suppressed.

Melatonin can regulate this suppressed immune system (Wichmann & et al., 1996). In cases of immune system deficiencies that develop with old age, melatonin has an enhancing effect on this system (Palaoğlu & Beşkonaklı, 1998). Melatonin activates immune system function either directly through the immune system cells through melatonin receptors or indirectly due to changes in steroid hormones (Hotchkiss & Nelson, 2002).

Effects of Melatonin on Sleep

Sleep is not necessary for melatonin secretion in metabolism. The important thing is the dark environment. In particular, increased melatonin release reduces body temperature. Thus, it creates a feeling of sleep. The effect of melatonin release on sleep is related to the onset and quality of sleep as well as the total sleep time. It is thought that melatonin, in particular, provides this effect through thermo regulation and hypothermic effects.

Melatonin has important functions in the electrical activity of the brain. It has been reported that people with sleep disorders have low serum melatonin levels (Wurtman & Zhdanova, 1995). Studies have reported that melatonin, which is used in delayed sleep phase syndrome, insomnia, restless legs syndrome, REM dysregulation, and fibromyalgia, increases sleep duration and quality in patients (Haimov & et al., 1995; Wade & et al., 2007).

Psychological Effect of Melatonin

A scientist named Lerner revealed the relationship between melatonin and human behavior and psychology. Studies have reported that melatonin levels in psychiatric diseases are related to the sleep cycle and depression (Lerner & Nordlund, 1978). Studies have reported that melatonin secretion levels of depressed patients decrease at night (Şener, 2010; Khaleghipour & et al., 2012). Additionally, after the use of melatonin for therapeutic purposes in depression patients, a decrease in depression symptoms and an improvement in sleep patterns were observed (Challet, 2007).

Studies have been conducted on melatonin levels in patients with bipolar psychological illness. Decreases in melatonin levels have been observed, especially in patients with bipolar disorder (Melo & et al., 2016; Lam & et al., 1990). Another study showed that patients with schizophrenia had low serum melatonin levels and circadian rhythm disorders (Suresh & et al., 2007). It has been reported that schizophrenia patients, during psychotic attacks, often have sleep problems. It is thought that melatonin can solve the sleep problems of patients with schizophrenia without disrupting the circadian rhythm (Shamir & et al., 2000).

Endocrinological Effects of Melatonin

Cortisol and melatonin levels act oppositely. Melatonin receptors are located in the adrenal gland. Therefore, when these receptors are stimulated with physiological doses, the adrenocorticotropic (ACTH) hormone suppresses the formation of cortisol (Liebmann & et al., 1997). In studies, increases in body weight levels were observed when high cortisol levels and low melatonin levels occurred (Guardiola-Lemaitre, 2007).

Melatonin levels, especially in patients with depression, it is at lower levels than in patients without it. Studies have shown that patients with depression have high cortisol levels in the evening. It has also been reported that bone degeneration occurs when the melatonin level is low and the cortisol level is high (Şener, 2010). It

has been determined that the risk of breast cancer is higher in people with low melatonin levels and high cortisol levels during the day (Hotchkiss & Nelson, 2002).

Humans have greater melatonin levels throughout pregnancy and childbirth than they do after giving birth (Wierrani & et al., 1997). Studies have shown that melatonin is the reason for the increase in twinning and ovulation rates. It has been reported that especially estrus is successfully stimulated and the survival level of the embryo increases with the increase in progesterone synthesis in granulosa cells (Uyar & Alan, 2008).

Anti-inflammatory Effect of Melatonin

Many studies have demonstrated the anti-inflammatory effects of melatonin (Galano, Tan & Reiter, 2011; Radogna, Diederich & Ghibelli, 2010; Bonnefont-Rousselot & Collin, 2010). Sepsis, asphyxia, etc. it has been reported that melatonin reduces the concentration of MDA (malondialdehyde) and inflammatory cytokines that occur as a result of disorders (Gitto & et al., 2004; Kücükakin & et al., 2009; Carrillo-Vico & et al., 2005).

Melatonin has anti-inflammatory effects in vivo and in vitro. Studies have reported that melatonin levels decrease in many infectious diseases such as pulmonary tuberculosis (Ozkan & et al., 2012) and HIV-1 (Nunnari & et al., 2003). Melatonin provides effective protection against bacteria and viruses thanks to its antioxidant, anti-inflammatory and immune modulating abilities (Srinivasan, Mohamed & Kato, 2012).

Melatonin Cancer Relationship

Melatonin is easily soluble in both the water and lipid phases. It reaches all intracellular components. In particular, cell organelles are protected from free radical damage by melatonin. Melatonin does its job of clearing these radicals by binding to the outer surface of the cell membrane. Melatonin bound to the outer surface traps and detoxifies free radicals before they pass into the membrane. It especially neutralizes radicals released by mitochondrial respiration.

Melatonin reaches the cell nucleus. Therefore, it protects DNA against oxidative damage (Reiter, 1993). Melatonin is a molecule that does not have a pro-oxidative function and does not oxidize. It never participates in radical-producing reactions (Beyer, Steketee & Saphier, 1998).

Additionally, melatonin provides repair for damaged DNA. Linoleic acid is a substance that ensures the growth, development, and proliferation of cancer cells. This substance cannot be produced in the body but must be taken from outside through food. Meanwhile, melatonin prevents linoleic acid from entering the cell and prevents the growth of cancer cells (Maestroni, 1998).

The most important enzyme that eliminates peroxides in the brain is the glutathione peroxidase enzyme. In addition to its antioxidant effect, melatonin has an activating effect on the glutathione peroxidase enzyme (Kuş & Sarsılmaz, 2002). Studies have shown that melatonin protects brain tissue from radical damage, activates antioxidant enzymes, and prevents lipid peroxidation, which is harmful to metabolism (Yazıcı & Köse, 2004).

Bone Protective Function of Melatonin

It has been reported that serum calcium levels decrease in cases where melatonin levels are suppressed. In other words, melatonin level has a direct effect on bones. In a study, the protective effect of melatonin against bone deformation in old rats was examined. This study showed that increasing melatonin levels reduced bone loss and increased bone strength in old rats (Ostrowska & et al., 2002; Tresguerres & et al., 2014). Melatonin is found in large amounts in the bone marrow. Therefore, it functions in the synthesis of bone proteins (osteoprotegerin) (Suzuki & et al., 2008).

Effects of Melatonin on Cortisol

Melatonin and cortisol act in opposite directions. Melatonin receptors and adrenocorticotropic hormone (ACTH)-mediated cortisol suppress its synthesis (Liebmann & et al., 2002). Studies

have shown that the amount of cortisol in the body decreases during sleeping hours. showed that the amount of melatonin was low, but the amount of melatonin peaked after a while (Şener, 2010).

In particular, studies have reported that high cortisol and low melatonin levels pave the way for the formation of various diseases. In particular, it has been reported that these diseases include cardiovascular diseases, osteoporosis, depression, and ease of weight gain (Millet & et al., 1999). Studies have shown that high cortisol and low melatonin levels lead to weight gain in metabolism (Guardiola-Lemaitre, 2007). In particular, studies have reported that the risk of breast cancer is higher in cases where the cortisol level is high and the melatonin level is low (Hotchkiss & Nelson, 2002).

Conclusion

Studies have shown that melatonin has vital duties and functions. It is a substance with antioxidant properties, especially since melatonin is a powerful free radical scavenger. It is a biological molecule that plays a role in many mechanisms in the human body, from the endocrine, muscle, and bone immune systems to sleep patterns, and plays a protective role against many diseases. It is a molecule that carries out vital functions.

References

Ballı, E. (2003). Melatonin functions. *Mersin University Faculty of Medicine Journal*. 4, 308–385.

Beyer, C. E., Steketee, J. D. & Saphier, D. (1998). Antioxidant properties of melatonin-an emerging mystery. *Biochem Pharmacol*. 56 (10), 1265-1272. Doi: 10.1016/s0006-2952(98)00180-4

Bonnefont-Rousselot, D. & Collin, F. (2010). Melatonin: action as antioxidant and potential applications in human disease and aging. *Toxicology*. 278 (1), 55-67. Doi: 10.1016/j.tox.2010.04.008

Carrillo-Vico, A., Lardone, P. J., Naji, L., Fernández-Santos, J. M., Martín-Lacave, I., Guerrero, J. M. & Calvo, J. R. (2005). Beneficial pleiotropic actions of melatonin in an experimental model of septic shock in mice: regulation of pro-/anti-inflammatory cytokine network, protection against oxidative damage and anti-apoptotic effects. *Journal of pineal research*. 3, 400-408. Doi: 10.1111/j.1600-079X.2005.00265.x

Challet, E. (2007). Minireview: Entrainment of the suprachiasmatic clockwork in diurnal and nocturnal mammals. *Endocrinology*. 148, 5648-5655. Doi: 10.1210/en.2007-0804

Claustrat, B., Brun, J. & Chazot, G. (2005). The basic physiology and pathophisology of melatonin. *Sleep Med Rev*. 9, 11-24. Doi: 10.1016/j.smrv.2004.08.001

Çetin, E. (2005). Melatonin and the immune system. *J Fac Vet Med Univ Erciyes*. 2 (2), 119–123.

Durkan, A., Ülkü, R. (2009). *Effects of Melatonin and N-acetylcysteine on Lung Ischemia and Reperfusion Injury (Experimental Study)*. Specialization Thesis, p. 14.

Emet, M., Ozcan, H., Ozel, L., Yayla, M., Halici, Z. & Hacimuftuoglu, A. A. (2016). Review of melatonin, its receptors and

drugs. *Eurasian J Med*. 48 (2), 135-141. Doi: 10.5152/eurasianjmed.2015.0267

Ferguson, S. A., Rajaratnam, S. M. & Dawson, D. (2010). Melatonin agonists and insomnia. *Expert Rev Neurother*. 10 (2), 305-318. Doi: 10.1586/ern.10.1

Galano, A., Tan, D. X. & Reiter, R. J. (2011). Melatonin as a natural ally against oxidative stress: a physicochemical examination. *J Pineal Res*. 51, 1-16. Doi: 10.1111/j.1600-079X.2011.00916.x

Gitto, E., Romeo, C., Reiter, R., Impellizzeri, P., Pesce, S., Basile, M., Antonuccio, P., Trimarchi, G., Gentile, C., Barberi, I. & Zuccarello, B. (2004). Melatonin reduces oxidative stress in surgical neonates. *Journal of pediatric surgery*. 39, 184- 189. Doi: 10.1016/j.jpedsurg.2003.10.003

Gomes, P. & Soares-da-Silva, P. (1999). L-DOPA transport properties in an immortalised cell line of rat capillary cerebral endothelial cells. *RBE 4. Brain Res*. 829 (1-2), 143-150. Doi: 10.1016/s0006-8993(99)01387-6.

Guardiola-Lemaitre, B. (2007). Melatoninergic receptor agonists and antagonists: therapeutic perspectives. *J Soc Biol*. 201, 105-113. Doi: 10.1051/jbio:2007012

Gupta, D., Riedel, L. & Frick, H. J. (1983). Circulating melatonin in children: In relation to puberty, endocrine disorders functional tests and racial origin. *Neuroendocrinol Lett*. 5, 63-78.

Haimov, I., Lavie, P., Laudon, M., Herer, P., Vigder, C. & Zisapel, N. (1995). Melatonin replacement therapy of elderly insomniacs. *Sleep*. 18, 598-603. Doi: 10.1093/sleep/18.7.598

Hardeland, R. (2012). Melatonin in aging and disease-multiple consequences of reduced secretion, options and limits of treatment. *Aging Dis*. 3 (2), 194- 225.

Hill, S. M., Belancio, V. P., Dauchy, R. T., Xiang, S., Brimer, S., Mao, L., Hauch, A., Lundberg, P. W., Summers, W., Yuan,

L., Frasch, T. & Blask, D. E. (2015). Melatonin: An inhibitor of breast cancer. *Endocr Relat Cancer*. 22 (3): R183-204. Doi: 10.1530/ERC-15-0030

Hilton, G. (2002). Melatonin and the pineal gland. *Journal of Neuroscience Nursing*. 34 (2), 74-8. Doi: 10.1097/01376517-200204000-00006

Hotchkiss, A. K. & Nelson, R. J. (2002). Melatonin and immune function: Hype or hypothesis? *Crit Rev Immunol*. 22, 351-371.

Ianaş, O., Olivescu, R. & Badescu, I. (1991). Melatonin involvement in oxidative processes. *Rom J Endocrinol*. 29 (3-4), 147-153.

Khaleghipour, S., Masjedi, M., Ahade, H., Enayate, M., Pasha, G., Nadery, F. & Ahmadzade, G. (2012). Morning and nocturnal serum melatonin rhythm levels in patients with major depressive disorder: an analytical cross-sectional study. *Sao Paulo Med J*. 130, 167-172. Doi: 10.1590/s1516-31802012000300006

Kücükakin, B., Gögenur, I., Reiter, R. J. & Rosenberg, J. (2009). Oxidative stress in relation to surgery: is there a role for the antioxidant melatonin? *Journal of Surgical Research*. 152, 338-347. Doi: 10.1016/j.jss.2007.12.753

Lam, R. W., Berkowitz, A. L., Berga, S. L., Clark, C. M., Kripke, D. F. & Gillin, J. C. (1990). Melatonin suppression in bipolar and unipolar mood disorders. *Psychiatry Res*. 33, 129-134. Doi: 10.1016/0165-1781(90)90066-e

Lerner, A. B. & Nordlund, J. J. (1978). Melatonin: clinical pharmacology. *J Neural Transm Suppl*. 13, 339-347.

Liebmann, P. M., Wölfler, A., Felsner, P., Hofer, D. & Schauenstein, K. (1997). Melatonin and the immune system. *Int Arch Allergy Immunol*. 112, 203-11. Doi: 10.1159/000237455

Macchi, M. M. & Bruce, J. N. (2004). Human pineal physiology and functional significance of melatonin. *Front Neuroendocrinol*. 25, 177-195. Doi: 10.1016/j.yfrne.2004.08.001

Maestroni, G. J. (2001). The immunotherapeutic potential of melatonin. *Expert Opin Investig Drugs*. 10: 467-476. Doi: 10.1517/13543784.10.3.467

Melo, M. C. A., Abreu, R. L., Linhares Neto, V. B., de Bruin, P. F. & de Bruin, V. M. (2016). Chronotype and circadian rhythm in bipolar disorder: A systematic review. *Sleep Med Rev*. 34, 46-58 Doi: 10.1016/j.smrv.2016.06.007

Millet, B., Touitou, Y., Poirier, M. F., Bourdel, M. C., Amado, I., Hantouche, E. G., Bogdan, A. & Olié, J. P. (1999). Obsessive-compulsive disorder: evaluation of clinical and biological circadian parameters during fluoxetine treatment. *Psychopharmacology (Berl).* 146, 268-274. Doi: 10.1007/s002130051116

Nunnari, G., Nigro, L., Palermo, F., Leto, D., Pomerantz R, & Cacopardo, B. (2003). Reduction of serum melatonin levels in HIV-1-infected individuals' parallel disease progression: correlation with serum interleukin-12 levels. *Infection*. 31, 379-382. Doi: 10.1007/s15010-003-4038-9

Ostrowska, Z., Kos-Kudla, B., Marek, B., Kajdaniuk, D., Staszewicz, P., Szapska, B. & Janusz Strzelczyk, J. (2002). The influence of pinealectomy and melatonin administration on the dynamic pattern of biochemical markers of bone metabolism in experimental osteoporosis in the rat. *Neuro Endocrinol Lett*. 23, 104-109.

Ozkan, E., Yaman, H., Cakir, E., Deniz, O., Oztosun, M., Gumus, S., Akgul, E. O., Agilli, M., Cayci, T., Kurt, Y. G., Aydin, I., Arslan, Y., Ilhan, N., Ilhan, N. & Erbil, M. K. & (2012). Plasma melatonin and urinary 6-hydroxymelatonin levels in patients with pulmonary tuberculosis. *Inflammation*. 35, 1429-1434. Doi: 10.1007/s10753-012-9456-3

Özcelik, F., Erdem, M., Bolu, A. & Gülsün, M. (2013). Melatonin: General features and its role in psychiatric disorders. *Current Approaches in Psychiatry*. 5 (2), 179-203. Doi: 10.5455/cap.20130512

Palaoğlu, Ö. S. & Beşkonaklı, E. (1998). Pineal gland and aging. *Turkish Journal of Geriatrics*. 1 (1), 13–18.

Pandi-Perumal, S. R., Trakht, I., Srinivasan, V., Spence, D. W., Maestroni, G. J., Zisapel, N. & Cardinali, D.P. (2008). Physiological effects of melatonin: role of melatonin receptors and signal transduction pathways. *Prog Neurobiol*. 85 (3), 335-353.

Radogna, F., Diederich, M. & Ghibelli, L. (2010.) Melatonin: a pleiotropic molecule regulating inflammation. *Biochemical pharmacology*. 80, 1844-1852. Doi: 10.1016/j.bcp.2010.07.041

Reiter, R. J. (1991). Melatonin. The chemical expression of darkness. *Mol Cell Endocrinol*. 79, 153-158. Doi: 10.1016/0303-7207(91)90087-9.

Reiter, R. J. (1993). Interactions of the pineal hormone melatonin with oxygen-centered free radicals: a brief review. *Braz J Med Biol Res*. 26 (11), 1141-1155.

Reiter, R. J. (1996). Functional aspects of the pineal hormone melatonin in combating cell and tissue damage induced by free radicals. *Eur J Endocrinol*. 134 (4), 412-420. Doi: 10.1530/eje.0.1340412

Reiter, R. J., Tan, D. X., Manchester, L.C., Simopoulos, A. P., Maldonado, M. D., Flores, L. J. & Terron, M. P. (2007). Melatonin in edible plants (phytomelatonin): Identification, concentrations, bioavailability and proposed functions. *World Rev Nutr Diet*. 97, 211-230. Doi: 10.1159/000097917

Scheer, F. & Czeisler, C.A. (2005). Melatonin, sleep, and circadian rhythms. *Sleep Med Rev*. 9 (1), 5-9. Doi: 10.1016/j.smrv.2004.11.004.

Shamir, E., Rotenberg, V. S., Laudon, M., Zisapel, N. & Elizur, A. (2000). First-night effect of melatonin treatment in patients with chronic schizophrenia. *J Clin Psychopharmacol.* 20, 691-694. Doi: 10.1097/00004714-200012000-00017

Srinivasan, V., Mohamed, M. & Kato, H. (2012). Melatonin in bacterial and viral infections with focus on sepsis: a review. *Recent Pat Endocr Metab Immune Drug Discov*. 6, 30-39. Doi: 10.2174/187221412799015317

Srinivasan, V., Spence, W. D., Pandi-Perumal, S. R., Zakharia, R., Bhatnagar, K.P. & Brzezinski, A. (2009). Melatonin and human reproduction: shedding light on the darkness hormone. *Gynecol Endocrinol*. 25, 779-785. Doi: 10.3109/09513590903159649

Suresh Kumar, P. N., Andrade, C., Bhakta, S. G. & Singh, N. M. (2007). Melatonin in schizophrenic outpatients with insomnia: a double-blind, placebo-controlled study. *J Clin Psychiatry.* 68, 237-241. Doi: 10.4088/jcp.v68n0208

Suzuki, N., Somei, M., Seki, A., Reiter, R. J. & Hattori, A. (2008). Novel bromomelatonin derivatives as potentially effective drugs to treat bone diseases. *J Pineal Res*. 45, 229-234. Doi: 10.1111/j.1600-079X.2008.00623.x

Şahna, E., Deniz, E. & Aksulu, H. E. (2006). Myocardial ischemia-perfusion injury and melatonin. *Anatolian Journal of Cardiology*. 6, 163-168.

Şener, G. (2010). The hormone of darkness: Melatonin. *Marmara Pharmacy Journal*. 14 (3), 112–20. Doi: 10.12991/201014445

Tresguerres, I. F., Tamimi, F., Eimar, H., Barralet, J. E., Prieto, S., Torres, J., Guirado, J. L. C. & Tresguerres, J. A. F. (2014). Melatonin dietary supplement as an anti-aging therapy for age-related bone loss. *Rejuvenation Res*. 17 (4), 341-346. Doi: 10.1089/rej.2013.1542

Uyar, A., & Alan, M. (2008). The effect of melatonin applications on ovulation and pregnancy in the early anoestrous period in sheep. *YYU Vet Fak Journal*. 19 (1), 47–54.

Üstündağ, H., Şentürk, E., & Gül, M. (2020) Melatonin and hyperthyroidism. *Arch Basic Clin Res*. 2 (2), 59-64. Doi: 10.5152/ABCR.2020.03

Vriend, J. & Reiter, R. J. (2015). Melatonin feedback on clock genes: a theory involving the proteasome. *J Pineal Res*. 58 (1), 1-11. Doi: 10.1111/jpi.12189

Wade, A. G., Ford, I., Crawford, G., McMahon, A. D., Nir, T., Laudon, M, & Zisapel, N. (2007). Efficacy of prolonged release melatonin in insomnia patients aged 55-80 years: quality of sleep and next-day alertness outcomes. *Curr Med Res Opin*. 23, 2597-605. Doi: 10.1185/030079907X233098

Waldhauser, F., Weiszenbacher, G., Tatzer, E., Gisinger, B., Waldhauser, M., Schemper, M. & Frisch, H. (1988). Alternations in nocturnal serum melatonin levels in humans with growth and aging. *J Clin Endocrinol Metab*. 66, 648-652. Doi: 10.1210/jcem-66-3-648

Wichmann, M. W., Haisken, J. M., Ayala, A. & Chaudry, I. H. (1996). Melatonin administration follwing hemorrhagic shock decreases mortality from subsequent septic challenge. *J Surg Res*. 65, 109-114. Doi: 10.1006/jsre.1996.0351

Wierrani, F., Grin, W., Hlawka, B., Kroiss, A. & Grünberger, W. (1997). Elevated serum melatonin levels during human late pregnancy and labour. *J Obstet Gynaecol*. 17, 449-451. Doi: 10.1080/01443619750112411

Wurtman, R. J. & Zhdanova, I. (1995). Improvement of sleep quality by melatonin. *Lancet.* 346, 1491. Doi: 10.1016/s0140-6736(95)92509-0

Yazıcı, C. & Köse, K. (2004). Melatonin: The antioxidant power of darkness. *E.Ü. Journal of Health Sciences.* 13 (2), 56–65.

CHAPTER XI

Compounds Contaınıng Aromatıc Rıng That Are Addıctıve

Arzu GÖBEK[1]
Hülya ÇELİK[2]

INTRODUCTION

Aromatic compounds are included in the chemical structure of many substances that cause addiction. Aromatics are compounds containing one or more benzene rings. Aromatic compounds are a large group of organic chemical compounds that differ from aliphatic compounds. These compounds are called "aromatics" because they have a pleasant odour. Compounds such as benzene and toluene, which contain aromatic groups, are also used in the

[1] Dr. Atatürk University, Faculty of Sciences, Department of Chemistry, Erzurum 25240, Turkey
[2] Doç.Dr. Agri Ibrahim Cecen University, Faculty of Pharmacy Basic Pharmaceutical Sciences Department / Fundamental Sciences of Pharmacy 04100, Turkey

composition of adhesives and paints that cause addiction (Doğan, M. S., & Çelik, H., 2023).

Any chemical substance that can cause abuse and addiction, called a "substance", can cause various changes in mood, perception, cognition and other brain functions and can be consumed in different ways. These substances can include illicit substances such as cannabis, heroin, cocaine, as well as prescription drugs such as amphetamines, benzodiazepines, other sedative and hypnotic drugs. In addition, substances such as volatiles, tobacco (nicotine), coffee (caffeine) and alcohol (ethanol), which are not subject to legal regulations or have limited legal regulation, can also be considered within this scope (Ceyhun, B., Oğuztürk, Ö., & Ceyhun, A. G., 2001). Addiction refers to a condition that includes processes such as increased misuse as a result of the development of tolerance to a substance, continued use despite the negative effects on life, and the emergence of withdrawal symptoms in case of reduction or cessation of substance use (Ugurlu, T. T., Sengül, C. B., & Sengül, C., 2012).

Addiction is a condition where people develop irregular habits and become unable to control their lives at the point where they become dependent on the substance. It is a debilitating condition that starts with small habits and eventually takes control of a person's behaviour and daily life. While this situation negatively affects the behaviour, willpower and regular life of individuals, it also causes serious harm to society. Considering that substance addiction is increasing day by day, addiction harms the individual as well as the society (Fraser, S., Moore, D., & Keane, H., 2014).

Addiction can be defined as a chronic brain disease that refers to the condition of continuing to take a substance despite the use of a substance causing mental, physical or social problems, the inability to quit despite the desire to quit, and the inability to control the desire to take the substance (Griffiths, M. D., 2017).

To explain in more detail, substance addiction:

- ✓ Continued substance intake despite knowing the negative consequences,
- ✓ Significant time and money is spent to obtain and use the addictive substance and then to recover from its negative effects,
- ✓ Social environment and activities are abandoned, and conflicts and problems are experienced with the person's family and environment,
- ✓ Prevents the fulfilment of the duties and responsibilities expected to be fulfilled by the person,
- ✓ The person is unable to resist substance intake despite experiencing many physical and psychological problems,
- ✓ When the substance is not taken, withdrawal symptoms appear in the person,
- ✓ It is a situation in which the amount of addictive substances is increasing with each passing day (O'Brien, C. P., 2006).

Some of the substances that cause addiction, from which they are obtained and what kind of changes they cause in the human body are examined in detail below:

COCAINE

Cocaine is known as a stimulant substance obtained from the coca plant. The mechanism of its effect occurs by inhibiting neuronal reuptake of monoamine neurotransmitters such as serotonin, noradrenaline and dopamine and increasing the concentrations of these neurotransmitters in the synaptic gap (Kılıç, F., 2016, Rasmussen *et. al*, 2001). It also inhibits sodium channels by showing local anaesthetic properties (Knuepfer, M. M., 2003). Although cocaine causes a high level of psychic dependence, it is not strong in terms of physical dependence. Therefore, withdrawal symptoms are quite mild. Effects such as dysphoria, depression, anxiety, muscle weakness, burnout, itching, pain, irritability, insomnia, nausea and

vomiting are observed (Ceyhun, B., Oğuztürk, Ö., & Ceyhun, A. G., 2001).

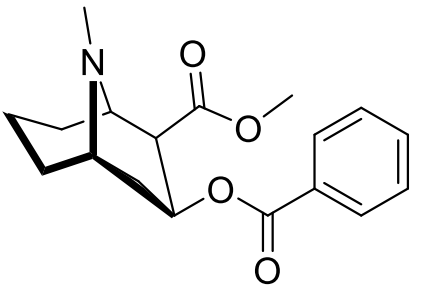

Figure 1. Chemical Structure of Cocaine.

The effect and addiction of cocaine

Cocaine is a substance that can be absorbed through all mucous membranes. Absorption through the nasal mucosa is preferable to oral use because the intensity and speed of action are much greater. When used through mucous membranes, it is not subject to first-pass effects. Vaginal, rectal and other mucosal contacts have also been trialled. However, the use of cocaine snorted through the nose can cause complications such as rhinitis, ethimoiditis mucosal erosions and perforation of the cartilaginous nasal septum. Intravenous use of the water-soluble form of cocaine hydrochloride is effective within 15-20 seconds, while subcutaneous and intramuscular injections are rarely seen. Inhalation use of the form of alkaloidal cocaine known as base or free base has become more popular due to its speed of action and euphorising effect. While the cocaine hydrochloride salt vaporises only at 195 °C, the alkaloid form of cocaine vaporises at 98 °C and can reach the heart from the pulmonary capillaries and then directly to the brain in as little as 7-10 seconds (Şatır *et. al*, 2000).

Cocaine use is not only associated with addiction, but also with various health and social problems. Some of these problems include decrease in work efficiency, problems in interpersonal relationships, financial difficulties, mood and cognitive

dysfunctions, psychiatric symptoms such as depression, paranoia, violence and suicidal tendencies, fatigue, weight loss, sleep problems and seizures. In addition, serious consequences such as traffic accidents and suicidal acts are also observed due to cocaine use (Washton, A. M., & Tatarsky, A., 1984).

Treatment of cocaine addiction

The development of new drugs for the treatment of cocaine addiction is ongoing and so far there is no fully effective treatment. However, as new treatments are developed, psychosocial treatment will be supported. Two important elements of the latest treatment methods are providing support to the patient and preventing relapse (Kampman, K. M., 2009).

During cocaine withdrawal, patients experience severe withdrawal syndrome. During this period, adrenaline and noradrenaline sensitivity increases and symptoms of anxiety and restlessness are observed. Propranolol can help reduce these symptoms. After stopping cocaine use, patients face a more challenging treatment process. At this stage, drugs such as baclofen, tiagabine, topiramate, disulfiram, modafinil are used to prevent relapse of cocaine addiction (Kampman, K. M., 2005).

AMPHETAMINE

Amphetamines are one of the most potent sympathomimetic amine drugs known for their central nervous system stimulant effect (Michel, R., & Adams, A. P., 1979). They are generally used in medical fields in the treatment of conditions such as narcolepsy, obesity, attention deficit and hyperactivity disorder (Berman *et. al.*, 2009). It is known as a substance frequently preferred by those who want to lose weight, students and those who have to work at night. In Turkey, its sale and use was banned in 1975 (Gökler, R., & Koçak, R., 2008).

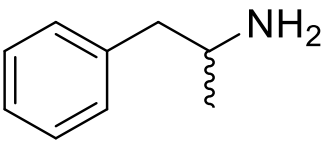

Figure 2. Chemical Structure of Amphetamine.

Effects and addiction of amphetamines

Amphetamine mainly acts by inhibiting the dopamine transporter molecule (DAT) and increasing dopamine release in the synaptic pathway. This effect may lead to the development of psychosis by causing an increase in dopamine in mesolimbic pathways in the central nervous system, and schizophrenia-like psychotic symptoms may occur (Altıntaş *et. al.*, 2007). Improper use of amphetamine may lead to complications such as weight loss, dental problems, epilepsy, miscarriage, premature birth as well as cardiovascular effects including hypertension and arrhythmia (Bruce, M., 2000).

Amphetamine is frequently used as a doping substance today because it increases physical performance by increasing excitability and euphoria. This substance is usually found in tablet forms sold under the name of "Kaptagon" and "Ecstasy" (Yedekci, A., & Onur, E., 2010).

The addictive potential of amphetamine carries the risk of damaging organs such as heart, kidney and liver and causing multiple organ failure and death. In acute use, it may lead to serious health problems such as myocardial infarction and arrhythmia with tachycardia, hypertension and hyperthermia (Song *et. al.*, 2010).

Amphetamine and theophylline act by metabolising and stimulating the central nervous system (Docherty, J. R., 2008). Acute or subchronic exposure to ecstasy and its use in combination with other abused substances may cause various disorders in the body. In the development of addiction, there is the potential to damage organs, multiple organ failure and risk of death. In acute use, conditions such as tachycardia, hypertension and hyperthermia may

lead to serious health problems such as myocardial infarction and arrhythmia (Song, *et. al.,* 2010).

Treatment of amphetamine addiction

In addition to psychosocial interventions, amphetamine-specific antipsychotic drugs that cause psychotic syndromes are also used in the treatment of amphetamine addiction (Vocci, F. J., & Montoya, I. D., 2009). Drugs such as Olanzapine, Quetiapine and Clozapine may decrease anxiety in addicts and decrease the desire to seek substances because they are serotonin 5HT1A partial agonists. Furthermore, in the treatment of amphetamine addiction, ondansetron, a serotonin 5-HT3 receptor antagonist, has been shown to reduce psychoactive substance seeking behaviour in animal experiments (Johnson, B. A., & Cowen, P. J., 1993).

However, there are not enough resources and research on the treatment of amphetamine addiction in our country and worldwide. Therefore, there is a need for effective agents to reduce withdrawal symptoms and psychoactive substance-seeking behaviour, and more research is needed in this field (Dankı *et. al.,* 2005).

MORPHINE

Morphine is a substance containing alcoholic hydroxyls attached to carbon number 3 in the phenanthrene core and methyl roots attached to the etamine bridge. In order to change the structural properties of morphine, new substances have been produced by adding various side chains instead of hydrogens of hydroxyls (Özden, S. Y., 1992).

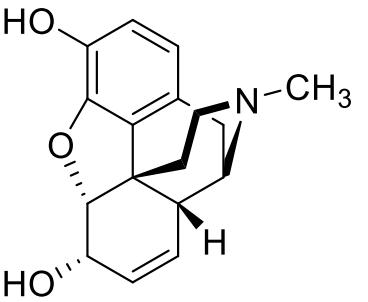

Figure 3. Chemical Structure of Morphine

Effect and addiction of morphine

Morphine and morphine-like agonists bind to μ-receptors in the central nervous system (Ling, W., & Wesson, D. R., 1990). As a result of this binding, effects such as analgesia, euphoria, respiratory depression, suppression of cough reflex and myosis are observed. Although tolerance develops against respiratory depression, analgesia, euphoria and sedation effects in repeated use of morphine, physical and physiological dependence occurs after a while (Howland, R. D., & Mycek, M. J., 2006). However, morphine addiction is different from other substance addictions. In other addictions, drug intake is continued even if the withdrawal syndrome that occurs after drug use is stopped, whereas in morphine addiction, the patient does not continue drug intake when the withdrawal syndrome reactions are over (Harold *et. al.*, 2007).

Withdrawal and withdrawal syndromes that may occur as a result of incorrect administration of morphine are manifested by serious rebound pharmacological effects of morphine. These effects may be observed as rhinorrhoea, lacrimation, yawning, tremor, piloerection, hyperventilation, hyperthermia, mydriasis, muscle pain, vomiting, diarrhoea and anxiety (Katzung, B. G., 2001).

Treatment of morphine addiction

Acute dependence resulting from a single injection of morphine usually leads to withdrawal syndrome symptoms within 4-

24 hours. Morphine exposure lasting for days and weeks may cause more severe withdrawal syndrome symptoms (Zhang, Z., & Schulteis, G., 2008). Within one hour when these symptoms are observed, the patient is given methadone not exceeding 30 milligrams. Methadone is an orally available, long-acting opioid antagonist drug (Kleber, H. D., 2007).

In many countries, the main pharmacological approach in the treatment of opioid addiction is maintenance treatment using opioid agonists. Buprenorphine, a partial opioid antagonist, is used as an alternative drug for patients who do not accept methadone treatment or do not show the desired course in methadone treatment (Evren *et. al*, 2000). In overdose of morphine and other opioids, treatment with naloxone is applied. Naltrexone effectively blocks the opioid effects in the patient (Rzasa Lynn, R., & Galinkin, J. L., 2018).

HEROİN

Heroin is a substance whose narcotic use is known to involve serious risks such as loss of respiration, nervous system depression and death. Heroin was synthesised from morphine by the Bayer Company in 1898. It is stated that heroin, which has 5 to 10 times the potency of morphine, is preferred among narcotic users (Sawynok, J., 1986).

However, the use of heroin is extremely risky due to its strong effects and addiction potential. Therefore, uncontrolled use of heroin can cause serious consequences and endanger the lives of users. It is important for individuals struggling with heroin addiction to seek professional help and be involved in the treatment process (Zhou *et. al*, 2023).

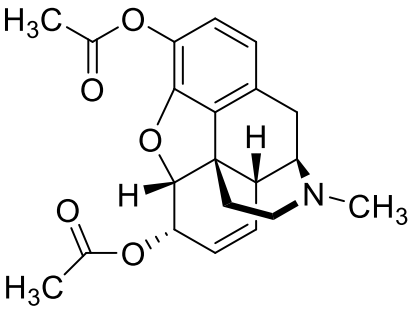

Figure 4. Chemical Structure of Heroin

Heroin was first produced in 1898 as an alternative anaesthetic to morphine and used in treatment for a while. However, it was discovered that heroin had a higher addiction potential than morphine (Van Ree *et. al*, 1999). Today, the use of heroin is legally prohibited worldwide and its use is subject to criminal sanctions. In addition to the addiction resulting from heroin use, serious health and safety problems such as intoxication, involvement in organised crimes and emergency services are also observed (Balcıoğlu *et. al*, 2008).

The effect and addiction of heroin

Heroin is chemically the acetylated form of morphine. It is rapidly metabolised in the liver to 6-monoacetylmorphine (6-MAM), which is hydrolysed to morphine. Morphine and 6-MAM molecules are responsible for the pharmacological effect of heroin (Goodman, L. S., 2009). Its analgesic effect is five times stronger than morphine and its use has been banned due to its very strong euphoria and addictive effect (Dural Ö., 2008). Heroin shows its effect depending on the way of use or some characteristic features (colour, physical state, water solubility, pH, stability, density, purity). Light brown heroin is generally available in Turkey (Ciccarone, D., 2009).

Heroin is used by wrapping it in a cigarette, snorting it, heating it on aluminium foil and inhaling the vapour and injecting it intravenously. It starts to show effect shortly after ingestion and its effect lasts for 6-8 hours. As a result of its use, symptoms such as

relaxation, disappearance of pain sensation, slowing down of heart and respiratory rate, shrinking of pupils, facial flushing, slowing down in speech and movements may be observed (Ögel, K., (,2005). Intravenous heroin use may increase the likelihood of infectious diseases such as hepatitis B, hepatitis C and HIV (Mırsal *et. al,* 2003). The reason for this situation is that the syringes used are not sterile, not cleaned well and sharing of syringes among addicts (Evren *et. al,* 2000). Spread of infectious diseases such as hepatitis and HIV threatens not only addicts but also the society (Evren, E. C., & Çakmak, D., 2002).

Heroin addiction is a chronic, relapsing disease that affects human genetics and is characterised by tolerance and high physical dependence (Levran *et. al,* 2008). Heroin addicted individuals usually live in a subculture specific to them and spend a large part of their time in drug-related activities with symptoms of obtaining drugs, "getting ready for flight", "walking around in a numb state", returning to normal and then withdrawing until their next dose (Kalyoncu A., & Mırsal H., 2000). The suicidal tendency of these individuals may increase with the severity of addiction (Koyuncu *et. al,* 2003).

Withdrawal syndrome symptoms such as dysphoria, insomnia, irritability, fatigue and substance seeking occur 8-12 hours after the last heroin intake. This process is characterised by the addicted individual experiencing the feelings of discomfort and need that arise with the decrease in the effects of heroin in the body. These withdrawal symptoms may encourage a new dose to be taken in order to maintain the addiction (Kleber, H. D., 2007).

Treatment of heroin addiction

In general, methadone maintenance treatment is applied in the treatment of heroin addiction (Kreek *et. al,* 2010). Since heroin especially affects opioid receptors, antagonists such as naloxone and naltrexone can eliminate some opioid effects of heroin by binding to these receptors and are used in addiction treatment. Since methadone is a substance from the opioid group like heroin, naltrexone may be

preferred for "drug-free treatment" (Kalyoncu *et. al*, 2000). Buprenorphine is used to treat disorders such as depression, dysphoria and anxiety observed in addicts (Maremmani *et. al*, 2009).

Treatment options may vary depending on the needs of the individual and the degree of addiction. Opioid agonists such as methadone and buprenorphine may help the addict to reduce withdrawal symptoms by affecting opioid receptors in the body. Antagonists, such as naltrexone, work by blocking the effects of opioids to reduce the person's dependence. Treatment usually involves a long-term and multidisciplinary approach, which includes psychosocial support, therapy and medication.

MARIJUANA

Marijuana is known as a substance obtained from the flower seed and dried leaves of the plant called Cannabis sativa. Marijuana is often used for recreational or medicinal purposes due to its psychotropic effects. Among the active components of this plant, tetrahydrocannabinol (THC) is the most prominent and, when used, causes psychoactive effects by affecting the central nervous system (Small, E., 2015).

The effects of marijuana can vary from person to person, but are generally associated with effects such as relaxation, increased pleasure, changes in perception and slowing of time. For this reason, marijuana has been the subject of legal, medical and social debate in many countries. Medical marijuana use may be legal in some places, and many studies and research into its use for various health conditions are ongoing. However, recreational use of marijuana may still be prohibited in some areas (Bayraktaroğlu *et. al*, 2004).

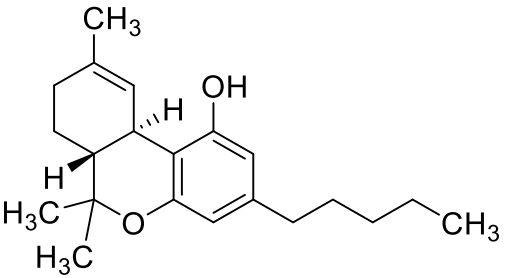

Figure 5. Chemical Structure of Marijuana

The effects and addiction of marijuana

Although the addictive potential of cannabis is low, it is clear that it is a drug that can be addictive although its potency is low. While its effect lasts for 2-4 hours when smoked as a cigarette, this period can increase up to 5-12 hours when taken orally. It can cause a series of effects on the immune system, respiratory system, cardiovascular system, central nervous system and cognitive functions during short or long-term use. In human and animal experiments, it has been determined that long-term intake of THC leads to a decrease in testosterone release, disorders in sperm production, motility and viability, and irregularities in the menstrual cycle. It has been reported that short-term cannabis use decreases prolactin secretion, and long-term use causes suppression of ovulation in women, galactorrhoea and gynaecomastia in men. Physiological dependence develops as a result of repeated use and withdrawal syndrome occurs when substance use is stopped. Depending on this situation, irritability, anger, depression, difficulty in sleeping, desire to use substance and decreased appetite are observed in addicts (Kumar et. al, 2001), (Budney et. al, 2007).

The active ingredient of cannabis is known as tetrahydrocannabinol (THC). THC is a component responsible for the psychoactive effects of cannabis. Although cannabis has the potential for addiction, the potential for addiction is generally lower compared to some other drugs. However, regular and long-term use can lead to addiction in individuals (Nahas et. al, 2002).

The use of cannabis can have a range of physical and psychological effects, whether short or long-term. These effects may include changes in the immune system, respiratory system, cardiovascular system, central nervous system and cognitive function. It has been reported that long-term THC intake can lead to hormonal changes, for example, decreased testosterone release, disturbances in sperm production and irregularities in the menstrual cycle in women (Karila *et. al*, 2014).

In addition, physiological dependence may develop as a result of repeated use of cannabis and withdrawal syndrome may occur when substance use is stopped. Withdrawal symptoms may include irritability, anger, depression, insomnia, craving for the substance and decreased appetite. It is therefore important to be informed about the potential risks and side effects of cannabis use (Smith, N. T., 2002).

Treatment of marijuana addiction

Treatment modalities for cannabis use disorders have developed significantly in recent years. Specific treatments have been developed for conditions such as weight loss, withdrawal syndrome and relapse in cannabis users. In the first stage of the treatment process, behavioural therapies are used to facilitate abstinence from cannabis. Medications such as nefazodone, marinol and buspirone are used to alleviate the withdrawal syndrome associated with stopping cannabis use. In addition, a synthetic delta-9-tetrahydrocannabinol called dronabinol has also been developed for this condition. Dronabinol acts as an agonist and has a reducing effect on the effects of cannabis on the body (Abhishek, D., & Choudhary, C. K., 2010).

Lysergic Acid Diethylamide (LSD)

Lysergic acid diethylamide (LSD) is one of the addictive substances commonly known as "club drugs" and is mostly consumed by adolescents and young adults in nightclubs (Wu *et. al,* 2006).

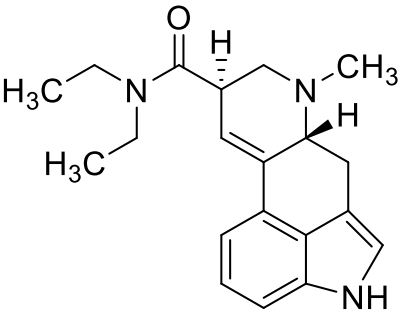

Figure 6. Chemical Structure of Lysergic acid diethylamide (LSD

The effect and addiction of LSD

LSD is a substance that can cause hallucinogenic effects and lead to exacerbation of psychosis. It can be found in different forms such as powder, gelatin capsules, tablets or sugar cubes coated with LSD, filter papers or postage stamps (Özden, H., 2010). Among ergot alkaloids, it is the one that shows the strongest effect on 5HT receptors (Green, A. R., 2008). The effect of LSD usually occurs within 30-60 minutes, reaches a peak in 1-6 hours and usually lasts up to 12 hours. Symptoms of acute toxicity may first appear as various digestive system disorders, followed by symptoms such as tremor, hyperglycaemia, hypertension, mydriasis and tachycardia. At high doses, panic reactions, intense anxiety, confusion and irritability may occur. Physical dependence and withdrawal syndrome are not observed, and physiological dependence is low (Schiff Jr, P. L., 2006).

Treatment of LSD addiction

Drugs from the SSRI (selective serotonin reuptake inhibitor) group can be used to prevent the desire to use again in individuals who stop using LSD. If a neuroleptic agent is chosen to treat the behavioural disorder, drugs such as haloperidol and risperidone may be preferred (Poole, R., & Brabbins, C., 1996).

PHENCYCLİDİNE

Phencyclidine (PCP) was introduced as an anaesthetic agent in the 1950s as part of clinical medicine. However, when its abuse increased in the early 1960s, its use as an anaesthetic was discontinued due to the cases of delirium it induced. Due to its schizophrenia-like effects, PCP was later used in schizophrenia research (Coşkunol, H., 2000).

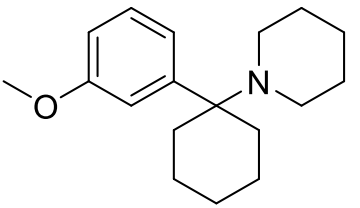

Figure 7. Chemical Structure of Phencyclidine (PCP)

The effect and addiction of phencyclidine

The effect of phencyclidine occurs through NMDA receptors (Thornberg, S. A., & Saklad, S. R., 1996). In both acute and chronic use, psychotoxic syndrome develops and the user may harm himself/herself and his/her environment. In addition to psychological effects, symptoms such as hyperthermia, tachycardia, hypertension, nystagmus, myoclonus and ataxia occur in the body (Winchester, J. F., 2002). When the substance is discontinued after high dose use, withdrawal syndrome is not observed, but hallucinations and tendency to violence are observed with intoxication. These delirium symptoms may persist for several months after drug withdrawal. Dependence varies depending on the dose and duration of use (Erickson, T. B., 2005).

Treatment of phencyclidine addiction

Firstly, substance use is stopped and urine acidification is applied to remove phencyclidine from the body. Intramuscular and oral antipsychotics or benzodiazepines are used for the resulting psychosis (60 mg Diazepam, 30 mg Haloperidol per day), but this

treatment should be as short-term as possible (Schuckit, M. A., 2006).

TOLUENE

Toluene-2,4-diisocyanate and toluene-2,6-diisocyanate are isomeric substances belonging to the isocyanate group and have a molecular structure of $C_9H_6N_2O_2$. Toluene, an aromatic hydrocarbon, carries a high risk, especially in terms of abuse potential (Yücel *et. al*, 2008). This chemical component is found as an organic solvent with neurotoxic properties in products such as paints, adhesives and thinners. It is reported that exposure to toluene may lead to neurological and psychiatric complications. It is known that these effects may occur as a result of prolonged inhalation among people exposed to toluene and those working in sectors such as paint, textile and leather products (Lim *et. al*, 2014).

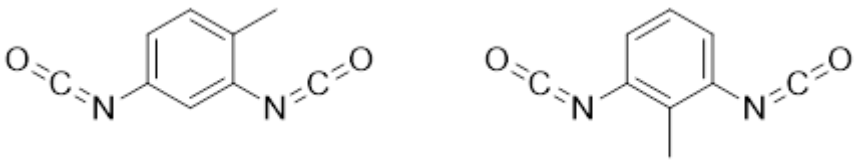

Figure 8. Chemical Structure of Toluene-2,4-diisocyanate and toluene-2,6-diisocyanate

It has been reported that adhesive materials contain toluene at a lower rate than paint thinner and that the euphoria and hallucinogenic effect of adhesive and the sedative and anaesthetic effect of paint thinner are higher (Salloum *et. al*, 2023). The psychological effects caused by toluene ingestion are associated with increased intraneuronal calcium levels and consequently increased dopamine release from presynaptic terminals (Rajendran *et. al*, 2022). Physiological effects of toluene include hypokalemia, respiratory suppression, metabolic acidosis, ventricular tachycardia, sinus bradycardia, vasospasm and cardiomyopathy. It has also been reported that chronic regular use may increase the risk of myocardial infarction (Ford *et. al*, 2014).

REFERENCES

Abhishek, D., & Choudhary, C. K. (2010). Genetics of morphine, yield and its candidate characters in opium poppy (Papaver somniferum L.). *Electronic Journal of Plant Breeding*, *1*(4), 649-655.

Altıntaş, K., Saatçioğlu, Ö., & Çakmak, D. (2007). Madde bağımlılığı ve psikoz. *Nöropsikiyatri Arşivi*, *44*(1), 34-40.

Balcıoğlu, İ., Çitken, A., & Doksat, M. K. (2008). Madde Bağımlılığının Hukukî Yönü. In *Yeni Symposium* (Vol. 46, No. 1, pp. 3-8).

Bayraktaroğlu, T., Kargı, E., Yeşilli, Ç., Numanoğlu, G., Borazan, A., & Üstündağ, Y. (2004). Erkekde kısa süreli marihuana (esrar) kullanımının beklenmedik etkileri: Jinekomasti ve oligoastenospermi. *Bağımlılık Dergisi*, *5*(1), 35-39.

Berman, S. M., Kuczenski, R., McCracken, J. T., & London, E. D. (2009). Potential adverse effects of amphetamine treatment on brain and behavior: a review. *Molecular psychiatry*, *14*(2), 123-142.

Bruce, M. (2000). Managing amphetamine dependence. *Advances in Psychiatric Treatment*, *6*(1), 33-39.

Budney, A. J., Roffman, R., Stephens, R. S., & Walker, D. (2007). Marijuana dependence and its treatment. *Addiction science & clinical practice*, *4*(1), 4.

Ceyhun, B., Oğuztürk, Ö., & Ceyhun, A. G. (2001). Madde kullanma eğilimi ölçeğinin geçerlik ve güvenilirliği. *Klinik Psikiyatri*, *4*(2), 87-93.

Ciccarone, D. (2009). Heroin in brown, black and white: structural factors and medical consequences in the US heroin market. *International Journal of Drug Policy*, *20*(3), 277-282.

Coşkunol, H. (2000). Şizofreni ve madde kullanım bozuklukları. *Şizofreni Dizisi*, *1*, 36-44.

Dankı, D., Dilbaz, N., Okay, T., Açıkgöz, Ç., Erdinç, I. B., & Telci, Ş. (2005). Madde Kullanimina Bağli Gelişen Psikotik Bozuklukta Atipik Antipsikotik Tedavisi: Bir Gözden Geçirme. *Journal of Dependence*, *6*, 136-141.

Docherty, J. R. (2008). Pharmacology of stimulants prohibited by the World Anti-Doping Agency (WADA). *British journal of pharmacology*, *154*(3), 606-622.

Doğan, M. S., & Çelik, H. (2023). Organic Compounds Containing Aromatic Structure Used in Pharmaceutical Production. *J Biochem Technol*, 14(2): 102-111.

EA, Ö. D. (2008). Farmakoloji (4. baskı). *Nobel tıp kitabevleri, İstanbul*.

Erickson, T. B. (2005). Pediatric toxicology: Diagnosis and management of the poisoned child. *(No Title)*.

Evren, E. C., Tamar, D., Babayağmur, B., & Çakmak, D. (2000). Opioid bağımlılığının tedavisinde buprenorfin: Metadonla karşılaştırma çalışmaları. *Klinik Psikofarmakoloji Bülteni-Bulletin of Clinical Psychopharmacology*, *10*, 205-212.

Evren, C., Tamar, D., Ögel, K., Çorapçıoğlu, A., & Çakmak, D. (2000). Damar yolu ile eroin kullanımı ve ilişkili bazı davranış biçimleri. *Klinik Psikiyatri Dergisi*, *3*(3), 185-191.

Evren, E. C., & Çakmak, D. (2002). Damar Yolu ile Eroin Kullananların Genel Özellikleri. *Nöropsikiyatri Arşivi,* 39(1): 20-26.

Ford, J. B., Sutter, M. E., Owen, K. P., & Albertson, T. E. (2014). Volatile substance misuse: an updated review of toxicity and treatment. *Clinical reviews in allergy & immunology*, *46*, 19-33.

Fraser, S., Moore, D., & Keane, H. (2014). *Habits: remaking addiction*. Springer.

Goodman, L. S. (2009). Goodman and Gilman Tedavinin Farmakolojik Temeli. *Nobel Tıp Kitabevleri*, 545-590.

Gökler, R., & Koçak, R. (2008). Uyuşturucu ve madde bağımlılığı. *Sosyal bilimler araştırmaları dergisi*, *3*(1), 89-104.

Green, A. R. (2008). Gaddum and LSD: the birth and growth of experimental and clinical neuropharmacology research on 5-HT in the UK. *British journal of pharmacology*, *154*(8), 1583-1599.

Griffiths, M. D. (2017). Behavioural addiction and substance addiction should be defined by their similarities not their dissimilarities. *Addiction*, *112*(10), 1718-1720.

Harold, K., Grant, D. M., & Mitchel, J. (2007). Principles of medical pharmacology. *Elsevier Canada Ltd*, *557*, 558-559.

Howland, R. D., & Mycek, M. J. (2006). Lippincotts Illustrated reviews, Pharmacology. *Teaching Learning*, *5*, 5.

Johnson, B. A., & Cowen, P. J. (1993). Alcohol-induced reinforcement: Dopamine and 5-HT3 receptor interactions in animals and humans. *Drug Development Research*, *30*(3), 153-169.

Kalyoncu A., & Mırsal H. (2000). Madde Bağımlılığında Bireysel Psikoterapi, Bağımlılık Dergisi, 1(2): 95-100.

Kalyoncu A, Mırsal H, Satır T. (2000). Opiat Bağımlılığında Antagonist Tedavi: Naltrexone, *Bağımlılık Dergisi*, 1(1): 43-49.

Kampman, K. M. (2005). New medications for the treatment of cocaine dependence. *Psychiatry (Edgmont)*, *2*(12), 44.

Kampman, K. M. (2009). New medications for the treatment of cocaine dependence. *Ann Ist Super Sanita*, *45*(2), 109-15.

Karila, L., Roux, P., Rolland, B., Benyamina, A., Reynaud, M., Aubin, H. J., & Lancon, C. (2014). Acute and long-term effects of cannabis use: a review. *Current pharmaceutical design*, *20*(25), 4112-4118.

Katzung, B. G. (2001). Introduction to autonomic pharmacology. *Basic and clinical pharmacology*, *13*, 87-109.

Kılıç, F. (2016). Bağımlılık ve Uyarıcı Maddeler/Addıctıon and Stımulant Drugs. *Osmangazi Tıp Dergisi*, *38*(1).

Kleber, H. D. (2007). Pharmacologic treatments for opioid dependence: detoxification and maintenance options. *Dialogues in clinical neuroscience*, *9*(4), 455-470.

Knuepfer, M. M. (2003). Cardiovascular disorders associated with cocaine use: myths and truths. *Pharmacology & therapeutics*, *97*(3), 181-222.

Koyuncu, A., Mırsal, H., Yavuz, M. F., Kalyoncu, Ö. A., & Beyazyürek, M. (2003). Eroin bağımlılarında intihar düşüncesi, planı ve girişimi.

Kreek, M. J., Borg, L., Ducat, E., & Ray, B. (2010). Pharmacotherapy in the treatment of addiction: methadone, *J Addict Dis.* 29(2): 200-216.

Kumar, R. N., Chambers, W. A., & Pertwee, R. G. (2001). Pharmacological actions and therapeutic uses of cannabis and cannabinoids. *Anaesthesia*, *56*(11), 1059-1068.

Levran, O., Londono, D., O'hara, K., Nielsen, D. A., Peles, E., Rotrosen, J., ... & Kreek, M. J. (2008). Genetic susceptibility to heroin addiction: a candidate gene association study. *Genes, Brain and Behavior*, *7*(7), 720-729.

Lim, S. K., Shin, H. S., Yoon, K. S., Kwack, S. J., Um, Y. M., Hyeon, J. H., ... & Lee, B. M. (2014). Risk assessment of volatile organic compounds benzene, toluene, ethylbenzene, and xylene (BTEX) in consumer products. *Journal of Toxicology and Environmental Health, Part A*, *77*(22-24), 1502-1521.

Ling, W., & Wesson, D. R. (1990). Drugs of abuse--opiates. *Western Journal of Medicine*, *152*(5), 565.

Maremmani, I., Pacini, M., Lamanna, F., Maremmani, A. G., Pani, P. P., Perugi, G., & Gerra, G. (2009). Predictors for non-relapsing in methadone-and buprenorphine-maintained heroin

addicts: a comparative study. *Heroin in addiction and related clinical problems*, 11(3): 41-44.

Mırsal, H., Kalyoncu, Ö. A., Pektaş, Ö., Tan, D., & Beyazyürek, M. (2003). Damar yolundan eroin kullananlarda hepatit B, hepatit C ve HIV yaygınlığı.

Michel, Rosalind., & Adams, A. P. (1979). Acute amphetamine abuse. Problems during general anaesthesia for neurosurgery. *Anaesthesia*, *34*(10), 1016-1019.

Nahas, G., Harvey, D. J., Sutin, K., Turndorf, H., & Cancro, R. (2002). A molecular basis of the therapeutic and psychoactive properties of cannabis (Δ9-tetrahydrocannabinol). *Progress in Neuro-Psychopharmacology and Biological Psychiatry*, *26*(4), 721-730.

O'Brien, C. P. (2006). Drug addiction and drug abuse. *Goodman and Gilman's the pharmacological basis of therapeutics*, *11*, 607-627.

Ögel, K. (2005). Madde kullanım bozuklukları epidemiyolojisi. *Türkiye Klinikleri Dahili Tıp Bilimleri Dergisi Psikiyatri*, *1*(47), 61-4.

Özden, S. Y. (1992). *Uyuşturucu Madde Bağımlılığı Teşhis-Tedavi-Tedbir*. Nobel Tıp Kitabevleri. İstanbul. 3-5, 330-331.

Özden, H. (2010). Bağımlılık Yapan Maddeler ve Etik Yaklaşım. *Bağımlılık Dergisi,* 6-7.

Poole, R., & Brabbins, C. (1996). Drug induced psychosis. *The British Journal of Psychiatry*, *168*(2), 135-138.

Rajendran, R., Ragavan, R. P., Al-Sehemi, A. G., Uddin, M. S., Aleya, L., & Mathew, B. (2022). Current understandings and perspectives of petroleum hydrocarbons in Alzheimer's disease and Parkinson's disease: a global concern. *Environmental Science and Pollution Research*, 1-22.

Rasmussen, S. G., Carroll, F. I., Maresch, M. J., Jensen, A. D., Tate, C. G., & Gether, U. (2001). Biophysical characterization of the cocaine binding pocket in the serotonin transporter using a fluorescent cocaine analogue as a molecular reporter. *Journal of Biological Chemistry*, *276*(7), 4717-4723.

Rzasa Lynn, R., & Galinkin, J. L. (2018). Naloxone dosage for opioid reversal: current evidence and clinical implications. *Therapeutic advances in drug safety*, *9*(1), 63-88.

Salloum, I. M., Stewart, C. M., & Abou-Saleh, M. T. (2023). Disorders Due to Substance Use: Inhalants. In *Tasman's Psychiatry* (pp. 1-41). Cham: Springer International Publishing.

Sawynok, J. (1986). The therapeutic use of heroin: a review of the pharmacological literature. *Canadian journal of physiology and pharmacology*, *64*(1), 1-6.

Schiff Jr, P. L. (2006). Ergot and its alkaloids. *American journal of pharmaceutical education*, *70*(5).

Schuckit, M. A. (2006). *Drug and alcohol abuse: A clinical guide to diagnosis and treatment*. Springer Science & Business Media.

Small, E. (2015). Evolution and classification of Cannabis sativa (marijuana, hemp) in relation to human utilization. *The botanical review*, *81*, 189-294.

Smith, N. T. (2002). A review of the published literature into cannabis withdrawal symptoms in human users. *Addiction*, *97*(6), 621-632.

Song, B. J., Moon, K. H., V Upreti, V., D Eddington, N., & J Lee, I. (2010). Mechanisms of MDMA (ecstasy)-induced oxidative stress, mitochondrial dysfunction, and organ damage. *Current pharmaceutical biotechnology*, *11*(5), 434-443.

Şatır, T. T., Kalyoncu, A., & Pektaş, Ö. (2000). Kokain kullanım bozukluğunda birbirini takip eden iki sürecin değerlendirilmesi. *Bağımlılık Dergisi*, *1*(1), 18-21.

Thornberg, S. A., & Saklad, S. R. (1996). A review of NMDA receptors and the phencyclidine model of schizophrenia. *Pharmacotherapy: The Journal of Human Pharmacology and Drug Therapy*, *16*(1), 82-93.

Ugurlu, T. T., Sengül, C. B., & Sengül, C. (2012). Bagimlilik Psikofarmakolojisi/Psychopharmacology of Addiction. *Psikiyatride Guncel Yaklasimlar*, *4*(1), 37.

Van Ree J. M, Gerrits M. A., & Vanderschuren L. J. (1999). Opioids, reward and addiction: an encounter of biology, psychology, and medicine, *The American Society for Pharmacology and Experimental Therapeutics*, 342-381.

Vocci, F. J., & Montoya, I. D. (2009). Psychological treatments for stimulant misuse, comparing and contrasting those for amphetamine dependence and those for cocaine dependence. *Current opinion in psychiatry*, *22*(3), 263.

Washton, A. M., & Tatarsky, A. (1984). Adverse effects of cocaine abuse. *NIDA Res Monogr*, *49*, 247-254.

Winchester, J. F. (2002). Dialysis and hemoperfusion in poisoning. *Advances in renal replacement therapy*, *9*(1), 26-30.

Wu, L. T., Schlenger, W. E., & Galvin, D. M. (2006). Concurrent use of methamphetamine, MDMA, LSD, ketamine, GHB, and flunitrazepam among American youths. *Drug and alcohol dependence*, *84*(1), 102-113.

Yedekci, A., & Onur, E. (2010). Bağımlılık yapıcı ilaçlar ve tayin yöntemleri. Türk Klinik Biyokimya Dergisi, 8(3), 125-131.

Yücel, M., Takagi, M., Walterfang, M., & Lubman, D. I. (2008). Toluene misuse and long-term harms: a systematic review of the neuropsychological and neuroimaging literature. *Neuroscience & Biobehavioral Reviews*, *32*(5), 910-926.

Zhang, Z., & Schulteis, G. (2008). Withdrawal from acute morphine dependence is accompanied by increased anxiety-like

behavior in the elevated plus maze. *Pharmacology Biochemistry and Behavior*, *89*(3), 392-403.

Zhou, H., Mahboob, A., Rasheed, M. W., Ovais, A., Siddiqui, M. K., & Cheema, I. Z. (2023). On QSPR Analysis of Molecular Descriptor and Thermodynamic Features of Narcotic Drugs. *Polycyclic Aromatic Compounds*, 1-21.